

Dissertation
zum Erwerb des Doktorgrades an der Medizinischen Fakultät
der Ludwig-Maximilians-Universität zu München



**Generation and characterization of CD19 CAR T cells
with CTLA-4/CD28 fusion receptor**

Jasmin Mahdawi

München

2023

Aus der Kinderklinik und Kinderpoliklinik
im Dr. von Haunerschen Kinderspital
Klinik der Universität München
Abteilung Pädiatrische Hämatologie und Onkologie
Ärztlicher Direktor: Professor Dr. Dr. Christoph Klein

**Generation and characterization of CD19 CAR T cells
with CTLA-4/CD28 fusion receptor**

Dissertation
zum Erwerb des Doktorgrades der Medizin
an der Medizinischen Fakultät der
Ludwig-Maximilians-Universität zu München

vorgelegt von
Jasmin Mahdawi
aus München

2023

Mit Genehmigung der Medizinischen Fakultät
der Universität München

Berichterstatter: Prof. Dr. Tobias Feuchtinger

Mitberichterstatter: Prof. Dr. Marion Subklewe

Prof. Dr. Andreas Humpe

Prof. Dr. Christoph Salat

Dekan: Prof. Dr. med. Thomas Gudermann

Tag der mündlichen Prüfung: 22.06.2023

Eidesstattliche Versicherung

Mahdawi, Jasmin

Name, Vorname

Ich erkläre hiermit an Eides statt, dass ich die vorliegende Dissertation mit dem Thema

Generation and characterization of CD19 CAR T cells with CTLA-4/CD28 fusion receptor

selbständig verfasst, mich außer der angegebenen keiner weiteren Hilfsmittel bedient und alle Erkenntnisse, die aus dem Schrifttum ganz oder annähernd übernommen sind, als solche kenntlich gemacht und nach ihrer Herkunft unter Bezeichnung der Fundstelle einzeln nachgewiesen habe.

Ich erkläre des Weiteren, dass die hier vorgelegte Dissertation nicht in gleicher oder in ähnlicher Form bei einer anderen Stelle zur Erlangung eines akademischen Grades eingereicht wurde.

München, 1. August 2023

Ort, Datum

Jasmin Mahdawi

Unterschrift der Doktorandin

Meiner Familie.

Table of contents

1	Abbreviations	1
2	Introduction.....	3
2.1	Acute lymphoblastic leukemia.....	3
2.2	Immunotherapy	5
2.3	CAR T cell therapy	6
3	Aims and objectives of this study.....	11
4	Materials.....	12
4.1	Equipment and software	12
4.2	Solutions, media and sera for cell culture	13
4.3	Consumables.....	14
4.4	Antibodies	16
5	Methods	18
5.1	CAR T cell generation	18
5.1.1	PBMC isolation and T cell activation	18
5.1.2	Virus generation	18
5.1.3	Retroviral CAR T cell transduction	19
5.2	Functionality assays	19
5.2.1	Checkpoint expression assay.....	19
5.2.2	Cytotoxicity assay	20
5.2.3	Intracellular cytokine stain (ICS).....	20
5.2.4	Proliferation assay	20
5.2.6	Activation assay with blinatumomab	21
5.2.7	Long-term assay.....	21
5.3	Generation and characterization of target cell lines	21
5.3.1	Transduction of cell lines.....	21
5.3.2	Immune checkpoint profile of cell lines	22
5.4	General cell culture.....	22
5.5	Flow cytometry	23
5.6	Software.....	23
5.7	Statistical analysis	23
6	Results	24
6.1	Checkpoint profiles of leukemic cells and T cells upon stimulation	24
6.2	CTLA-4 overexpression leads to reduced T cell functionality	27
6.3	Generation of anti-CD19 CAR T cells with CTLA-4/CD28 fusion receptor is feasible.....	29

6.4	CAR T cells with CTLA-4/CD28 fusion receptor show high CD19-specific functionality	32
6.5	CAR T cells with CTLA-4/CD28 fusion receptor obtain similar activation capacity compared to conventional first generation CAR T cells.....	34
6.6	19_3z_CTLA_28 CAR T cells exhibit comparable cytotoxic capability to conventional first and second generation CAR T cells	35
6.7	CAR T cells with CTLA-4/CD28 fusion receptor show slightly enhanced cytokine secretion in presence of CD80 and CD86.....	37
6.8	CAR T cells with CTLA-4/CD28 fusion receptor obtain superior long-term functionality....	39
7	Discussion.....	42
7.1	The role of immune checkpoints on T cell interaction with malignant cells in acute lymphoblastic leukemia.....	42
7.2	Successful generation of anti-CD19 specific CAR T cells.....	42
7.3	Inhibitory effect of CTLA-4 on T cells	43
7.4	Abrogation of the inhibitory CTLA-4 signal.....	44
7.5	Potential enhancement of conventional CAR T cells by CTLA-4/CD28 fusion receptor in specific settings	45
7.6	Clinical potential of the CTLA-4/CD28 fusion receptor.....	46
8	Summary	48
9	Zusammenfassung.....	49
10	Literature.....	50
11	Supplements.....	55
11.1	Primer sequences.....	55
11.2	T cell sequences	55
11.2.1	Sequence of 19_3z CAR.....	55
11.2.2	Sequence of 19_3z_CTLA CAR.....	55
11.2.3	Sequence of 19_3z_CTLA_CD28 CAR	56
11.2.5	Sequence of 19_BB_3z CAR	57
11.2.6	Sequence of 19_BB_3z_CTLA CAR	57
11.2.7	Sequence of 19t CAR.....	58
11.2.8	Sequence for CTLA-4 overexpression.....	58
11.3	Vector Maps.....	59
11.3.1	Vector map of pMP71	59
11.3.2	Vector map of gag/pol (pcDNA3.1-MLV-g/p).....	59
12	Publication list	60

1 Abbreviations

19_3z	1 st generation CAR T cells	CNS	Central nervous system
19_3z_BB_CTLA	2 nd generation CAR T cells with CTLA-4 overexpression	CoALL	Cooperative acute lymphoblastic leukemia study
19_3z_CTLA	1 st generation CAR T cells with CTLA-4 overexpression	CR	Complete remission
19_3z_CTLA_28	1 st generation CAR T cells with fusion receptor	CRS	Cytokine release syndrome
19_BB_3z	2 nd generation CAR T cells	CTLA-4	Cytotoxic T-lymphocyte-associated protein 4
19t	Truncated CAR, control CAR	DC	Dendritic cells
ADP	Adenosine diphosphate	DMSO	Dimethyl sulfoxide
AIEOP-BFM ALL	Associazione italiana ematologia oncologia pediatrica – Berlin-Frankfurt-Munster acute lymphoblastic leukemia study	E:T	Effector : target
ALL	Acute lymphoblastic leukemia	EC	Extracellular
ATP	Adenosine triphosphate	EMA	European Medicine Agency
B	B cells	ENTPD1	Ectonucleoside triphosphate diphosphohydrolase 1
BFM-ALL	Berlin-Frankfurt-Munster acute lymphoblastic leukemia study	FACS	Fluorescence-activated cell sorting
BTLA	B- and T-cell lymphocyte attenuator	FBS	Fetal bovine serum
CAR	Chimeric antigen receptor	FC	Fold change
CD	Cluster of differentiation	FDA	U.S. Food and Drug Administration
CEACAM1	Carcinoembryonic antigen-related cell adhesion molecule 1	HMGB1	High mobility group protein B1
		HSCT	Hematopoetic stem cell transplantation
		HSVgD	Herpes simplex virus glycoprotein D

HSA	Human serum albumin	PCR	Polymerase chain reaction
HVEM	Herpes virus entry mediator	PD-1	Programmed cell death 1
IC	Intracellular	PD-L1	Programmed cell death 1 ligand 1
ICOS-L	Inducible T-cell co-stimulator ligand	PtdSer	Phosphatidylserine
ICS	Intracellular cytokine stain	PVR	Poliovirus receptor
IFN-γ	Interferon gamma	ScFv	Single chain variable fragment
IntReALL	International study for treatment of childhood relapsed acute lymphoblastic leukemia	T	T cells
LAG-3	Lymphocyte-activation gene 3	T_{CM}	Central memory T cells
LSEctin	Liver and lymph node sinusoidal endothelial cell C-type lectin	T_{EFF}	Effector T cells
LT-α	Lymphotoxin- α	T_{EM}	Effector memory T cells
MHC	Major histocompatibility complex	TIGIT	T-cell immunoreceptor with Ig and ITIM domains
MRD	Minimal residual disease	TIM-3	T-cell immunoglobulin and mucin domain 3
n	Number	TM	Transmembrane
NK	Natural killer cells	T_N	Naïve T cells
NKT	Natural killer T cells	TNF-α	Tumor necrosis factor alpha
ns	Not significant	T_{SCM}	Stem cell-like memory
NT5E	Ecto-5'-nucleotidase	WBC	White blood cell count

2 Introduction

2.1 Acute lymphoblastic leukemia

Epidemiology

Acute lymphoblastic leukemia (ALL) is the most common malignant disease in childhood and the most frequent cause of death from cancer under 20 years of age¹. The malignant lymphoid progenitor cells can be either of T or B cell origin, however approximately 80-85% are of B cell origin. Age and gender distribution shows an increased incidence of ALL in children between two to five years of age, as well as a 1.2:1 boys to girls gender ratio².

In 1948, Farber et al. reported the first patient achieving temporary leukemia remission induced by chemotherapy³. Since the 1960s, the survival rates of children have increased from less than 10% up to 90% (Figure 1) due to progressive improvements in therapeutic options⁴. Despite remarkably enhanced survival rates, prognosis of relapsed or refractory ALL in children remains poor⁵.

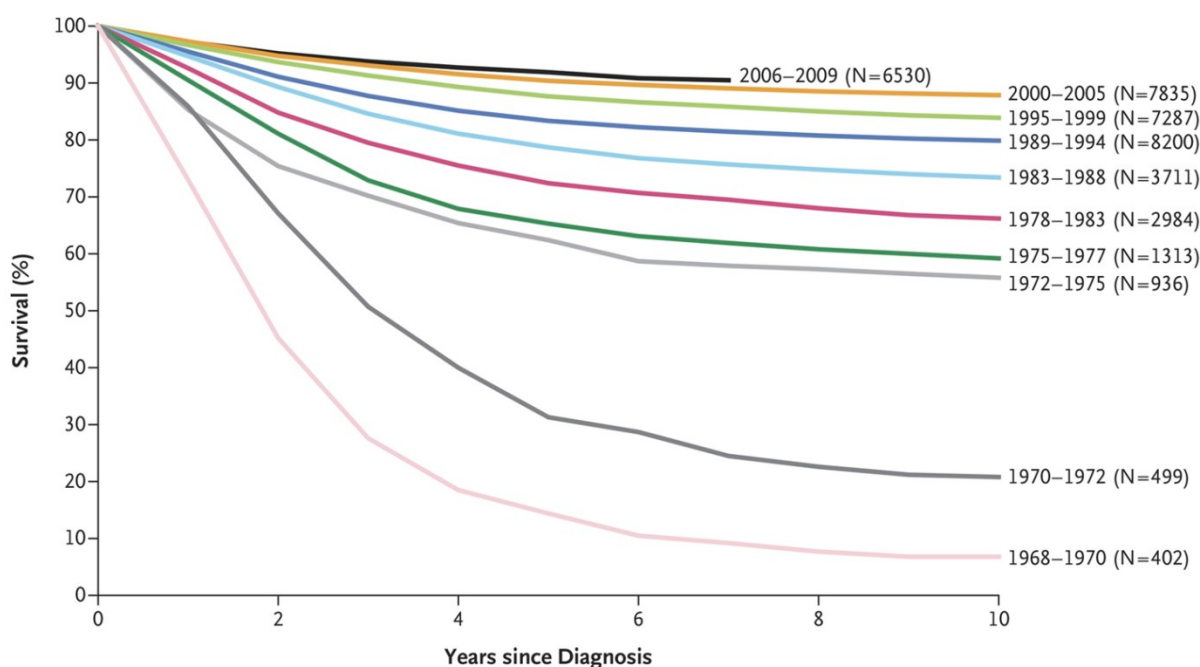


Figure 1 Overall survival of children with acute lymphoblastic leukemia (ALL) from 1968-2009.

Survival rates of children diagnosed with acute lymphoblastic leukemia has increased from approximately 10% in the 1960s up to 90% in 2009 (Figure adapted from Hunger and Mullighan 2015)¹.

Prognostic stratification

Stratification of newly diagnosed pediatric ALL and prediction of treatment failure is based on different markers such as age, white blood cell count (WBC), central nervous system (CNS) involvement and

immunophenotype of leukemic cells at initial diagnosis. Patients between one and ten years of age with WBC under 50 000/ μ l, less than 5 leucocytes/ μ l in cerebrospinal fluid and absence of CNS involvement are defined as standard-risk patients⁵. Children not meeting these parameters are classified as high risk. Risk-stratification allows treatment with less toxic regimens for patients at standard risk, while high-risk patients can be provided with a more aggressive therapy. Additionally, response to initial therapy has been shown to be a powerful predictor. Complete remission (CR) is defined as less than 5% detectable blasts in microscopy at the end of induction⁵. An even more sensitive method to quantify induction outcome is the evaluation of minimal residual disease (MRD) by flow cytometry or polymerase chain reaction (PCR). Best clinical outcomes were achieved for MRD negative patients at end of induction therapy, while MRD positive patients were more likely to relapse⁶.

Standard treatment

Pediatric patients with ALL are assigned and treated according to therapeutic study protocols like AIEOP-BFM ALL and ALLTogether, which have almost the same treatment backbone. All standard treatment plans include induction, consolidation, maintenance and extra compartment therapy. The induction phase lasts four to six weeks and consists of three or four chemotherapy drugs. Remission can be achieved in approximately 95% of all patients⁵. Induction is followed by intensive phases of multi-agent chemotherapy over a period of several months, aiming for eradication of submicroscopic residual disease that may have remained after obtaining CR. Maintenance phase is the final and longest phase of chemotherapy and consists of daily and weekly oral chemotherapy for myelosuppression and periodic intrathecal chemotherapy. Specific CNS therapy is given to all patients, regardless of initial CNS involvement by intrathecal or systemic administration of blood-brain barrier penetrating chemotherapy. Historically, cranial irradiation was part of treatment protocols, but has been largely abandoned due to its late effects, including secondary malignant neoplasm and cognitive deficits⁵.

Remarkable progress in diagnosis and treatment of pediatric ALL over the last decades has resulted in high overall survival rates for patients at standard-risk. Still, 15% to 20% of patients with ALL will suffer disease relapse, which is the most common cause of treatment failure⁵. Even with intensive therapy that may include hematopoietic stem cell transplantation (HSCT), overall survival rates of patients with relapsed ALL is below 40%⁷. Immunotherapy has emerged as a promising approach for treatment of relapsed and refractory ALL in children.

2.2 Immunotherapy

The role of the immune system in treatment of malignancy

Gaining knowledge about the role of the human immune system in cancer surveillance is indispensable for understanding the way immunotherapeutic options can be used to treat childhood leukemia. In the most simplified manner, tumor cells can be recognized by the immune system due to tumor-specific antigens, which can result in tumor cell killing⁸. Nonetheless, malignant cells can evade this mechanism in numerous ways, including down-regulation of tumor-specific antigens and upregulation of inhibitory immune checkpoints like cytotoxic T-lymphocyte associated protein 4 (CTLA-4) and programmed death receptor (PD-1) on T cells⁹. The aim of cancer immunotherapy is to enhance or induce the immune response against tumor cells.

Immune checkpoint inhibitors

T cell homeostasis is regulated by the expression of inhibitory and stimulatory surface markers on T cells¹⁰. Antibodies against inhibitory checkpoint molecules on the T cell or tumor cell surface can improve T cell activation and immune surveillance¹¹. Patients with highly immunogenic malignancies, like melanoma, have been reported to benefit from this approach (e.g. anti-PD-1, anti-CTLA-4)^{12,13}, whereas immune checkpoint blockade has not shown far-reaching success as therapeutic option in pediatric ALL to date. However, previous work of our group has shown the relevance of checkpoint molecules in acute lymphoblastic leukemia¹⁴. The profile of co-inhibitory and co-stimulatory surface markers differed significantly between ALL blasts and B precursor cells of healthy donors¹⁴. Inhibitory immune checkpoint molecules like PD-L1 have been upregulated on leukemic blasts upon T cell attack, leading to suppression of T cell activation¹⁴. Although ALL is described as a malignancy with low immunogenicity, individual cases of favorable responses to immune checkpoint blockade in ALL have been reported for pediatric patients with B-ALL and T-ALL upon administration of pembrolizumab (anti-PD-1)^{14,15}.

Bispecific T cell engager blinatumomab

Antibody-based therapies like monoclonal antibodies, antibody-drug conjugates or bispecific T cell engagers (BiTEs) allow therapeutic effects mainly to be targeted to tumor cells, while non-tumor cells are ideally being spared. Blinatumomab is an anti-CD3/anti-CD19 bispecific T cell engager, binding to CD3 on T cells and linking them to CD19 positive B(-precursor) cells. Thus, TCR-mediated activation and killing of the targeted cells is enabled due to spatial proximity. Blinatumomab was approved by the U.S. Food and Drug Administration (FDA) for treatment of relapsed or refractory B-precursor ALL of adults in 2014 and extended in 2018 for treatment of children¹⁶.

Pediatric data on the efficacy of blinatumomab rely on a phase I/II clinical trial. Von Stackelberg et al. demonstrated the achievement of complete remission for 30% of refractory and 48% of relapsed patients within the first two cycles of treatment¹⁷. Blinatumomab was included into standard relapse protocols (IntReALL) for treatment of advanced pediatric ALL in Germany.

Recent advances have shown the possibility to harness the power of the immune system to eradicate malignant cells. An even more promising immunotherapeutic approach for the treatment of acute lymphoblastic leukemia emerged with the adoptive transfer of T cells modified with a chimeric antigen receptor (CAR).

2.3 CAR T cell therapy

Structure of CAR T cells

Chimeric antigen receptors are synthetically engineered receptors that can target surface molecules on leukemic cells independent of MHC¹⁸. The basic structure of CARs consists of extracellular immunoglobulin-derived heavy and light chains linked to a T cell activating CD3 ζ domain (Figure 2). By variation of the single chain variable fragment (scFv), different tumor surface antigens can be targeted¹⁹. As CD19 is present in most B cell leukemia but not any normal tissue other than B cells, it is the most attractive and currently most investigated target for CARs.

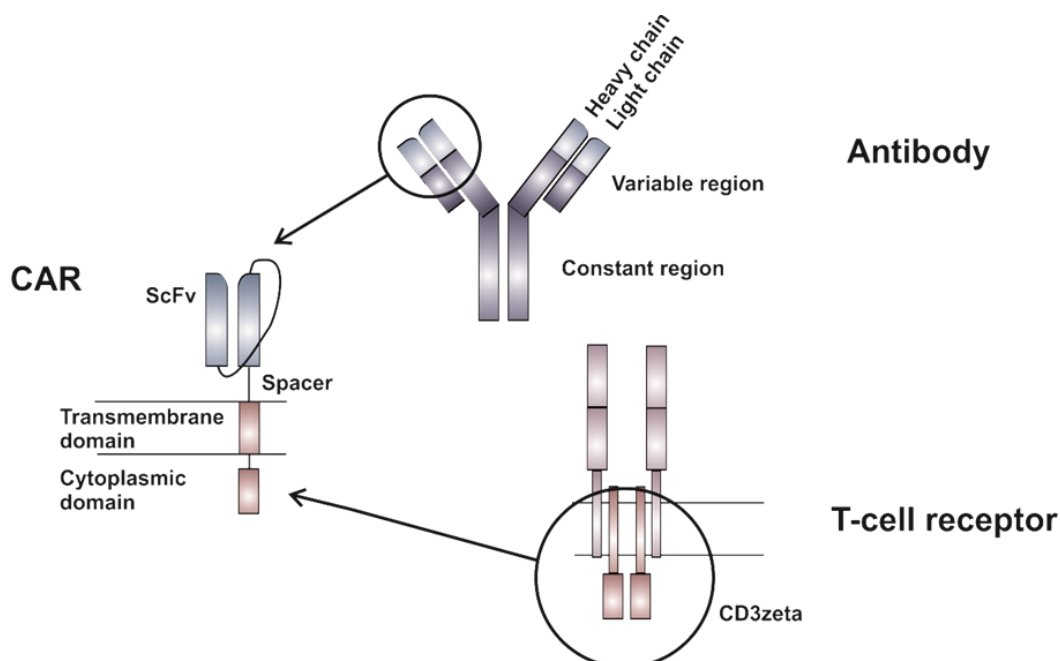


Figure 2 CAR structure.

CARs are built of an extracellular immunoglobulin-derived single chain variable fragment (scFv) and an intracellular CD3 ζ chain. Both domains are linked by a spacer and transmembrane domain. Costimulatory domains (e.g. 4-1BB and CD28) are often included intracellularly for improved clinical functionality. Hence, antibody-mediated recognition is translated into T cell receptor-based signaling through the CAR. CAR: chimeric antigen receptor, ScFv: single chain variable fragment. Schematic illustration was kindly provided by Franziska Blaeschke.

This minimal equipped – first generation – CAR has laid the foundation for further improvements of CARs (Figure 3). Second generation CARs additionally contain one costimulatory molecule such as CD28 or 4-1BB in the intracellular compartment. In third generation CARs two costimulatory domains are included to increase T cell activation, proliferation and persistence, although these constructs have shown limited efficacy compared to second generation CAR T cells²⁰.

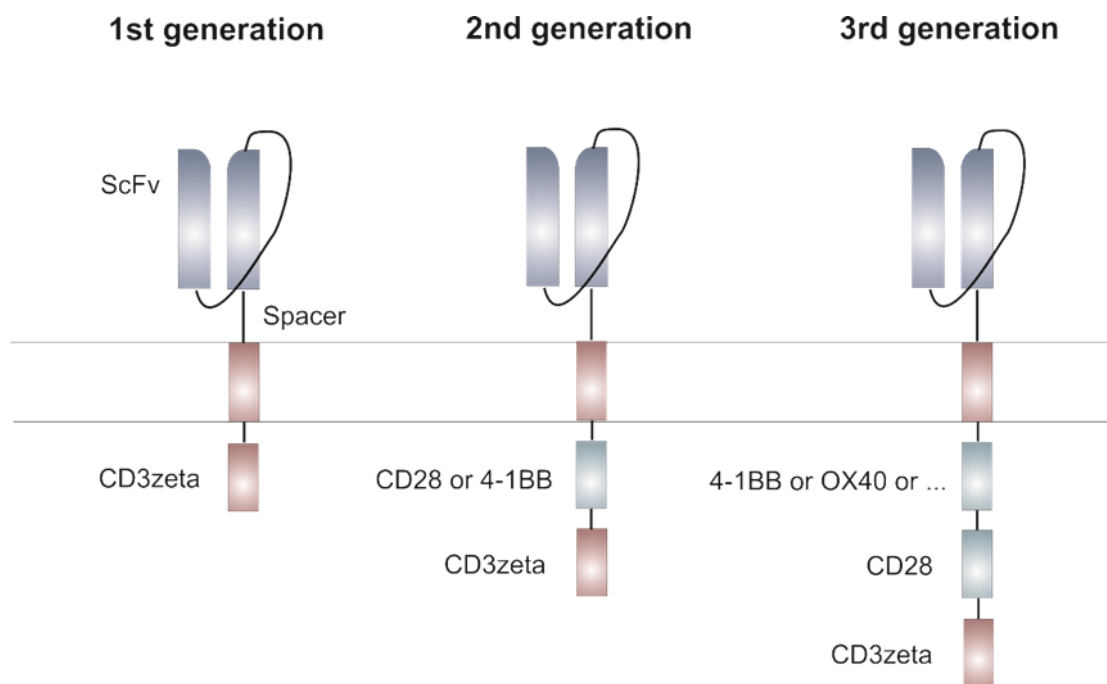


Figure 3 CAR T cell generations.

The intracellular part of first generation CARs contains only a CD3 ζ chain, whereas second generation CARs have one additional costimulatory domain like 4-1BB or CD28. Third generation CARs combine two costimulatory domains. ScFv: single chain variable fragment. Schematic illustration was kindly provided by Franziska Blaeschke.

Clinical administration

In August 2017 the FDA approved tisagenlecleucel, a second generation anti-CD19 CAR T cell therapy, for treatment of relapsed and refractory B-ALL in children and young adults^{21,22}. The European Medicine Agency (EMA) followed this example with the approval of tisagenlecleucel for the same indication in June 2018²³.

For clinical manufacturing of CAR T cells, T cells are usually collected via leukapheresis, ex vivo retro- or lentivirally transduced with the CAR, expanded for several days and reinfused to the patient (Figure 4)²⁴. Prior to CAR T cell infusion, patients receive chemotherapy inducing lymphodepletion, to enhance CAR T cell expansion and persistence *in vivo*²⁵. Significantly longer overall survival was seen in patients receiving fludarabine/cyclophosphamide regimen compared with those who received alternative regimens²⁶.

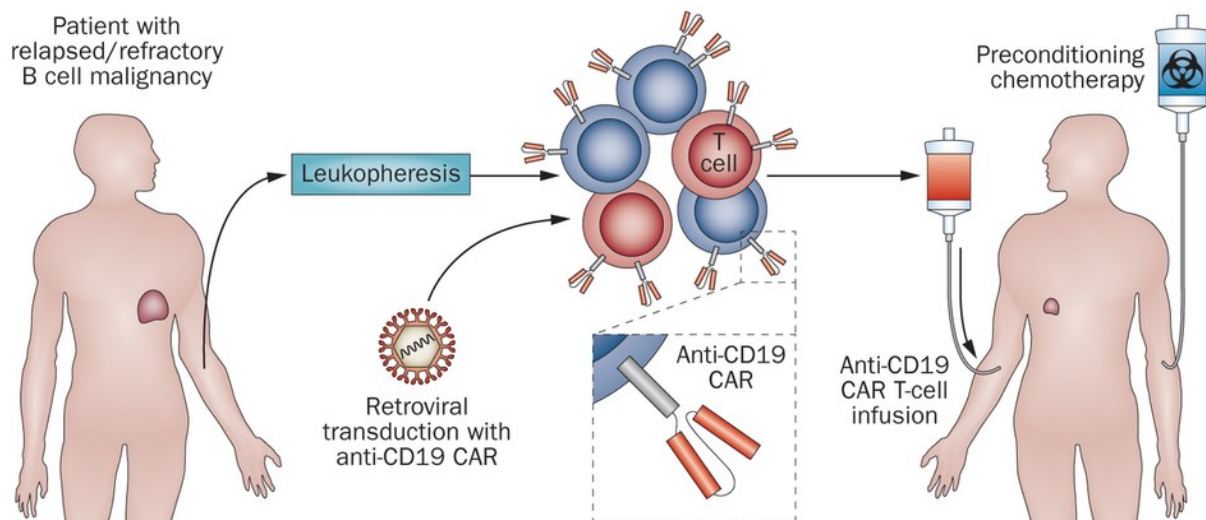


Figure 4 Clinical administration of CAR T cells.

T cells derived from patients with B cell malignancies are lenti- or retrovirally transduced with an anti-CD19 CAR. The CAR T cells are expanded in vitro and reinfused into the patient (Figure adapted from Klebanoff et al. 2014)²⁷.

While first generation CAR T cells showed no clinical efficacy, great results were achieved for second generation anti-CD19 CAR T cells in children and adults. Initial response rates of up to 90% were observed in heavily pretreated patients with CD19-positive refractory or relapsed acute lymphoblastic leukemia in several pediatric clinical trials^{26,28,29}. Recent data of a phase II study, including analysis of the efficacy and safety of tisagenlecleucel in children and young adults with B-precursor ALL revealed an overall remission rate of 81%²⁹. 95% of these patients were negative for minimal residual disease by day 28 after infusion of CAR T cells. Adverse events were experienced by nearly all patients.

CAR T cell mediated toxicities

CAR T cell mediated toxicities have been reported for all trials investigating anti-CD19 CAR T cell therapy. The most frequently reported specific toxicities are B cell aplasia, cytokine release syndrome (CRS) and neurotoxicity³⁰.

B cell aplasia is an expected on-target off-tumor side effect, which results from anti-CD19 CAR T cells eliminating non-malignant CD19⁺ B cells. Most patients receive immunoglobulin replacement in order to reduce the risk for opportunistic infections³¹.

CRS is an inflammatory response syndrome characterized by high fever, increased serum cytokines and in severe cases, hemodynamic instability, multiorgan toxicity and even death³⁰. Risk factors for severe CRS include high tumor burden (>50% marrow blasts) before initiation of therapy, spread of leukemia during lymphodepleting chemotherapy, high T-cell dose, and inflammatory processes³². The IL-6 receptor antagonist tocilizumab has been shown to ameliorate CRS, while not impairing CAR T cell functionality³⁰ and is FDA-approved for this indication³³.

CRS occurring after CAR T cell infusion is frequently accompanied by neurotoxicity characterized by headaches, delirium, aphasia, seizures and reduced consciousness²⁶. Although most neurological side effects are reversible with supportive care, severe cases of cerebral edema, followed by death have been reported³⁴.

Recently published data of murine models revealed that monocyte-derived IL-1 and IL-6 are responsible for CAR T cell-mediated CRS and neurotoxicity. IL-1 blockade by anakinra administration may successfully overcome both toxicities^{35,36}.

Limitations of CAR T cell therapy

Product manufacturing failures, lack of CAR T cell persistence and loss or modulation of target antigen can be limitations for achieving durable remission with CAR T cell therapy (Figure 5)³⁷. Patients having a T cell response against the murine part of the CAR showed restricted CAR T cell persistence³⁸. As more patients are being treated and longer follow-up data is becoming available, it was seen that approximately 30-50% of patients with CAR T cell induced remission, will suffer disease relapse^{28,39}. The majority of relapses occur within the first 12 months^{28,39}. Relapses can be divided in relapse of antigen-positive leukemia (CD19⁺) and relapse correlated with antigen loss (CD19⁻). CD19⁺ relapses are associated with insufficient CAR T cell persistence *in vivo*²⁸. So called CD19⁻ relapses can be caused by various mechanisms. CD19 antigen loss can be due to CD19 isoforms with disrupted target epitope and/or reduced surface expression, generated through alternative splicing⁴⁰. Independent of antigen loss, outgrowing of preexisting CD19⁻ malignant B cell progenitors, particularly in patients with BCR-ABL1 ALL has been reported⁴¹. Another mechanism for evading CAR T cells is lineage switching, by patients having transformation to AML following ALL-specific therapy^{42,43}. A rare case of CAR transduction into a single leukemic B cell has led to masking of CD19 on target cells and thus resulted in an escape of CAR T cell therapy⁴⁴. Recently published data of a CAR therapy relapse model in immunocompromised mice has revealed antigen-low tumor relapses due to trogocytosis of CAR T cells, an active process in which the target antigen is transferred to T cells. Reduction of antigen density on target cells has led to hampered T cell activity and to this end, escape of antigen-low tumors⁴⁵.

Remarkable results of CAR T cell therapy have been seen for CD19 positive leukemia and lymphoma. However, the extension of CAR T cells to solid cancers and targeting other surface antigens has been more difficult and is under clinical investigation³⁷.

With immunotherapy becoming a cornerstone in cancer treatment, the way has been paved for novel therapeutic options for heavily pretreated children with relapsed or refractory acute lymphoblastic leukemia. To achieve long-term overall survival, it is essential to disclose the potential interaction between leukemic and T cell, increase the CAR *in vivo* persistence and detect as well as evade possible escape mechanisms of tumor cells.

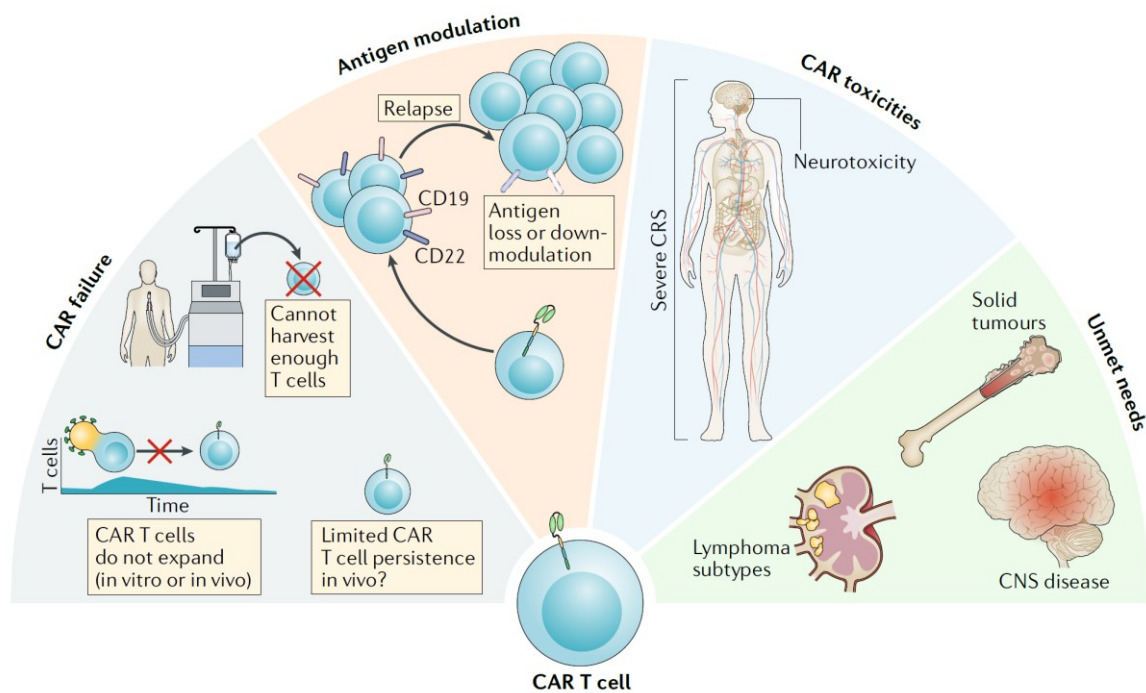


Figure 5 Limitations of CAR T cell therapy.

First, insufficient CAR T cell generation, expansion and persistence can cause CAR T cell failure. Second, antigen loss or downregulation of CD19 on malignant B cells demonstrates an escape mechanism and leads to resistance to CAR T cell therapy. Third, CAR T cell mediated toxicities can be fatal, potentially leading to reduced therapeutic benefit in patients suffering CRS and/or neurotoxicity. Finally, unmet needs, including lymphoma subtypes, solid tumors or CNS involvement remain areas of ongoing investigation to optimize response rates (Figure source: Shah et al. 2019)³⁷.

3 Aims and objectives of this study

Despite revolutionary improvements in treatment of childhood acute lymphoblastic leukemia (ALL), the potential interaction between T cells and malignant cells is not fully understood. Although ALL is considered as a low immunogenic malignancy, the role of immune checkpoints for treatment success or failure should not be underestimated. This study aims at elucidating part of these mechanisms and harnessing its therapeutic potential to improve CAR T cell therapy for pediatric ALL.

We first analyzed the immune checkpoint profile of leukemic cell lines and CAR T cells before and after activation, to get a better understanding of possible interactions. Several interaction partners were revealed that might diminish CAR T cell functionality. Here, we focused on the inhibitory molecule CTLA-4 that is expressed on T cells upon activation and its ligands CD80/CD86. Therefore, we generated CAR T cells that express a CTLA-4/CD28 fusion receptor on the cell surface. This fusion receptor is meant to convert the inhibitory CTLA-4 mediated signal into a T cell stimulation via the intracellular CD28 domain. CAR T cell constructs with and without fusion receptor were characterized by flow cytometry and compared regarding viability, expansion, transduction rate, cellular composition, phenotype as well as short and long-term functionality upon antigen contact.

With collecting *in vitro* functionality data of CAR T cells with CTLA-4/CD28 fusion receptor the foundation for future *in vivo* experiments has been laid.

4 Materials

4.1 Equipment and software

Equipment/software	Name, Manufacturer
Autoclaves	VX-55, VX-150, DX-65, Systec, Linden, Germany
Cell counting auxiliaries	Cell Counting Chamber Neubauer, Chamber Depth 0.1 mm, Paul Marienfeld, Lauda-Königshofen, Germany
Centrifuges	Multifuge X3R and Mini Centrifuge Fresco 17, Heraeus, Hanau, Germany
Cleaner Box	UVC/T-M-AR, DNA-/RNA UV-cleaner box, Biosan, Riga, Latvia
Cooling units	Cooler (4 °C) Comfort No Frost, Liebherr, Biberach an der Riß, Germany
	Cryogenic Freezer MVE 600 Series, Chart, Luxemburg
	Freezer (-20 °C) Premium No Frost, Liebherr, Biberach an der Riß, Germany
	Freezer (-86 °C) HERAfreeze HFC Series, Heraeus, Hanau, Germany
	Freezer (-86 °C) HERAfreeze HFU T Series, Heraeus, Hanau, Germany
	Thermo Scientific Cryo 200 liquid nitrogen dewar, Thermo Fisher Scientific, Waltham, Massachusetts, USA
Flow cytometer	BD FACSAria III, BD, Franklin Lakes, New Jersey, USA
	BD LSRFortessa Cell Analyzer, BD, Franklin Lakes, New Jersey, USA
	MACSQuant Analyzer 10, Miltenyi Biotec, Bergisch Gladbach, Germany
Freezing container	Nalgene Mr. Frosty, Thermo Fisher Scientific, Waltham, Massachusetts, USA
Gel Imager	Gel iX20 Imager, Intas Science Imaging, Göttingen, Germany
Heat block	Eppendorf ThermoMixer comfort, Eppendorf, Hamburg, Germany
Incubator	HERAcell 240, 150i CO ₂ Incubator, Thermo Fisher, Waltham, Massachusetts, USA
Laminar flow hood	HERAsafe, Thermo Fisher, Waltham, Massachusetts, USA
	Uniflow KR130, Uniequip, Planegg, Germany
Magnetic cell separator	MACS MultiStand, Miltenyi Biotec, Bergisch Gladbach, Germany
	MidiMACS Separator, Miltenyi Biotec, Bergisch Gladbach, Germany
	QuadroMACS Separator, Miltenyi Biotec, Bergisch Gladbach, Germany
Microscope	Axiovert 25, Carls Zeiss Microscopy, Jena, Germany
	Leica DM IL, Leica Microsysteme, Wetzlar, Germany
Spectrophotometer	Nanodrop ND-1000 spectrophotometer, Nanodrop Technologies, Wilmington, Delaware, USA
Pipettes (electrical)	Easypet 3, Eppendorf, Hamburg, Germany
Pipettes (manual)	2.5 µl, 20 µl, 200 µl, 1000 µl Eppendorf Research, Eppendorf, Hamburg, Germany
Power Supply	Biorad Power Pac 200, Biorad, Hercules, California, USA
Scale	R 200 D, Sartorius AG, Göttingen, Germany

Software	BD FACSDiva 8.0.1, BD Biosciences, Franklin Lakes, New Jersey, USA
	CorelDRAW Graphics Suite, Corel Corporation, Ottawa, Kanada
	FlowJo 10.0.7r2, Ashland, Oregon, USA
	Gel iX20 Imager Windows Version, Intas Science Imaging, Göttingen, Germany
	GraphPad PRISM 8.0, La Jolla, California, USA
	MACSQuantify, Miltenyi Biotec, Bergisch Gladbach, Germany
	Microsoft Office 2016, Redmond, Washington, USA
Thermocycler	peqSTAR 96 Universal Gradient, Isogen, Utrecht, Netherlands
Vacuum pump	Vakuumsytem BVC 21 NT, Vacuubrand, Wertheim, Germany
Water bath	LAUDA Aqualine AL 18, LAUDA-Brinkmann, Delran, New Jersey, USA

4.2 Solutions, media and sera for cell culture

Solution/ Medium/Serum	Order number	Manufacturer
100 bp DNA Ladder Ready to Load	01-11-00050	Solis BioDyne, Tartu, Estonia
Agarose	50004	Seakem Le Agarose, DMA, Rockland, Maine, USA
Albiomin 5 % infusion solution human albumin (HSA)	623 050	Biotest, Dreieich, Germany
Biocoll separating solution	L6115	Biochrom, Berlin, Germany
BLINCYTO® (Blinatumomab)	-	Amgen, Thousand Oaks, California, USA
Brefeldin A	5936	Sigma-Aldrich, Steinheim, Germany
CellTrace Violet Proliferation Kit	C34557	Invitrogen, Thermo Fisher Scientific, Life Technologies Cooperation, Eugene, Oregon, USA
Compensation beads	552843	BD Biosciences, San Diego, California, USA
	130-097-900, 130-104-693	MACS Comp Bead Kit anti mouse/anti REA, Miltenyi Biotec, Bergisch Gladbach, Germany
Dimethylsulfoxid	D5879	Honeywell, Seelze, Germany
	4720.4	Carl Roth, Karlsruhe, Germany
DMEM	FG1445	Biochrom, Berlin, Germany
DNA Clean & Concentrator -5	D4014	Zymo Research, Irvine, California, USA
DNA Gel Loading Dye (6X)	R0611	Thermo Fisher Scientific, Waltham, Massachusetts, USA
Dulbeccos phosphate buffer saline (PBS)	14190-250	Gibco, Life Technologies, Darmstadt, Germany
Ethidium bromide	2218.1	Roth, Karlsruhe, Germany
FcR Blocking Reagent	130-059-901	Miltenyi Biotec, Bergisch Gladbach, Germany
Fetal Bovine Serum	F0804	Sigma-Aldrich CHEMIE, Steinheim, Germany
Fix & Perm Cell Permeabilization Kit	GAS004	Life Technologies, Frederick, Maryland, USA
Heparin sodium 25,000 I.U./5ml		Ratiopharm, Ulm, Germany

HEPES-Buffer (1M)	L 1613	Biochrom, Berlin, Germany
Human AB serum		Human AB serum was kindly provided by Prof. R. Lotfi, University Hospital Ulm, Institute for Transfusion Medicine and German Red Cross Blood Services Baden-Württemberg—Hessen, Institute for Clinical Transfusion Medicine and Immunogenetics, both from Ulm, Germany
IL-7, IL-15 (human, premium grade)	130-95-363, 130-095-764	Miltenyi Biotec, Bergisch Gladbach, Germany
L-Glutamine 200 mM	K 0283	Biochrom, Berlin, Germany
MicroBeads (CD4, CD8, CD56)	130-045-101, 130-045-201, 130-050-401	Miltenyi Biotec, Bergisch Gladbach, Germany
Non-Essential Amino Acids	11140-035	Gibco, Life Technologies, Darmstadt, Germany
Penicillin/Streptomycin	15140-122	Gibco, Life Technologies, Darmstadt, Germany
Protamine sulfate	P3369	Sigma-Aldrich CHEMIE, Steinheim, Germany
Q5 High-Fidelity DNA Polymerase	M0491S	New England BioLabs, Frankfurt am Main, Germany
QIAamp DNA Mini Kit	51306	QIAGEN, Hilden, Germany
RetroNectin Reagent	T100A	Takara, Saint-Germain-en-Laye, France
Sodium pyruvate	11360-039	Gibco, Life Technologies, Darmstadt, Germany
Staphylococcal enterotoxin B	4881	Sigma-Aldrich CHEMIE, Steinheim, Germany
TAE Buffer	A4686	TAE buffer (50x), Applichem, Darmstadt, Germany
TexMACS GMP Medium	170-076-307	Miltenyi Biotec, Bergisch Gladbach, Germany
T cell TransAct, human	130-111-160	Miltenyi Biotec, Bergisch Gladbach, Germany
TransIT-293 Transfection Reagent	Mirumir2704	Mirus Bio LLC, Madison, Wisconsin, USA
Trypan blue	15250-061	Gibco, Life Technologies, Darmstadt, Germany
Tween 20	9127.1	Carl Roth, Karlsruhe, Germany
VLE RPMI 1640 Medium	F1415	Biochrom, Berlin, Germany

4.3 Consumables

Consumable	Order number	Name, Manufacturer
Cannula	851.638.235	Safety-Multifly-Needle, Sarstedt, Nümbrecht, Germany
Cell culture dish	664 160	Cellstar Greiner Labortechnik, Kremsmünster, Austria
Cell culture flasks with ventilation caps	83.3910.002, 83.3911.002, 83.3912.002	T25, T75, T175, Sarstedt, Nümbrecht, Germany
Cell culture multiwell plates, 6 well	657160	Cellstar Greiner Labortechnik, Kremsmünster, Austria
Cell culture multiwell plates, 24 well	3524	Costar Corning Incorporated, Corning, New York, USA
Cell culture multiwell plates, 48 well	3548	Costar Corning Incorporated, Corning, New York, USA

Cell culture multiwell plates, 96 well	163320	Nunclon Delta Surface, Thermo Fisher Scientific, Waltham, Massachusetts, USA
Compresses	18507	Gauze Compresses 10 x 10 cm, Nobamed Paul Danz, Wetter, Germany
Cover slips	C10143263NR1	Menzel-Gläser 20 x 20 mm, Gerhard Menzel, Braunschweig, Germany
FACS buffers and solutions	130-092-747, 130-092-748, 130-092-749	Running Buffer, Storage Solution, Washing Solution, Miltenyi Biotec, Bergisch Gladbach, Germany
	340345, 340346, 342003	FACS clean/rinse/flow, Becton, Dickinson and Company (BD), Franklin Lakes, New Jersey, USA
Freezing tubes	72.379	Cryo Pure Gefäß 1.8 ml, Sarstedt, Nümbrecht, Germany
Magnetic separation columns	130-042-401, 130-042-901	LS Columns, LD Columns, Miltenyi Biotec, Bergisch Gladbach, Germany
Pasteur pipettes	747720	Glass Pasteur Pipettes 230 mm, Brand, Wertheim, Germany
Pipette tips	70.1130.217, 70.760.213, 70.760.212, 70.762.211	0.1-2.5 µl, 10 µl, 20 µl, 100 µl, 2-200 µl, 1000 µl, Sarstedt, Nümbrecht, Germany
Reaction vessels	62.554.502	15 ml, Sarstedt, Nümbrecht, Germany
	4440100	50 ml, Orange Scientific, Braine-l'Alleud, Belgium
	72.690.550	1.5 ml, Sarstedt, Nümbrecht, Germany
Round bottom tubes with cell strainer snap cap	352235	5 ml Polystyrene Round Bottom Tube, Falcon, Corning Science, Taunaulipas, Mexico
Safety gloves	9209817	Vaso Nitril Blue, B. Braun Melsungen, Melsungen, Germany
Serological pipettes	86.1685.001, 86.1253.001, 86.1254.001	5 ml, 10 ml, 25ml Serological Pipette, Sarstedt, Nümbrecht, Germany
Skin disinfectant	975512, 306650	Sterilium Classic Pure, Sterilium Virugard, Hartmann, Heidenheim, Germany
Sterile filters	SE2M229104, SE2M230104	0.2µm, 0.45µm, Carl Roth, Karlsruhe, Germany
Surface disinfectant	CLN-1006.5000	Ethanol 80 % MEK/Bitrex, CLN, Niederhummel, Germany
Syringe	309658	3ml, Becton, Dickinson and Company (BD), Franklin Lakes, New Jersey, USA
	4606728V	10ml, B. Braun Melsungen, Melsungen, Germany
	4617509F	50ml, Omnifix, B. Braun Melsungen, Melsungen, Germany

4.4 Antibodies

Fluorochrome	Antigen	Clone	Order number	Manufacturer
7AAD	Viability dye		420404	Biolegend, San Diego, California, USA
APC	CD10	HI10a	312210	Biolegend, San Diego, California, USA
APC	CD14	TÜK4	130-115-559	Miltenyi Biotec, Bergisch Gladbach, Germany
APC	CD56	NCAM16.2	341027	Becton, Dickinson and Company (BD), Franklin Lakes, New Jersey, USA
APC	CD86	IT2.2	305412	Biolegend, San Diego, California, USA
APC	CD95	DX2	130-092-417	Miltenyi Biotec, Bergisch Gladbach, Germany
APC	CTLA-4	BNI3	555855	Becton, Dickinson and Company (BD), Franklin Lakes, New Jersey, USA
APC	HVEM	122	318808	Biolegend, San Diego, California, USA
APC	PD-1	EH12.2H7	329908	Biolegend, San Diego, California, USA
APC-Cy7	CD62L	DREG-56	304814	Biolegend, San Diego, California, USA
APC-Vio 770	CD8	REA734	130-110-681	Miltenyi Biotec, Bergisch Gladbach, Germany
APC-Vio770	CD3	REA613	130-113-136	Miltenyi Biotec, Bergisch Gladbach, Germany
APC-Vio770	CD4	VIT4	130-113-773	Miltenyi Biotec, Bergisch Gladbach, Germany
BB515	CD19	HIB19	564456	Becton, Dickinson and Company (BD), Franklin Lakes, New Jersey, USA
BUV395	CD3	SK7	564001	Becton, Dickinson and Company (BD), Franklin Lakes, New Jersey, USA
BUV496	CD8	RPA-T8	564804	Becton, Dickinson and Company (BD), Franklin Lakes, New Jersey, USA
BUV737	CD56	NCAM16.2	564447	Becton, Dickinson and Company (BD), Franklin Lakes, New Jersey, USA
BV421	CD137	4B4-1	309820	Biolegend, San Diego, California, USA
BV421	CD137L	5F4	311507	Biolegend, San Diego, California, USA
BV421	CD39	A1	328214	Biolegend, San Diego, California, USA
BV421	CD56	HCD56	318328	Biolegend, San Diego, California, USA
BV421	CD80	2D10	305222	Biolegend, San Diego, California, USA
BV421	CTLA-4	BNI3	369606	Biolegend, San Diego, California, USA
BV421	Galectin-9	9M1-3	348919	Biolegend, San Diego, California, USA
BV421	ICOS-L	2D3 B7-H2	564276	Becton, Dickinson and Company (BD), Franklin Lakes, New Jersey, USA
BV421	PD-1	EH12.2H7	329920	Biolegend, San Diego, California, USA
BV421	PD-L1	29E.2A3	329714	Biolegend, San Diego, California, USA

BV421	TIM-3	F38-2E2	345007	Biolegend, San Diego, California, USA
BV650	CD69	FN50	563835	Becton, Dickinson and Company (BD), Franklin Lakes, New Jersey, USA
BV650	PD-1	EH12.2H7	329950	Biolegend, San Diego, California, USA
BV785	CD95	DX2	305646	Biolegend, San Diego, California, USA
FITC	CD48	BJ40	336705	Biolegend, San Diego, California, USA
FITC	CD73	AD2	344016	Biolegend, San Diego, California, USA
FITC	Anti-c-myc	14D3	130-092-472	Miltenyi Biotec, Bergisch Gladbach, Germany
Pacific Blue	TNF- α	MAb11	502920	Biolegend, San Diego, California, USA
PE	CD112	TX31	337410	Biolegend, San Diego, California, USA
PE	CD19	LT19	130-113-169	Miltenyi Biotec, Bergisch Gladbach, Germany
PE	CD25	M-A251	356104	Biolegend, San Diego, California, USA
PE	CD45RO	UCHL1	304206	Biolegend, San Diego, California, USA
PE	CD56	REA196	170-078-057	Miltenyi Biotec, Bergisch Gladbach, Germany
PE	CD70	113-16	355104	Biolegend, San Diego, California, USA
PE	CEACAM1	ASL-32	342304	Biolegend, San Diego, California, USA
PE	IFN- γ	25723.11	340452	Becton, Dickinson and Company (BD), Franklin Lakes, New Jersey, USA
PE	LAG-3	11C3C65	369305	Biolegend, San Diego, California, USA
PE	OX40	Ber-ACT35	350003	Biolegend, San Diego, California, USA
PE	OX40-L	ik-1	558164	Becton, Dickinson and Company (BD), Franklin Lakes, New Jersey, USA
PE	TIGIT	MBSA44	12-9500-41	eBioscience/ Thermo Fisher Scientific, Waltham, Massachusetts, USA
PE-Cy7	CD155	SKII.4	337614	Biolegend, San Diego, California, USA
PE-Cy7	CTLA-4	L3D10	349914	Biolegend, San Diego, California, USA
PE-Vio 770	CD3	REA613	130-113-140	Miltenyi Biotec, Bergisch Gladbach, Germany
PE-Vio 770	CD45RO	REA611	130-113-560	Miltenyi Biotec, Bergisch Gladbach, Germany
PE-Vio 770	CD69	REA824	130-112-615	Miltenyi Biotec, Bergisch Gladbach, Germany
VioBlue	CD62L	145/15	130-098-699	Miltenyi Biotec, Bergisch Gladbach, Germany
VioGreen	CD4	REA623	130-113-230	Miltenyi Biotec, Bergisch Gladbach, Germany

5 Methods

Sections 5.1, 5.2.1, 5.2.2, 5.2.3, 5.3.1 and 5.4 to 5.7 were adapted from MD thesis of Antonia Apfelbeck: Generation and Characterization of CD19 CAR T cells with PD-1_CD28 fusion receptor (Ludwig-Maximilians-University, Munich).

5.1 CAR T cell generation

5.1.1 PBMC isolation and T cell activation

Cells were derived from 100 ml peripheral blood of healthy donors. All donors gave written informed consent before venous puncture for heparin blood collection. Peripheral blood mononuclear cells (PBMCs) were generated *via* density gradient centrifugation. Therefore, heparin blood was diluted 1:2 with PBS and carefully layered on 15 ml Biocoll. After centrifugation at 800 g for 30 minutes without brake PBMCs were aspirated. T cells were isolated using CD4 MicroBeads and CD8 MicroBeads according to the manufacturer's information. T cells were cultured in TexMACS GMP medium supplemented with 2.5% human AB serum and 12.5 ng/ml interleukins 7 and 15. Isolated T cells were activated with T cell TransAct, human as suggested in the supplier's information and washed two days after activation.

5.1.2 Virus generation

Producer cells (293Vec-RD114 cells) were previously generated for all constructs according to published literature^{46,47}. Untransduced producer cells were kindly provided by Manuel Caruso, BioVec Pharma, Québec, Canada.

Virus was harvested by aspirating supernatant of 293VEC-RD114 cells. Supernatant was filtered with a 0.45µm filter, frozen and stored at -80 °C.

For verification of the constructs a PCR followed by Sanger sequencing was performed. Therefore, genomic DNA of transduced producer cells was isolated with the QIAamp DNA Mini Kit according to the manufacturer's information. For PCR, isolated genomic DNA was amplified using Q5 High-Fidelity DNA Polymerase according to the supplier's information. The thermocycler setting consisted of initial denaturation at 98 °C for 30 seconds, 35 cycles of 98 °C for 10 seconds, 60 °C for 20 seconds and 72 °C for 60 seconds, and a final elongation step of 72 °C for 2 minutes. For electrophoresis, gel was loaded with DNA Gel Loading Dye (6X) according to the supplier's information. PCR products were concentrated and purified Bands DNA Clean and Concentrator kit according to the supplier's information and sent for Sanger sequencing (Eurofins genomics). Primer (see 11.1) and CAR sequences (see 11.2) are shown in the supplements.

5.1.3 Retroviral CAR T cell transduction

Transduction process was performed two days after T cell isolation. 24-well plates were coated with 2.5 µg RetroNectin Reagent per well either overnight at 4 °C or for 2 hours at 37 °C. Plates were blocked with 2% Albumin Fraction V in PBS for 30 minutes and afterwards washed with a 1:40 dilution of HEPES 1M in PBS. 1 ml of thawed virus supernatant was centrifuged on coated wells at 3000 g for 90 minutes at 32 °C. Supernatants were discarded and 1×10^6 T cells in 1ml TexMACS GMP medium/2.5% human AB serum + 12.5 ng/ml interleukins 7 and 15 were added per well. For untransduced control, same amount of T cells was added to RetroNectin coated wells. Plates were centrifuged at 450 g for 10 minutes at 32 °C and on day 2 after transduction T cells were washed to remove virus.

T cells were cultured in TexMACS GMP medium/2.5% human AB serum + 12.5 ng/ml interleukins 7 and 15 throughout the expansion process. Every two to three days, new medium was added to the cell culture. Expansion rate and viability was assessed every two or three days under light microscope after diluting the cells 1:2 with trypan blue. On day 12 after transduction, cells were harvested and frozen as described in 3.4.

For characterization of the final product, cellular composition, phenotype and transduction rate was analyzed by flow cytometry on day 12 after transduction by staining for CD3, CD4, CD8, CD56, CTLA-4, c-myc, CD14, CD19, for CD62L, CD45RO and CD95.

T cell phenotype was determined as follows: T_N : CD62L⁺, CD45RO⁻, CD95⁻; T_{SCM} : CD62L⁺, CD45RO⁻, CD95⁺; T_{CM} : CD62L⁺, CD45RO⁺, CD95⁺; T_{EM} : CD62L⁻, CD45RO⁺, CD95⁺; T_{EFF} : CD62L⁻, CD45RO⁻, CD95⁺.

5.2 Functionality assays

For functionality assays all T cell conditions were adjusted to the lowest transduction rate within the donor, which was determined on day 12 after transduction, by adding untransduced T cells. The effector count was calculated on the number of CAR⁺ T cells for every condition.

5.2.1 Checkpoint expression assay

Before CAR T cells were frozen, checkpoint surface expression was evaluated by flow cytometry. T cells were stained for CTLA-4, TIGIT, LAG-3, PD-1, TIM-3, 4-1BB, OX40 and CD69. All panels included CD3, CD8, CD56, CD62L, CD45RO, CD95 and c-myc to identify T cell subsets. Cells were co-cultured with CD19⁺ K562 cells and CD19⁺ CD80⁺ CD86⁺ K562 cells for 48 hours at an effector to target ratio of 1:1. For evaluation of the initial surface expression of the checkpoints, T cells without target cell co-culture were stained.

5.2.2 Cytotoxicity assay

On day 13 after transduction NK(T) cells were depleted with CD56 MicroBeads according to the supplier's information. In a FITC c-myc single stain the transduction rate was reevaluated and all conditions were adjusted to the lowest transduction rate within the donor by adding untransduced cells. K562 cells were used as target cells, labeled according to CellTrace Violet cell Proliferation Kit and co-cultured with CAR T cells at different effector to target ratios. Cells were co-cultured for 48 hours. Effector count was calculated on the number of CAR⁺ T cells. Absolute cell count of CellTrace Violet positive cells was measured and killing rate was calculated with following formula: $100 - (100 / \text{targets only} * \text{targets left in co-culture})$. "Targets only" describes target cell lines without co-cultured effector cells and were used as reference. Experiments were performed in technical duplicates and measured on a MACSQuant Analyzer 10.

5.2.3 Intracellular cytokine stain (ICS)

For ICS, either T cells on day 13 after transduction or thawed T cells were used. In the latter case CAR T cells were thawed and rested in TexMACS GMP medium/2.5% human AB serum + 12.5 ng/ml interleukin 7 and 15 for 2 to 10 hours. T cells were co-cultured with target cells at a 1:1 ratio for 24 hours. For positive control, T cells were stimulated with 1 µg/ml Ionomycin and 1 µg/ml phorbol 12-myristate 13-acetate (PMA) 22 hours after co-culture. 24 hours after co-culture, 10 µg/ml Brefeldin A was added. Stimulation was stopped with cold PBS 26 hours after co-culture and T cells were washed. T cells were stained for CD3, CD4, CD8, CD56 and c-myc to identify T cell subsets. Intracellular stain for IFN-γ and TNF-α was performed with Fix & Perm cell Fixation & Permeabilization Kit according to the supplier's information.

5.2.4 Proliferation assay

For proliferation assay, thawed or fresh T cells and K562 cells were used. Thawed T cells were rested for two hours in TexMACS GMP medium/2.5% human AB serum + 12.5 ng/ml interleukin 7 and 15. T cells were labeled according to CellTrace Violet cell Proliferation Kit and co-cultured with target cells at a 1:1 ratio for 72 hours. An SEB positive control (final concentration 10 µg/ml) was performed. T cells cultured without target cells were used as negative control. For proliferation assay with blinatumomab, 500 pg/ml blinatumomab was added to co-culture. Cells were stained for CD19, CD3, CD4, CD8 and c-myc. Experiments were performed in technical triplicates.

5.2.6 Activation assay with blinatumomab

The activation capacity of T cells was measured through surface expression of activation markers on T cells. Fresh T cells and K562 cells were co-cultured at a 1:1 ratio for 24 hours. 500 pg/ml blinatumomab was added at time point of co-culture, to enable an interaction between T cells and target cells in absence of the CAR. T cells were stained for 4-1BB, CD69 and CD25, additionally to CD3, CD4 and CD8. Initial surface expression was measured by staining of T cells without co-culture. T cells co-cultured with target cells in the absence of blinatumomab served as controls. Experiments were performed in technical triplicates and evaluated *via* flow cytometry.

5.2.7 Long-term assay

T cells were thawed and rested overnight in TexMACS GMP medium/2.5% human AB serum + 12.5 ng/ml interleukin 7 and 15. For cytotoxicity measurement, T cells were treated as described in 3.2.2 and incubated with CD80⁺ CD86⁺ Daudi cells at an effector to target ratio of 0.2:1, for ICS at a ratio of 1:1. Every three to four days T cells were re-stimulated with Daudi cells over a period of 19 days. 24 hours after the first, fourth and sixth stimulation extracellular stain for CD3, CD25, CTLA-4, PD-1 and intracellular stain for IFN- γ and TNF- α was conducted according to 5.2.3. Cytotoxicity assay was performed 24 hours after each stimulation. Experimental setting is shown in the results section (Figure 16). Absolute cell count of CellTrace Violet positive Daudi cells was detected by flow cytometry and killing rate was calculated with formula explained in 5.2.2. Experiments were performed in technical triplicates.

5.3 Generation and characterization of target cell lines

5.3.1 Transduction of cell lines

CD19_pMP71/ CD80_pMP71/ CD86_pMP71 and helper plasmids MLV env (pALF-10A1-env) and MLV gag/pol (pcDNA3.1-MLV-g/p) were transfected into HEK 293T cells using TransIT-293 Transfection Reagent according to the supplier's information. Helper plasmids were kindly provided by Sebastian Kobold, Department of Clinical Pharmacology, Ludwig-Maximilians-University of Munich. Vector map of pcDNA3.1-MLV-g/p is shown in the supplements (see 11.3.2) and pALF-10A1 is described in Stitz et al.⁴⁸. Vector pMP71 was kindly provided by Christopher Baum, Department of Experimental Hematology, Hannover Medical School, and a vector map is shown in the supplements (see 11.3.1). After 48 hours, viral supernatant was harvested and used for transduction of K562 and Daudi cells. 24-well plates were coated with 2.5 μ g RetroNectin reagent overnight at 4 °C. Plates were blocked with 2% Albumin Fraction V in PBS for 30 minutes and washed with a 1:40 dilution of HEPES 1M in PBS.

Virus supernatant was centrifuged at 500 g for 5 minutes at 32 °C and filtered with a 0.45 µm filter. 1 ml of virus supernatant was centrifuged on coated wells at 3000 g for 90 minutes at 32 °C. Supernatant was discarded and 1×10^6 K562 and Daudi cells in RPMI + 10% fetal bovine serum (FBS) + 1% penicillin streptomycin + 1% L-glutamine were added per well. 4 µg of protamine sulfate and 1% HEPES 1M were added. On day 2 after transduction, cells were washed to remove virus. Cells were sorted for CD19⁺ CD80⁺ CD86⁺ K562 and CD80⁺ CD86⁺ Daudi cells at a FACSAria III and cultured in RPMI + 10% fetal bovine serum (FBS) + 1% penicillin/streptomycin + 1% L-glutamine.

5.3.2 Immune checkpoint profile of cell lines

Checkpoint expression on target cell lines Raji, Nalm-6, Nalm-16, Jeko, Daudi and K562 was analyzed by flow cytometry. Cell lines were seeded at 1×10^6 cells per ml in RPMI + 10% fetal bovine serum (FBS) + 1% penicillin/streptomycin + 1% L-glutamine and stimulated with 10 ng/ml TNF-α and 100 ng/ml IFN-γ. Unstimulated cells served as control. After 48 hours cells were stained for ICOS-L, CD48, OX40-L, 4-1BBL, CD70, 4-1BB, CD86, CD80, HVEM, TIM-3, LAG-3, PD-L1, Galectin-9, CD155, CD73, CEACAM1, CD39 and CD112. To prevent unspecific antibody binding, FcR blocking was performed prior to staining. Analyses were performed *via* flow cytometry.

5.4 General cell culture

Cells were cultured at 37 °C with 5% CO₂.

Cell lines were cultured in RPMI + 10% fetal bovine serum (FBS) + 1% penicillin/streptomycin + 1% L-glutamine and splitted at least every five days in a 1:10 ratio. Identity of cell lines was verified by STR analysis regularly.

Cell lines were frozen in RPMI + 20% fetal bovine serum (FBS) + 1% penicillin/streptomycin + 1% L-glutamine containing 10% dimethyl sulfoxide (DMSO). Primary T cells were frozen in 5% human serum albumin (HSA) containing 10% DMSO. After cells were frozen in a freezing container at -80 °C, they were transferred to liquid nitrogen (-179° C) for preservation.

For thawing, cells were rapidly warmed in the water bath, transferred to prewarmed RPMI medium and washed in TexMACS GMP medium.

5.5 Flow cytometry

Antibodies for flow cytometry staining were titrated prior to use. PBS + 1% fetal bovine serum (FBS) was used as staining buffer. Cells were stained for 10 minutes at 4 °C and washed once with buffer. For stains with K562 cells, Fc receptor block was used according to the manufacturer's information. Except for the checkpoint expression assay, all measurements were performed at a MACSQuant Analyzer 10. Checkpoint expression assay was measured at a BD LSRFortessa Cell Analyzer.

5.6 Software

Flow cytometry data was analysed using FlowJo 10.

Schematic illustrations in Figure 2, Figure 3, and Figure 10A were created with CorelDRAW and kindly provided by Franziska Blaeschke.

Graphs were created with GraphPad Prism 8.

5.7 Statistical analysis

Statistics were performed with GraphPad Prism 8. Statistical differences between experimental conditions were examined using paired Student's t test for experiments with $n \geq 3$ individual donors and unpaired t test for experiments with $n < 3$ donors in technical triplicates and for checkpoint staining on target cell lines. A p value of < 0.05 indicates significant (*), < 0.01 very significant (**), and < 0.001 extremely significant (***) differences. Mean and standard error mean is shown unless stated otherwise.

6 Results

6.1 Checkpoint profiles of leukemic cells and T cells upon stimulation

To gain a better understanding of the interaction between leukemic cells and T cells, several leukemic and control cell lines were stained for stimulatory (ICOS-L, CD48, OX40-L, 4-1BBL, CD70, 4-1BB), bivalent (CD80, CD86) and inhibitory (HVEM, TIM-3, LAG-3, PD-L1, Galectin-9, CD155, CD73, CD112) surface markers in at least three independent experiments.

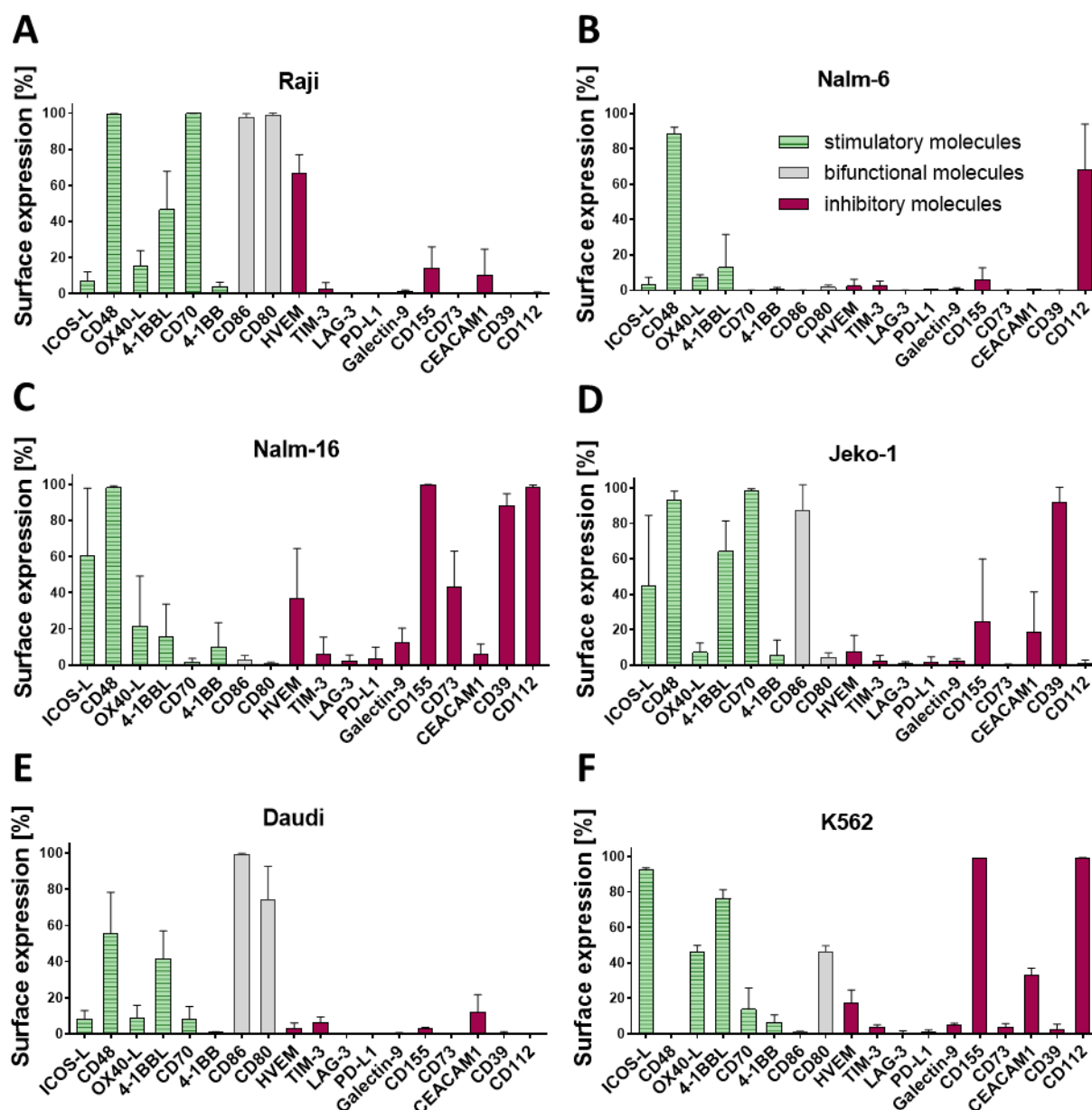


Figure 6 Checkpoint profile of leukemic and control cell lines.

Flow cytometry analysis of stimulatory and inhibitory surface molecules on Raji (A), Nalm-6 (B), Nalm-16 (C), Jeko-1 (D), Daudi (E) and K562 (F) cells showed differing checkpoint profiles on the tested leukemic and control cell lines (n=3). Further explanations on co-stimulatory and co-inhibitory immune checkpoints can be found in Table 1.

Different checkpoint profiles for the tested cell lines could be detected. Raji (Figure 6A) and Jeko-1 cells (Figure 6D) showed a more stimulatory profile, while Nalm-16 (Figure 6C) expressed mainly inhibitory molecules. For Nalm-6 (Figure 6B), Daudi (Figure 6E) and K562 cells (Figure 6F) a balanced ratio of stimulatory and inhibitory checkpoint markers was observed.

Table 1 Overview of co-stimulatory and co-inhibitory surface molecules regulating T-cell responses (Table adapted from Feucht et al. 2016)¹⁴

Molecule	Synonyme	Cellular Expression	Ligand	Main function
ICOS-L	CD275	B, T, NKT, monocytes	ICOS	stimulation
CD48	-	B, T, NK, DC, monocytes, macrophages, mast cells granulocytes	CD2 CD244	stimulation
OX40-L	CD134	B, T, DC, macrophages	OX40	stimulation
4-1BBL	CD137L	B, T, DC, monocytes, macrophages	CD137	stimulation
CD70	CD27L	B, T, DC	CD27	stimulation
4-1BB	CD137	B, T, DC, NK, granulocytes	4-1BBL	stimulation
CD86	B7.2	B, T, DC, monocytes, macrophages, mast cells	CD28 CTLA-4	stimulation inhibition
CD80	B7.1	B, T, DC, monocytes, macrophages, mast cells	CD28 CTLA-4 PD-L1	stimulation inhibition inhibition
HVEM	CD270	B, T, DC	BTLA CD160 HSVgD	inhibition inhibition inhibition
TIM-3	CD366	T, NK, DC, monocytes, macrophages	Galectin-9 PtdSer HMGB1 CEACAM1	inhibition inhibition inhibition inhibition
LAG-3	CD223	T, NK	MHC-II LSEctin	Inhibition inhibition
PD-L1	B7-H1; CD274	B, T, NK, DC, monocytes, macrophages, mast cells	PD-1 CD80	inhibition inhibition
Galectin-9	-	T, DC, granulocytes	TIM-3	inhibition
CD155	PVR	monocytes	CD226 TGIT	inhibition inhibition
CD73	NT5E	B, T, NK	ATP ADP	Inhibition inhibition
CEACAM1	CD66a	B, T, DC, macrophages		inhibition
CD39	ENTPD1	B, T, DC, monocytes, macrophages	ATP ADP	Inhibition inhibition
CD112	Nectin-2	monocytes	CD226	inhibition

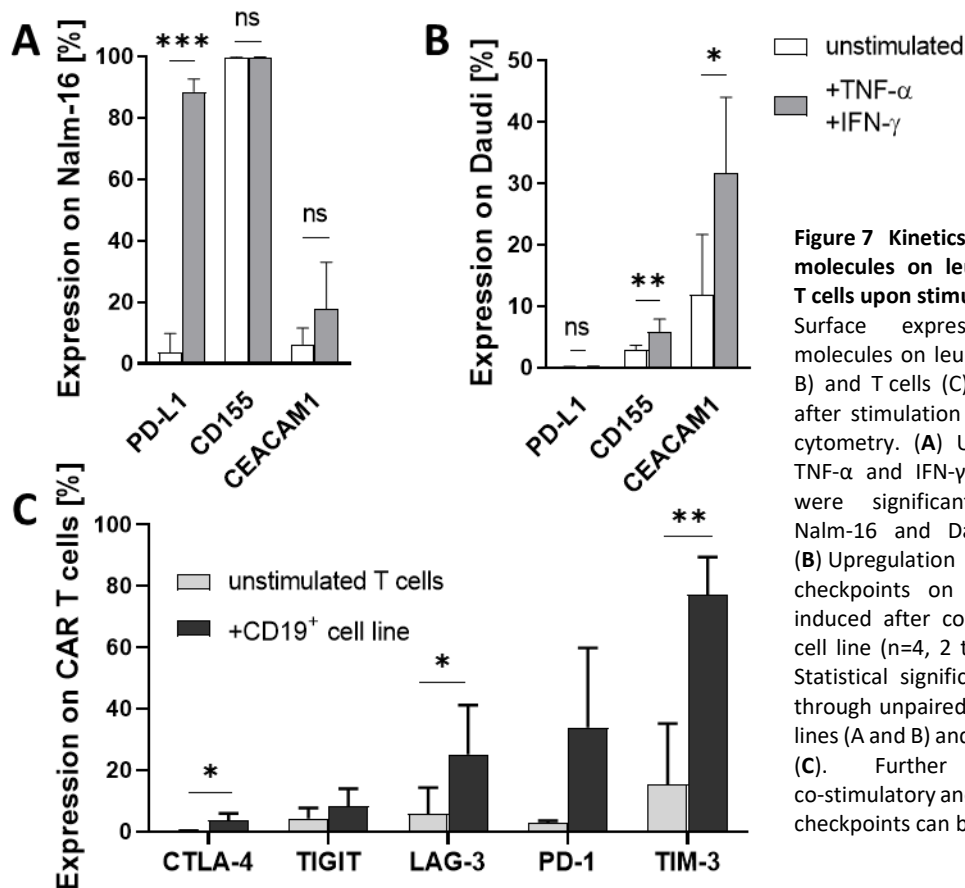


Figure 7 Kinetics of inhibitory molecules on leukemic cell lines and T cells upon stimulation.

Surface expression of inhibitory molecules on leukemic cell lines (A and B) and T cells (C) before and 48 hours after stimulation was detected by flow cytometry. (A) Upon stimulation with TNF- α and IFN- γ , inhibitory molecules were significantly upregulated on Nalm-16 and Daudi cell lines ($n \geq 3$). (B) Upregulation of inhibitory checkpoints on CAR T cells could be induced after co-culture with a CD19⁺ cell line ($n=4$, 2 two biological donors). Statistical significance was determined through unpaired multiple t test for cell lines (A and B) and paired t test for T cells (C). Further explanations on co-stimulatory and co-inhibitory immune checkpoints can be found in Table 1.

To mimic the influence of tumor and T cell interaction, cell lines were incubated with the inflammatory T_{H1} cytokines IFN- γ and TNF- α for 48 hours. Cells were stained for the same checkpoints as described above. Most notably, inhibitory markers like CD155 (mean 2.8% upregulated to 5.9%; $p=0.030$) and CEACAM1 (mean 11.9% upregulated to 31.7%; $p=0.045$) on Daudi cells (Figure 7B) were significantly upregulated after stimulation. The mean surface expression of PD-L1 on Nalm-16 cells (Figure 7A) increased remarkably from 3.8% to 88.5% ($p=0.0004$) upon stimulation. Expression levels of all other co-inhibitory and co-stimulatory molecules showed no significant differences compared to unstimulated cells (data not shown).

To investigate changes in checkpoint profile of CAR T cells upon activation, first generation CAR T cells (19_3z) were co-cultured with CD19⁺ K562 cells. CTLA-4, TIGIT, LAG-3, PD-1 and TIM-3 surface expression on T cells was measured before and 48 hours after incubation with the cell line. A significant increase in mean surface expression of the inhibitory markers CTLA-4 (0.3% to 3.9%; $p=0.048$), LAG-3 (5.9% to 25.2%; $p=0.041$) and TIM-3 (15.5% to 77.2%; $p=0.004$) was observed (Figure 7C).

These results indicate that leukemic cell lines have differing profiles of stimulatory and inhibitory surface molecules that are subject to stimulation, while CAR T cells respond with an overexpression of inhibitory markers upon target cell contact.

6.2 CTLA-4 overexpression leads to reduced T cell functionality

To detect the impact of CTLA-4 on anti-leukemic T cell response, T cells were overexpressed with CTLA-4 and stimulated with either CD19⁺ or CD19⁺ CD80⁺ CD86⁺ K562 cells. Blinatumomab was added to the co-culture, enabling an interaction between T cells and target cells. For evaluation fold change of proliferating cells treated with or without blinatumomab was calculated.

The proliferative potential of T cells was significantly decreased due to CTLA-4 overexpression, when being co-cultured with CD19⁺ (p<0.0001) and CD19⁺ CD80⁺ CD86⁺ K562 cells (p=0.006) (Figure 8).

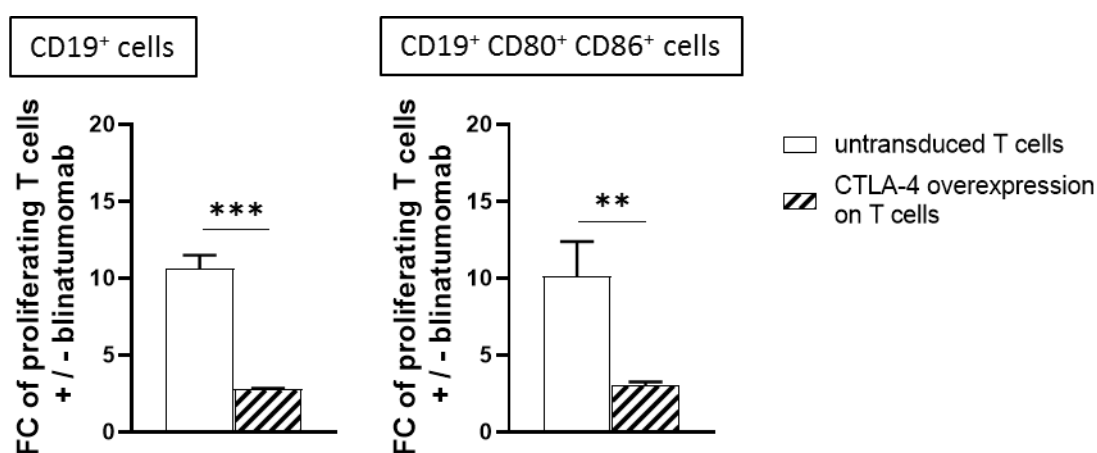


Figure 8 Inhibitory effect of CTLA-4 on proliferative potential of T cells upon target recognition induced by blinatumomab. Proliferative potential of T cells was determined via flow cytometry 72 hours after co-culture. Evaluation was performed by calculation of the fold change of proliferating T cells treated with and without blinatumomab. T cells with CTLA-4 overexpression showed decreased proliferative capacity, when being co-cultured with CD19⁺ K562 cells (left) and CD19⁺ CD80⁺ CD86⁺ K562 cells (right) (n=3, technical replicates of one donor). Statistical significance was determined through unpaired t test. *P<0.05, **P<0.01, ***P<0.001. FC: fold change.

Surface expression of activation markers 4-1BB and CD25 was measured before and after contact with CD19⁺ and CD19⁺ CD80⁺ CD86⁺ target cells, to compare activation potential of T cells with and without CTLA-4 overexpression. A decrease in 4-1BB expression was detectable on CTLA-4 overexpressing T cells after co-culture with both cell lines (Figure 9B and E). Changes in CD25 surface expression remained small.

Next, it was tested whether this effect could be recapitulated in CAR T cells. For this purpose, CTLA-4 was retrovirally overexpressed in conventional first (19_3z vs. 19_3z_CTLA) and second generation (19_BB_3z vs. 19_BB_3z_CTLA) CAR T cells (Figure 9A). Second generation CAR T cells additionally contained an intracellular 4-1BB domain.

Decreased expression levels of 4-1BB and CD25 were observed in first generation CAR T cells with CTLA-4 overexpression, regardless of the presence of its ligands CD80 and CD86 on target cell surface (Figure 9C and F). Comparable effects were seen in second generation CAR T cells overexpressing CTLA-4 (Figure 9D and G).

Collectively, it could be shown that the overexpression of CTLA-4 on T cells and CAR T cells significantly limited both, proliferation and activation potential upon target cell contact.

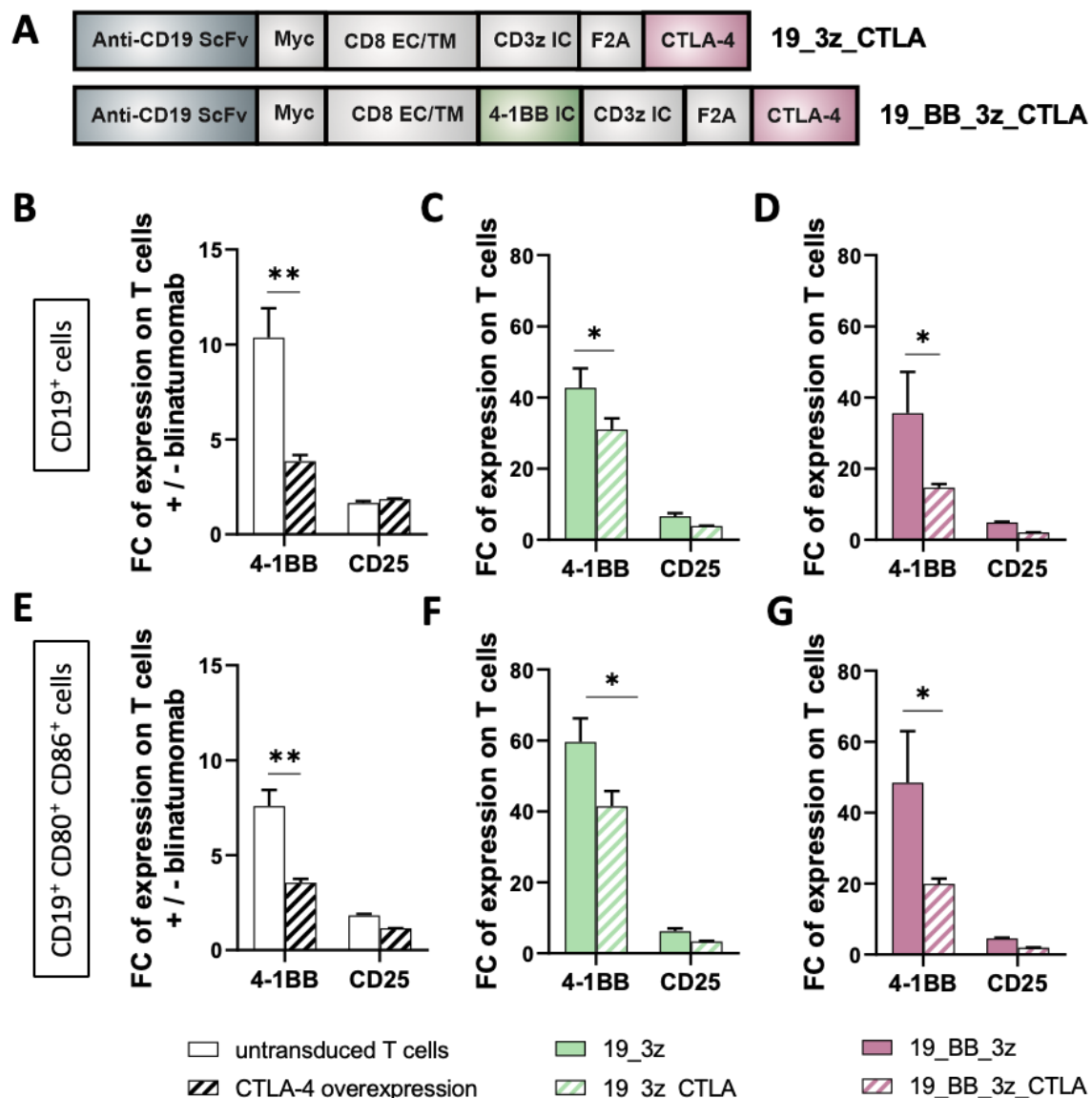


Figure 9 Reduced activation capacity due to CTLA-4 overexpression on wildtype and CAR T cells.

(A) Schematic structure of first and second generation CAR constructs with CTLA-4 overexpression. (B-G) Surface expression of activation markers 4-1BB and CD25 was detected by flow cytometry 24 hours after co-cultivation with CD19⁺ K562 cells (upper row) and CD19⁺ CD80⁺ CD86⁺ K562 cells (bottom row). (B and E) The presence of CD19⁺ target cells and blinatumomab resulted in a reduced surface expression of activation markers on CTLA-4 overexpressing T cells. (C and F, D and G) Decreased expression of 4-1BB and CD25 was observed in first generation (C and F) and second generation (D and G) CAR T cells overexpressing CTLA-4. Fold changes were calculated on cells with and without target cell contact (n=3, technical replicates of one donor). Schematic illustration was kindly provided by Franziska Blaeschke. Statistical significance was determined through unpaired t test. FC: fold change.

6.3 Generation of anti-CD19 CAR T cells with CTLA-4/CD28 fusion receptor is feasible

To circumvent the suppressing effect of CTLA-4 on CAR T cells, a bi-cistronic construct was designed. The construct consisted of a conventional first generation CAR connected to a CTLA-4/CD28 fusion receptor (Figure 10A). Equimolar translation of two separate proteins (CAR and fusion receptor) was mediated by an F2A linker. The fusion receptor contained the extracellular and transmembrane domain of CTLA-4 fused to the intracellular domain of CD28, which is meant to turn the inhibitory CTLA-4 signal into CD28-mediated T cell stimulation (19_3z_CTLA_28).

All CAR constructs were designed in collaboration with Sebastian Kobold (Department of Clinical Pharmacology, Ludwig-Maximilian-University of Munich) and Franziska Blaeschke. Virus supernatant producing cells were generated in our facility and used for retroviral transduction of CAR T cells. First generation CAR (19_3z) consisted of an anti-CD19 single chain variable fragment, a c-myc tag for flow cytometry based CAR detection, a CD8 extracellular and transmembrane domain and an intracellular CD3 ζ chain. Second generation CAR (19_BB_3z) additionally contained a costimulatory molecule (4-1BB) in the intracellular compartment. 19t served as a negative control since it lacked the CD3 ζ chain and therefore did not provide a signal to T cells. A schematic overview of the tested CAR constructs is given below (Figure 10A).

T cells were successfully transduced two days after activation. Twelve days after transduction, a mean transduction rate of 85% (range 75.6 to 92.9%) for 19_3z, 76% (range 59.1 to 90.0%) for 19_3z_CTLA_28 and 79% (range 43.2 to 78.7%) for 19_BB_3z was achieved (Figure 10B). The surface expression of CTLA-4 was significantly higher on the fusion receptor CAR and correlated with the CAR expression (Figure 10C and D). This led to the assumption that the CTLA-4 expression on 19_3z_CTLA is mediated by the CTLA-4/CD28 fusion receptor, while CTLA-4 expression on 19_3z shows the amount of endogenous CTLA-4 expression. Exemplary FACS plots of one donor showing the co-expression of CAR and CTLA-4/CD28 fusion receptor extra- and intracellularly can be seen in Figure 10D.

T cells were generated and cultivated for 14 days in total. Throughout the generation process, a mean viability of 94.8% was observed (Figure 11A). On day twelve after transduction, CAR T cells reached expansion rates of nearly 100 fold (Figure 11B). Phenotypical analyses of the end product revealed a mainly stem-cell and central memory like phenotype with no significant differences between the tested CAR constructs (Figure 11C). After PBMC isolation followed by T cell separation and cultivation for 14 days, a pure T cell product with 67.9% CD4+, 21.7% CD8+, 3.0% CD4+ CD8+ and 7.1% natural killer T cells could be generated for first generation CAR T cells with CTLA-4/CD28 fusion receptor (Figure 11D). Other tested constructs showed no significant differences in cellular composition (data not shown).

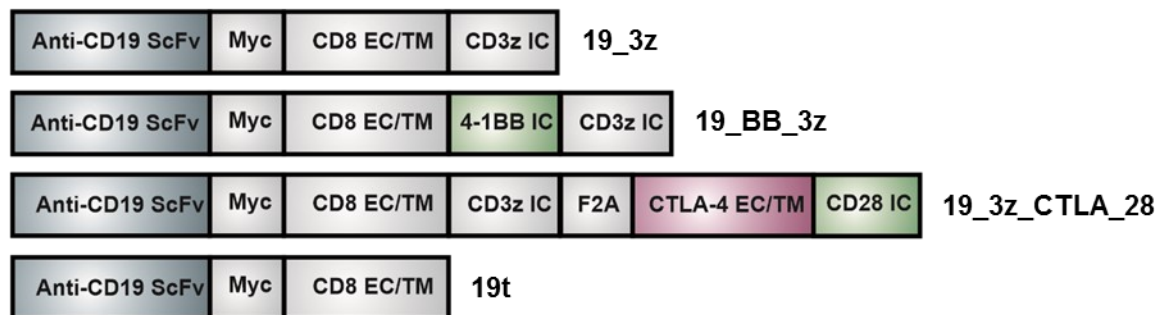
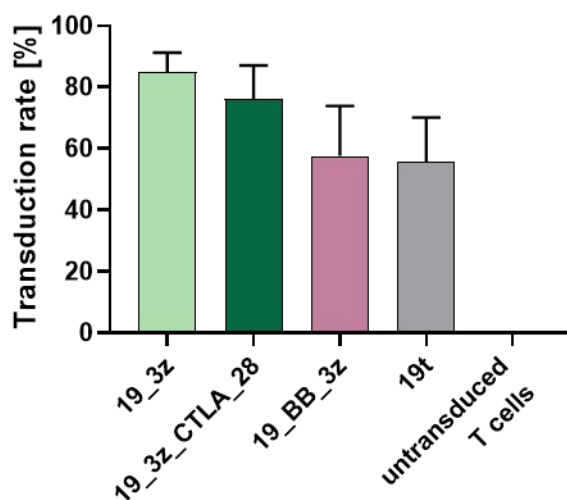
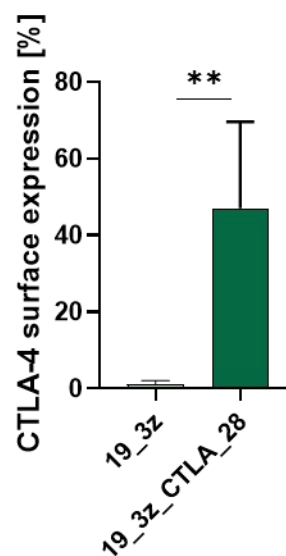
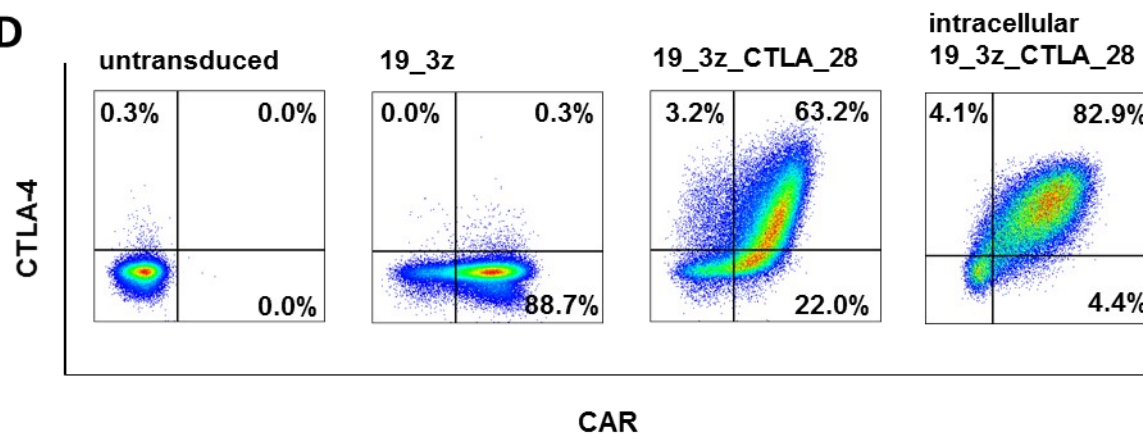
A**B****C****D**

Figure 10 Retroviral transduction of CAR T cells with CTLA-4/CD28 fusion receptor.

(A) Schematic structure of tested CAR constructs. 19t served as a negative control since it lacks the CD3 ζ chain. (B and C) Transduction rates of CAR and CTLA-4/CD28 fusion receptor were detected by flow cytometry 12 days after transduction ($n \geq 4$ individual donors). Statistical significance was determined through paired t test. (D) Representative FACS plots of one donor show simultaneous expression of CAR and CTLA-4 on T cells extra- and intracellularly. Schematic illustration was kindly provided by Franziska Blaeschke. ScFv: single chain variable fragment, EC: extracellular, TM: transmembrane, IC: intracellular.

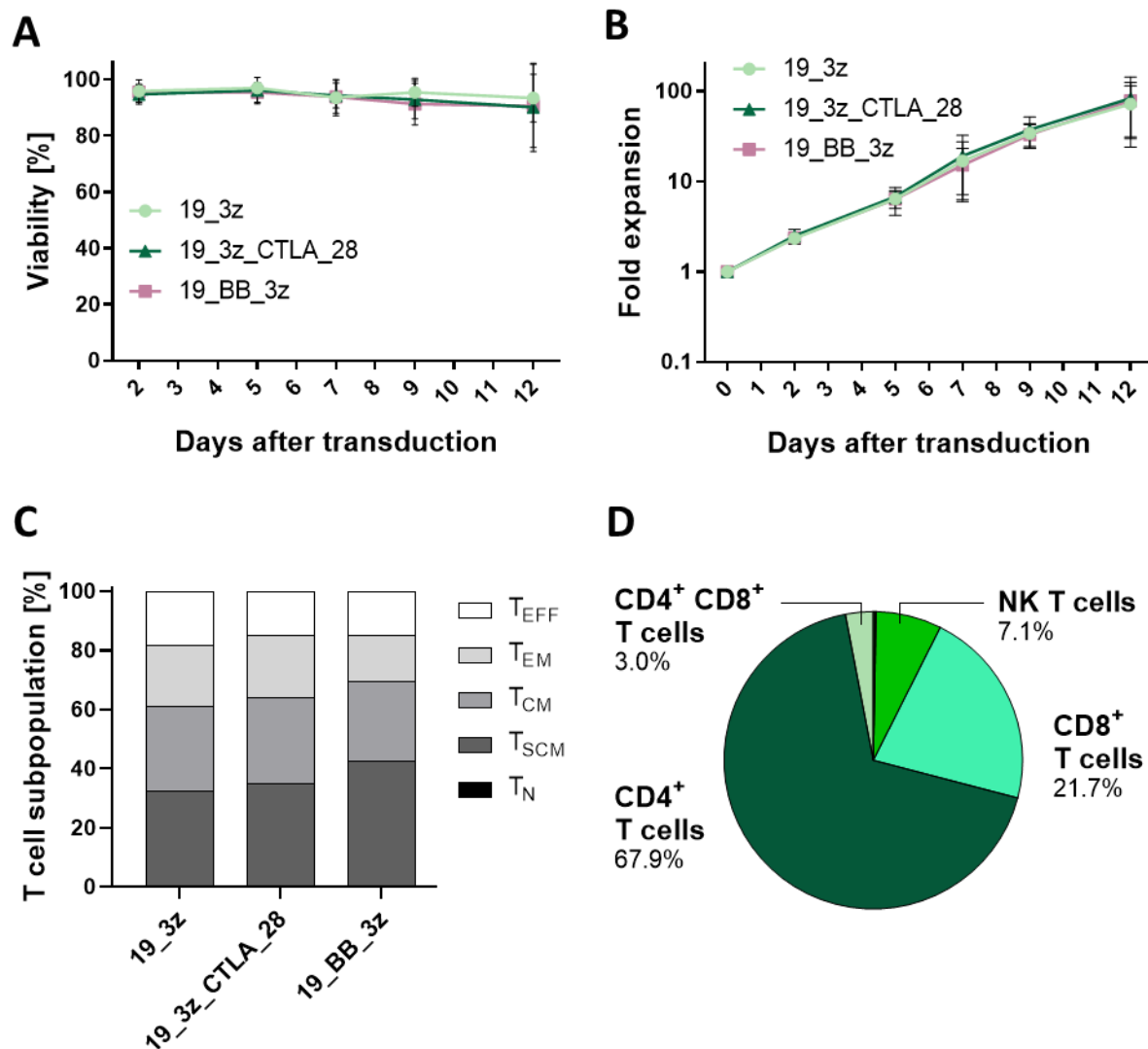


Figure 11 Characterization of CAR T cells with CTLA-4/CD28 fusion receptor.

Viability and expansion of CAR T cells were evaluated through cell count by trypan blue staining every two to three days. Phenotypical analyses and cellular composition were determined by flow cytometry. **(A)** A mean viability of 94.8% for all tested constructs could be achieved ($n \geq 3$, individual donors). **(B)** First generation CAR, first generation CAR with CTLA-4/CD28 fusion receptor and second generation CAR T cells reached expansion rates near 100 fold. **(C)** All CAR T cell products showed a mainly stem cell-like and central memory like phenotype on day 12 after transduction. No significant differences between the tested constructs were detected. T cell subsets were determined by analysis of CD62L, CD45RO and CD95 expression ($n \geq 3$, individual donors). **(D)** 12 days after transduction a pure CD4-dominant T cell product was observed. Pie chart exemplarily shows cellular composition of first generation CAR T cells with CTLA-4/CD28 fusion receptor. Other tested CAR constructs did not differ significantly (data not shown) ($n \geq 3$, individual donors). Paired t test was performed to evaluate statistical significance. T_N: naïve T cells, T_{SCM}: stem cell-like memory T cells, T_{CM}: central memory T cells, T_{EM}: effector memory T cells, T_{EFF}: Effector T cells. NK T cells: Natural killer T cells.

The production of first and second generation CAR T cells, as well as first generation CAR T cells with CTLA-4/CD28 fusion receptor was feasible. High viability and expansion rates were achieved during the production process. Analyses of the final products' subpopulations and cellular composition revealed comparable characteristics for all tested CAR T cell constructs.

6.4 CAR T cells with CTLA-4/CD28 fusion receptor show high CD19-specific functionality

To study the functionality of the newly designed first generation CAR T cells with CTLA-4/CD28 fusion receptor, co-culture assays with CD19⁺ K562 and CD19⁻ wildtype K562 cells were performed.

Phenotypical analyses revealed a shift from central memory like towards a more mature T cell phenotype with significantly higher amounts of effector memory ($p=0.083$) and effector T cells ($p=0.022$) 48 hours after antigen recognition (Figure 12A).

CAR T cells with CTLA-4/CD28 fusion receptor were able to produce cytokines upon CD19⁺ target cell contact. After 24 hours a mean of 44.1% IFN- γ positive and 20.3% TNF- α positive CAR T cells were detectable. This effect was CAR specific, since secretion of both cytokines was significantly lower (IFN- γ $p=0.023$, TNF- α $p=0.004$) when co-cultured with CD19⁻ target cells (Figure 12B).

The surface expression of activation markers 4-1BB and CD69 was significantly increased (4-1BB up to 66.9 fold, $p=0.010$; CD69 up to 25.0 fold, $p=0.038$) after 48 hours of co-culture with CD19⁺ cells compared to unstimulated T cells (Figure 12C).

High proliferative potential of CAR T cells upon antigen recognition could be shown (Figure 12D). 72 hours after co-culture with CD19⁺ target cells a mean of 87.5% of all T cells within the 19_3z_CTLA_28 population compared to only 3.2% in untransduced T cells started to proliferate. This effect was CAR mediated, since gating on proliferating subsets revealed that a mean of 93.8% were CAR⁺ and only 7.8% CAR⁻ T cells ($p<0.0001$).

After being co-cultured for 48 hours at several E:T ratios, CAR T cells with CTLA-4/CD28 fusion receptor showed an E:T ratio dependent cytotoxic capacity. Mean killing rates of 73.1% could be achieved for a 1:1 E:T ratio, while for the 19t control only 15.7% was seen ($p=0.002$). The specificity of this effect was shown by co-culturing the 19_3z_CTLA_28 CAR T cell with CD19⁻ target cells. In absence of CD19 on target cells CAR T cells with CTLA-4/CD28 fusion receptor showed a significantly decreased mean cytotoxic effect of 26.2% for 1:1 ($p=0.006$) and 4.9% for 0.1:1 ($p=0.045$) E:T ratio.

In summary, CD19-specific functionality of the newly designed first generation CAR with CTLA-4/CD28 fusion receptor could be demonstrated including cytokine secretion as well as activation, proliferation and cytotoxic capacity.

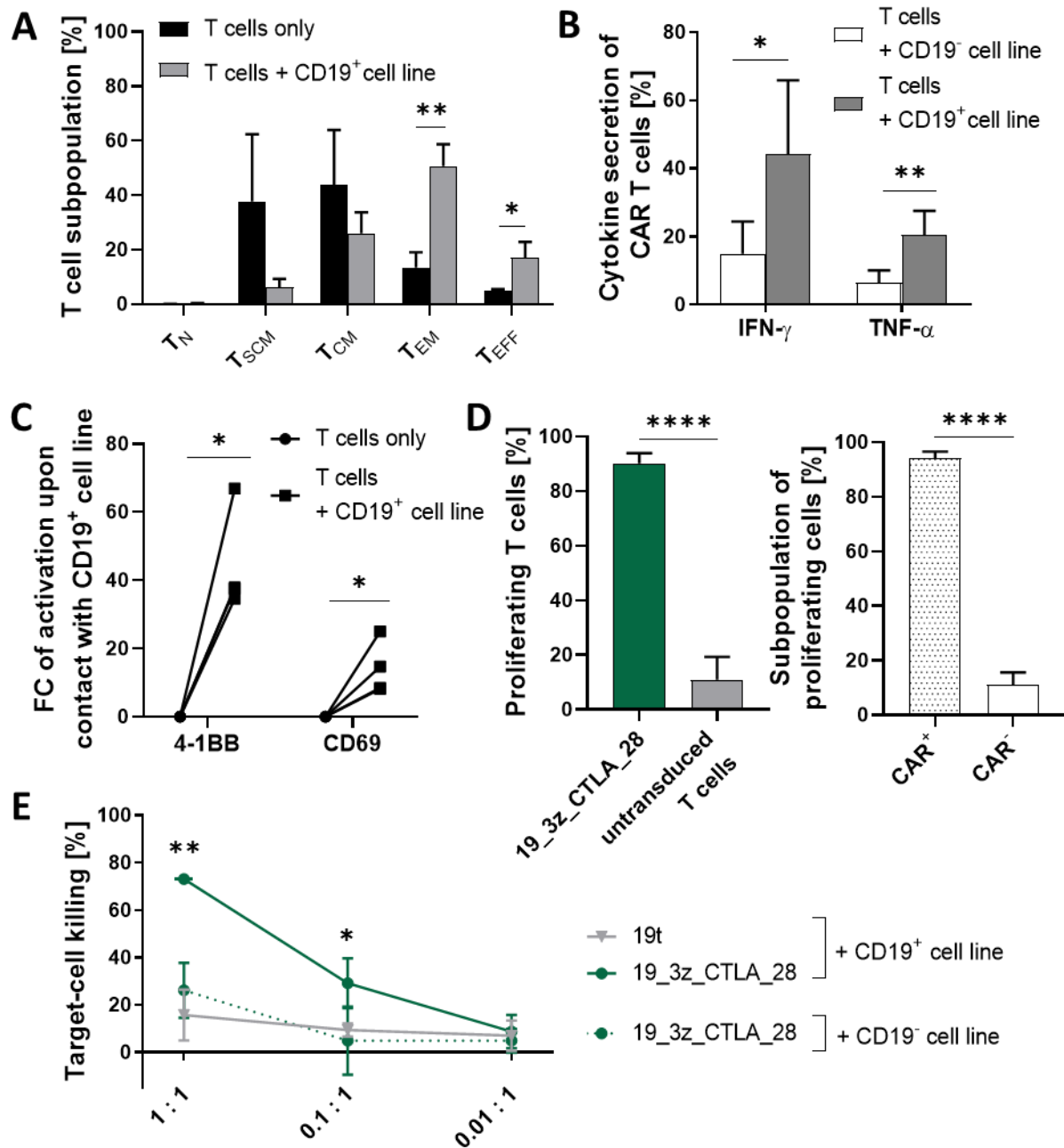


Figure 12 CD19-specific functionality of first generation CAR T cells with CTLA-4/CD28 fusion receptor.

Functionality of 19_3z_CTLA_28 CAR was determined in flow cytometry based assays. (A) Phenotypical analyses were performed before and 48 hours after co-culture with CD19⁺ K562 cells. The T cell distribution turned from a mostly central memory like to an effector memory phenotype. Effector memory and effector T cells increased significantly after target cell contact ($n \geq 3$, individual donors). (B) Intracellular cytokine stain (ICS) was performed 24 hours after co-cultivation with CD19⁺ and CD19⁻ K562 cells. 19_3z_CTLA_28 CAR showed significantly higher amounts of IFN- γ and TNF- α positive CAR T cells upon antigen recognition ($n \geq 3$, individual donors). (C) Expression of activation markers was evaluated before and 48 hours after co-culture with CD19⁺ K562 cells. Upon target cell contact, 4-1BB and CD69 expression increased on 19_3z_CTLA_28 CAR ($n \geq 3$, individual donors). (D) A high proliferative capacity was detectable 72 hours after CD19 antigen contact within the 19_3z_CTLA_28 CAR population but not in the untransduced control (left, $p < 0.0001$). Gated on T cell subpopulations, this effect was mainly mediated by CAR⁺ T cells (right, $p < 0.0001$). (E) For cytotoxicity measurement CAR T cells were co-cultured with CD19⁺ K562 and K562 wildtype cells in several E:T ratios (x-axis). CAR T cells showed significant higher CD19-dependent killing capacities at varying E:T ratios compared to the 19t negative control. Statistical significance was determined through paired t test for $n \geq 3$ individual donors (A,B,C,E) and unpaired t test for technical replicates of two donors (D). 19t: control CAR. IFN- γ : interferon gamma. TNF- α : tumor necrosis factor alpha. E:T ratio: effector to target ratio.

6.5 CAR T cells with CTLA-4/CD28 fusion receptor obtain similar activation capacity compared to conventional first generation CAR T cells

Next, we tested if the presence of the CTLA-4/CD28 fusion receptor influenced the activation potential of CAR T cells. Therefore, first generation CAR T cells and first generation CAR T cells with CTLA-4/CD28 fusion receptor were co-cultured either with CD19⁺ K562 or with CD19⁺ CD80⁺ CD86⁺ K562 cells for 48 hours.

In co-culture with CD19⁺ cells, no significant difference in the expression of the activation markers 4-1BB, OX40 and CD69 was detectable between 19_3z CAR and 19_3z_CTLA_28 CAR T cells (Figure 13A).

With the additional presence of CD80 and CD86 on CD19⁺ target cells still no difference in expression levels of 4-1BB and OX40 was observed on first generation CAR T cells with and without fusion receptor. CD69 surface expression was slightly increased in 19_3z_CTLA_28 CAR T cells ($p=0.031$) (Figure 13B).

Thus, it could be shown that the presence of CTLA-4/CD28 fusion receptor does not impair the activation potential of first generation CAR T cells.

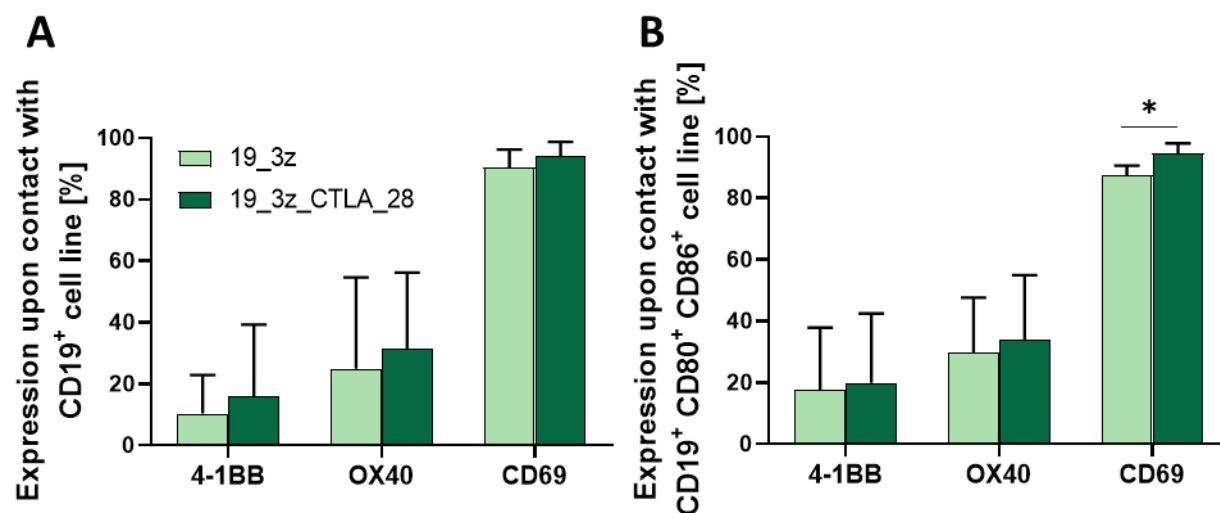


Figure 13 Surface expression of activation markers on CAR T cells after target cell contact.

Expression of activation markers 4-1BB, OX40 and CD69 was measured by flow cytometry 48 hours after co-culture. (A) First generation CAR T cells with CTLA-4/CD28 fusion receptor showed similar expression levels of activation markers compared to conventional first generation CAR T cells when being co-cultured with CD19⁺ cells. (B) The presence of CD80 and CD86 on target cells led to comparable surface expression of 4-1BB and OX40, while CD69 was slightly but significantly increased in first generation CAR T cells with CTLA-4/CD28 fusion receptor ($n \geq 3$, individual donors). Statistical significance was determined through paired t test.

6.6 19_3z_CTLA_28 CAR T cells exhibit comparable cytotoxic capability to conventional first and second generation CAR T cells

For comparative analysis of killing capacities, first generation CAR T cells with and without fusion receptor and second generation CAR T cells were co-cultured with CD19⁺ K562 cells at different E:T ratios for 48 hours, before being evaluated by flow cytometry.

CD19⁺ K562 cells were specifically killed in an E:T ratio dependent manner by all tested CAR T cell constructs (range 66.5 to 81.9% at 1:1 E:T ratio), while untransduced T cells showed mean killing rates of 4.3% (for 1:1 E:T ratio) (Figure 14A). 19_3z, 19_BB_3z and 19_3z_CTLA_28 showed no significant differences in killing capacities at any E:T ratio.

In presence of additional CD80 and CD86 on target cells same behavior was seen with killing rates between 74.8 and 84.8% for CAR T cells at the 1:1 E:T ratio (Figure 14B).

In order to distinguish between the effects of the two ligands of CTLA-4, CD80 and CD86, CAR T cells were co-cultivated with either CD19 CD80 or CD19 CD86 expressing target cells. Target cells were killed in an E:T ratio dependent manner with no significant difference in killing potential of the tested CAR T cells (Figure 14C and D).

In summary, the CTLA-4/CD28 fusion receptor did not diminish the cytotoxic capacity of first generation CAR T cells. 19_3z_CTLA_28 CAR T cells showed no inferiority of killing potential compared to second generation CAR T cells.

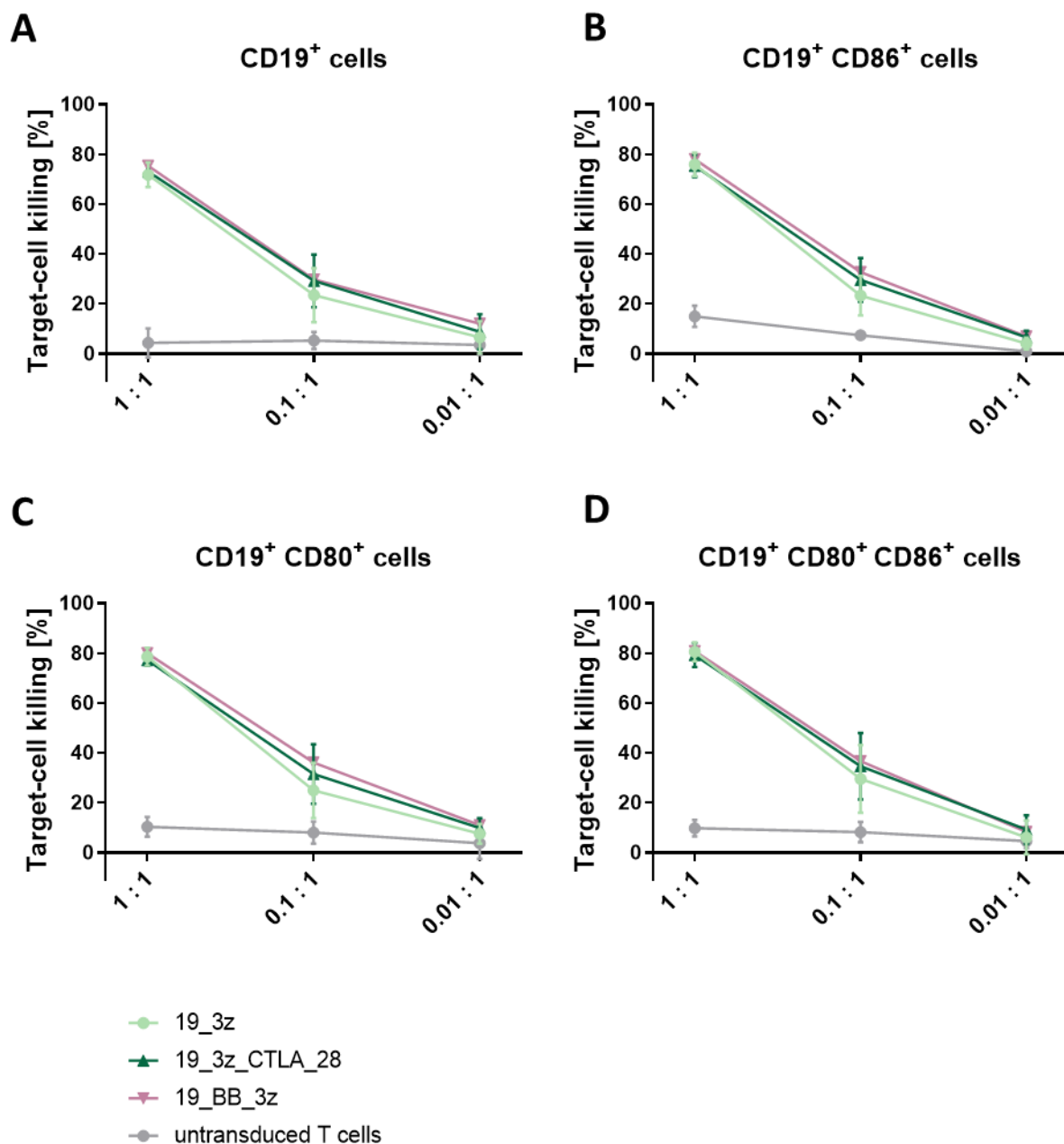


Figure 14 Short-term cytotoxicity of CAR T cells with CTLA-4/CD28 fusion receptor.

Cytotoxicity in CD19⁺ (A), CD19⁺ CD80⁺ CD86⁺ (B), CD19⁺ CD80⁺ (C) and CD19⁺ CD86⁺ (D) K562 cells after CAR T cell contact detected by flow cytometry at several E:T ratios (x-axis) 48 hours after co-culture. CAR T cells were able to specifically kill target cells in an E:T ratio dependent manner. No significant differences in killing capacities were detected, comparing first generation CAR with CTLA-4/CD28 fusion receptor to conventional first and second generation CAR T cells ($n \geq 3$, individual donors). Statistical significance was determined through paired t test.

6.7 CAR T cells with CTLA-4/CD28 fusion receptor show slightly enhanced cytokine secretion in presence of CD80 and CD86

The capability of CAR T cells for cytokine secretion was tested in co-culture with either CD19⁺ or CD19⁺ CD80⁺ CD86⁺ K562 cells, followed by intracellular staining of IFN- γ and TNF- α after 48 hours and evaluation in flow cytometry.

When co-cultured with CD19⁺ K562 cells, IFN- γ and TNF- α secretion of 19_3z, 19_BB_3z and 19_3z_CTLA_28 CAR did not differ significantly in all tested CAR constructs (Figure 15A and B).

19_3z_CTLA_28 CAR showed a mean of 20.3% TNF- α positive and 22.9% IFN- γ CAR T cells after co-culture with CD19⁺ targets. The additional presence of CD80 and CD86 on target cells led to a further increase to a mean of 35.3% (range 22.7 to 57.0%, $p=0.014$) TNF- α and 60.1% (range 43.5 to 81.3%, $p=0.032$) IFN- γ positive CAR T cells (Figure 15A and B).

19_BB_3z CAR T cells showed no superiority in IFN- γ and TNF- α secretion compared to 19_3z_CTLA_28 CAR T cells regardless of CD80 CD86 presence on target cell line (Figure 15A and B).

To confirm these results, an ICS with Daudi cells was performed, allowing the evaluation of cytokine secretion capacity of CAR T cells in a lymphoma system (Figure 15C). First generation CAR T cells with and without fusion receptor were co-cultured with CD80⁺ CD86⁺ Daudi cells for 24 hours. Significant higher amounts of IFN- γ (mean 72.1%, range 71.5 to 73.1%) and TNF- α (mean 42.3%, range 40.8 to 43.6%) positive CAR T cells were detectable in 19_3z_CTLA_28 CAR T cells, compared to 19_3z CAR T cells (IFN- γ $p=0.002$, TNF- α $p=0.004$).

To ensure the specificity of cytokine secretion in presence of the CAR, 19_3z_CTLA_28 CAR T cells were co-cultured with CD19⁻, CD19⁻ CD80⁺ CD86⁺ and CD19⁺ CD80⁺ CD86⁺ K562 cells (Figure 15D). Only the presence of CD19 led to production of IFN- γ (mean 68.4%, range 64.4 to 70.1%) and TNF- α (mean 30.0%, range 26.8 to 34.0) in CAR T cells with CTLA-4/CD28 fusion receptor. A significantly lower mean fraction of IFN- γ (15.5%, $p=0.0005$) and TNF- α (7.7%, $p=0.0009$) positive CAR T cells was seen in co-culture with CD19⁻ CD80⁺ CD86⁺ target cells. The presence of CD80 and CD86 on CD19⁻ target cells led to no significant difference in cytokine secretion of T cells.

In conclusion, increased levels of cytokine secretion in first generation CAR T cells with fusion receptor compared to conventional CAR T cells were confirmed with two different cell lines. Second generation CAR T cells did not show superiority in terms of cytokine secretion.

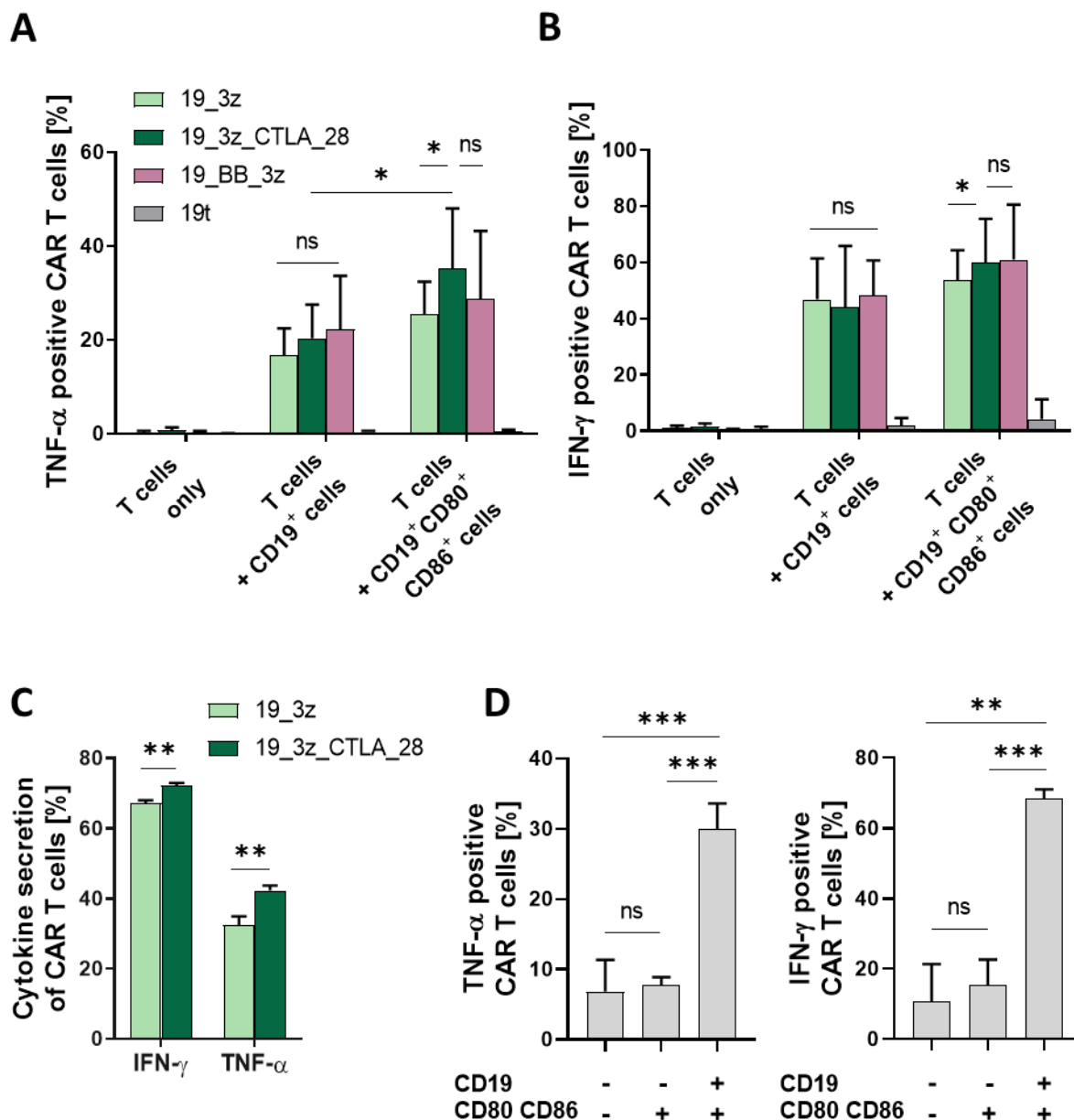


Figure 15 Intracellular cytokine staining of CAR T cells upon stimulation with target cell lines.

Intracellular cytokine stain was performed before and 24 hours after co-culture with target cells and evaluated by flow cytometry. (A and B) CAR T cells with fusion receptor exhibited similar amounts of TNF- α and IFN- γ positive CAR T cells compared to conventional first and second generation CAR T cells, in co-culture with CD19⁺ K562 cells. In presence of CD80 and CD86 on target cells 19_3z_CTLA_28 showed significantly higher amounts of TNF- α ($p=0.014$) and IFN- γ ($p=0.032$) positive CAR T cells in comparison to 19_3z CAR and achieved same levels as 19_BB_3z CAR T cells ($n \geq 3$, individual donors). (C) In co-culture with CD80⁺ CD86⁺ Daudi cells significantly more IFN- γ ($p=0.002$) and TNF- α ($p=0.004$) positive CAR T cells were observed in 19_3z_CTLA_28 ($n = 3$, technical replicates of one donor). (D) 19_3z_CTLA_28 CAR T cells were co-cultured with CD19⁻, CD19⁻ CD80⁺ CD86⁻ and CD19⁺ CD80⁺ CD86⁺ K562 cells. Significantly lower expression levels of TNF- α and IFN- γ were detected in co-culture with CD19⁻ CD80⁻ CD86⁻ ($p<0.0001$ for TNF- α , $p=0.001$ for IFN- γ) and CD19⁻ CD80⁺ CD86⁺ target cells ($p=0.0009$ for TNF- α , $p=0.0005$ for IFN- γ) ($n = 4$, technical replicates of two donors). Statistical significance was determined through paired t test for $n \geq 2$ individual donors (A,B,D) and unpaired t test for technical replicates of one donor (C). IFN- γ : interferon gamma. TNF- α : tumor necrosis factor alpha. E only: effector without target cell contact. Ns: not significant.

6.8 CAR T cells with CTLA-4/CD28 fusion receptor obtain superior long-term functionality

To assess the efficacy of CAR T cells over time a long-term assay for detection of CAR T cell functionality upon serial stimulation was established. In this model, first generation CAR T cells and first generation CAR T cells with CTLA-4/CD28 fusion receptor were co-cultured with CD80⁺ CD86⁺ Daudi cells and re-stimulated every three to four days. Activation and exhaustion markers were stained on day two, twelve and 19. ICS and Cytotoxicity measurements were performed as depicted below (Figure 16).

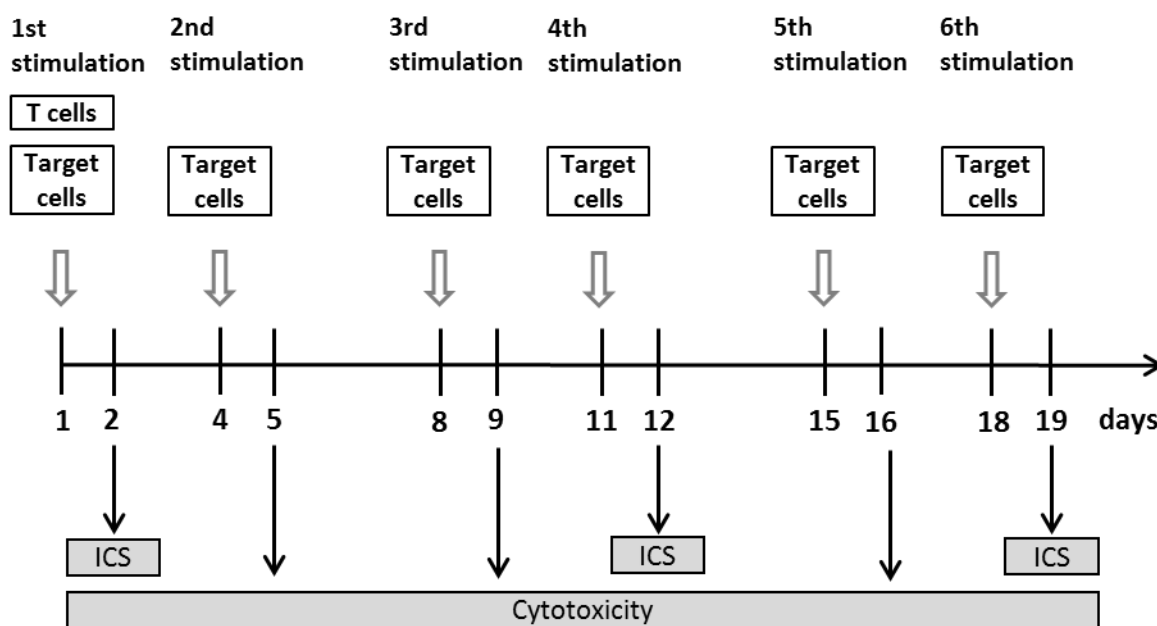


Figure 16 Workflow of a long-term assay for detection of cytokine secretion and cytotoxicity of CAR T cells over time. CAR T cells were serially co-cultured with CD80⁺ CD86⁺ Daudi cells at a 0.2:1 E:T ratio for cytotoxicity assay and 1:1 E:T ratio for ICS. Re-stimulation was performed every two to three days. Cytotoxicity was determined 24 hours after each stimulation for six times. ICS, activation and exhaustion panel were stained on day two, twelve and 19. Assays were evaluated via flow cytometry. ICS: Intracellular cytokine stain, E:T ratio: effector to target ratio.

CAR expression on T cells was evaluated via flow cytometry with every ICS and could be ensured over time (data not shown). The expression of CTLA-4 remained stable and high in 19_3z_CTLA_28 CAR, assuming this to be the fusion receptor, whereas an increase of endogenous CTLA-4 could be observed in conventional first generation CAR T cells (mean 30.2 to 46.9%) (Figure 17A).

Mean PD-1 surface expression decreased in both CAR T cell constructs (76.0 to 52.6% for 19_3z, 73.1 to 49.4% for 19_3z_CTLA_28) upon serial stimulation. 19_3z_CTLA_28 showed significant lower levels of PD-1 at any time (day 2 $p=0.036$, day 12 $p=0.017$) (Figure 17B).

Surface expression of activation marker CD25 remained consistently high even after repetitive co-culture in both CAR T cell conditions (83.2 to 94.7%). CD25 surface expression was significantly higher on 19_3z_CTLA_28 although with minor differences, indicating a superior activation potential of CAR T cells with fusion receptor (day 2 $p=0.002$, day12 $p=0.0001$) (Figure 17C).

As previously described in chapter 6.7, CAR T cells with CTLA-4/CD28 fusion receptor showed significantly higher levels of IFN- γ and TNF- α positive CAR T cells compared to conventional CAR T cells upon stimulation with CD80⁺ CD86⁺ Daudi cells for 24 hours (Figure 17A and B). Upon repetitive stimulation for three times, reduced amounts of cytokine secretion and no differences between the CAR T cells with and without fusion receptor were observable.

Upon serial stimulation, the mean killing potency was 37.4% (range 24.0 to 51.0%) for 19_3z and 52.8% (range 34.3 to 66.2%) for 19_3z_CTLA_28. In contrast to the cytotoxicity assay using CD19⁺ K562 (Figure 14), a significant difference in cytotoxic capacities of 19_3z_CTLA_28 compared to conventional 19_3z CAR T cells was observed with Daudi cell line.

Taken together, long-term efficacy of CAR T cells could be shown *in vitro*. CAR T cells with CTLA-4/CD28 fusion receptor can outcompete conventional first generation CAR T cells in terms of cytokine secretion and killing capacities in this specific setting.

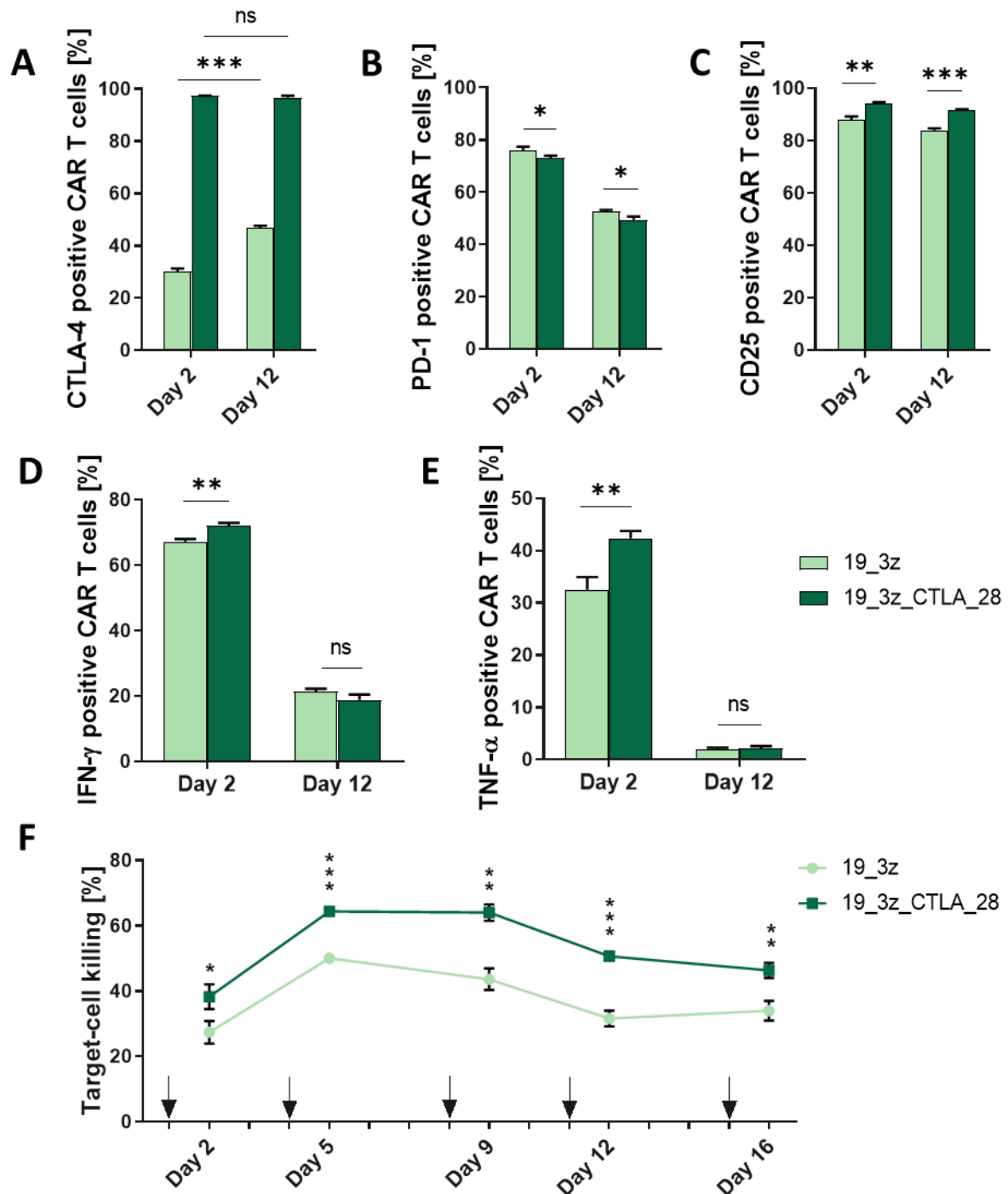


Figure 17 Long-term functionality of CAR T cells with CTLA-4/CD28 fusion receptor.

CAR T cells were serially co-cultured with CD80⁺ CD86⁺ Daudi cells at a 1:1 E:T ratio for ICS, exhaustion, activation and at 0.2:1 E:T ratio for cytotoxicity measurements. Restimulation was performed every three to four days. (A) Surface expression of CTLA-4 in 19_3z_CTLA_28 CAR remained stable over time, assuming this to be the fusion receptor. Increased expression of endogenous CTLA-4 on 19_3z was seen upon serial stimulation ($p < 0.0001$). (B) Exhaustion marker PD-1 was significantly higher expressed on conventional CAR T cells compared to CAR T cells with CTLA-4/CD28 fusion receptor upon repetitive stimulation ($p = 0.036$ day 2, $p = 0.017$ day 12). (C) Surface expression of activation marker CD25 was increased in 19_3z_CTLA_28 CAR T cells ($p = 0.002$ day 2, $p = 0.0001$ day 12) (D and E) On day 2 after co-culture significantly higher levels of IFN- γ and TNF- α positive CAR T cells were detected in 19_3z_CTLA_28. On day 12 reduced cytokine secretion and no differences between the CAR constructs were observable. (F) Target-cell killing was evaluated every 24 hours after stimulation. Arrows mark time point of stimulation with target cells. 19_3z_CTLA_28 CAR T cells showed stable serial killing potency as well as significantly higher killing percentages compared to 19_3z CAR T cells over time ($n = 3$, technical replicates of one donor). Statistical significance was determined through unpaired t test. IFN- γ : interferon gamma. TNF- α : tumor necrosis factor alpha.

7 Discussion

7.1 The role of immune checkpoints on T cell interaction with malignant cells in acute lymphoblastic leukemia

Despite revolutionary improvements in treatment of childhood ALL^{17,31,49}, the reason is unknown why some patients respond to therapy, while others are non-responders or relapse after primarily achieved remission. Emerging evidence indicates that the role of expression of co-inhibitory molecules and loss of co-stimulatory molecules is not negligible in effector-target cell interaction for hematologic malignancies⁵⁰. Previous work of our group revealed that leukemic cells have the potential to evade immune surveillance by T cells through expression of inhibitory surface molecules¹⁴. Antibodies against inhibitory surface markers are successfully administered in patients with highly immunogenic malignancies^{12,13}. For leukemia, the role of immune checkpoints needs to be further investigated to reveal possible mechanisms of interaction between T cells and leukemic cells. This study aims at elucidating part of these mechanisms and harnessing its therapeutic potential to improve CAR T cell therapy for pediatric ALL.

Different baseline expression profiles of inhibitory and stimulatory surface markers on several leukemic cell lines were observed. Upon stimulation, the checkpoint profiles of both, cell lines and T cells changed, most notably by upregulation of inhibitory markers (PD-L1, CEACAM1, CD155 on target cells; CTLA-4, LAG-3 and TIM-3 on T cells). CTLA-4, LAG-3 and TIM-3 are transiently expressed on functional effector T cells and crucial for negative regulatory pathways⁵¹. However, higher and permanent expression of inhibitory receptors are characteristics of exhausted T cells⁵². T cell exhaustion is associated with the expression of multiple inhibitory markers, loss of effector functions and therefore inadequate response to persisting infections and tumors⁵¹.

These variable expression profiles on both sides are consistent with the literature, describing inter-individual T cell responses of patients against ALL and might provide a potential explanation for the differing therapeutic success of immunotherapy in children with relapsed and refractory ALL^{14,53}.

7.2 Successful generation of anti-CD19 specific CAR T cells

CAR T cell constructs were successfully generated from PBMCs of healthy donors. The CAR included the CD19 scFv from clone FMC63, which has been used for anti-CD19 CAR T cell therapy in several clinical trials^{34,54}. A CD8 transmembrane domain was incorporated in the CAR design, since incorporation of CD8 in the transmembrane domain had shown functional advantages over other tested transmembrane domains⁵⁵. For second generation CAR T cells, 4-1BB was included as co-stimulatory domain, due to its longer *in vivo* persistence compared to CD28⁵⁶. Retroviral

transduction of T cells has already shown success in clinical use²⁶ and was chosen as viral delivery system in our approach. High CAR transduction rates between 43.2% and 92.9% were achieved, varying due to inter-individual differences. Differences in transduction rates between the tested constructs were observed, most likely caused by not-standardized virus titer or length of the transduced insert. High viability and up to 100 fold expansion were detected during manufacturing process. The final CAR T cell product showed a CD4 T cell dominant cellular composition, as well as a central and stem cell memory phenotype, which is known to be favorable for a functionally active CAR T cell product⁵⁷. The generated CAR T cells were able to specifically kill CD19⁺ target cells even at low E:T ratios and secreted IFN- γ and TNF- α upon target cell contact. Phenotypical analyses revealed a shift from central memory like towards a more mature T cell phenotype upon antigen recognition. High activation potential was determined, measured by the surface expression of the activation markers 4-1BB and CD69 after target cell co-culture. High proliferative capacity after CD19 antigen contact was detected in the transduced T cell population compared to untransduced T cells. Investigation of subpopulations within the proliferating T cells revealed that this effect was mainly mediated by CAR⁺ T cells.

7.3 Inhibitory effect of CTLA-4 on T cells

To detect the inhibitory effect on T cells, CTLA-4 was retrovirally overexpressed in primary human T cells. Decreased proliferative and activation capacity were observed upon antigen contact, in line with the inhibitory effects of CTLA-4 described in literature^{58,59}.

Endogenous CTLA-4 plays a key role in maintaining self-tolerance in T cells⁶⁰. It is expressed on T cells and mainly stored in intracellular vesicles⁶¹. Since CTLA-4 is a CD28 homolog with a 100-fold higher affinity for the B7 family members CD80 (B7-1) and CD86 (B7-2)⁶², the relative amount of CD28:B7 and CTLA-4:B7 binding determines whether a T cell will undergo activation or anergy⁶³. As CTLA-4 is upregulated upon TCR ligation⁵⁰, it negatively regulates excessive activation of T cells⁶⁴. Unfortunately, this constitutes a potential vulnerability that can be exploited by tumor cells to evade immune surveillance of T cells^{64,60}. For instance, in multiple myeloma patients, CD86 was expressed by tumor cells, while CTLA-4 was upregulated on T cells, leading to reduced activity of tumor-specific T cells⁶⁵. Clinical administration of the anti-CTLA-4 antibody ipilimumab increased the overall survival rates in heavily pretreated patients with metastatic melanoma, which has led to its approval in 2011⁶⁶. Systemic blockade of CTLA-4 signaling was associated with auto-immune side effects, involving the gastrointestinal, endocrinal, cardiovascular, renal and dermatological system^{67,68}.

First attempts at selectively blocking CTLA-4 signaling in tumor-specific T cells were published in 2012 for autologous⁶⁹ and in 2017 for allogenic adoptive T cell therapy⁷⁰. Genetic modification of tumor-antigen specific CD4 and CD8 donor T cells with a CTLA4-CD28 chimera gene, in which the

intracellular signaling domain of CTLA-4 apart from seven amino acids was replaced with the CD28 signaling domain, resulted in significantly increased graft-versus-tumor effects in several murine tumor models⁷⁰. In contrast to that approach, the design of our CTLA-4/CD28 fusion receptor contained the complete intracellular domain of CTLA-4. Here, the CTLA-4/CD28 fusion receptor was incorporated into CAR T cells. In a CAR T cell model, the first T cell activating signal is mediated by the CAR and is much stronger compared to the T cell receptor signal^{19,64}. The second signal which is provoked by the expression of co-stimulatory and co-inhibitory molecules⁶⁴ could then be interfered by co-transduction of a CTLA-4/CD28 fusion receptor that would ideally amplify the anti-tumor efficacy of CAR T cells. Investigations in presence of CTLA-4 ligands CD80 and CD86 on target cell lines allowed more differentiated observations on the efficacy of the CTLA-4/CD28 fusion receptor.

7.4 Abrogation of the inhibitory CTLA-4 signal

This study aimed at reversing the inhibiting effect of CTLA-4 on CAR T cells to a stimulatory CD28 signal through simultaneous transduction of CAR and CTLA-4/CD28 fusion receptor into T cells. The bi-cistronic fusion receptor design contained the extracellular and transmembrane domain of CTLA-4 fused to the intracellular domain of CD28, which is meant to turn the inhibitory CTLA-4 signal into CD28-mediated T cell stimulation. Here, the complete intracellular domain of CTLA-4 was replaced with CD28. In contrast to anti-CTLA-4 blocking antibodies, the newly designed fusion receptor could benefit from the additional co-stimulation through CD28 and therefore potentially leads to stronger T cell activation. Anti-tumor functionality of the designed construct on CAR T cells could be shown *in vitro* by co-culture assays with target cell lines expressing the CAR-specific antigen CD19 as well as the ligands of the fusion receptor CD80 and CD86. Unspecific activation of CAR T cells via the CTLA-4 domain of the fusion receptor could be excluded, since CD80 and CD86 positive target cells did not activate T cells in absence of CD19 CAR signaling.

Since the surface expression of CTLA-4 was significantly higher on the fusion receptor CAR and correlated with the CAR expression, we assumed that the CTLA-4 expression on 19_3z_CTLA_28 is mediated by the fusion receptor, while CTLA-4 expression on 19_3z shows the amount of endogenous CTLA-4 expression. In this setting it is not distinguishable whether the CTLA-4 expression on CAR T cells with CTLA-4/CD28 fusion receptor is mediated by the fusion receptor or endogenous CTLA-4. Therefore, the question raises, how the CTLA-4/CD28 fusion receptor abrogates the inhibitory effects of endogenous CTLA-4 on T cells. Shin et al. investigated genetically modified T cells with a CTLA-4 mutant named CTLA4-CD28 chimera gene⁶⁹. The group illustrated two possible explanations for the superiority of the CTLA4-CD28 chimera gene that are used as basis to interpret this data. Since the CAR and the CTLA-4/CD28 fusion receptor are linked by a 2A peptide simultaneous transcription of the

genes can be ensured. High expression levels of CTLA-4/CD28 fusion receptor on 19_CTLA_3z and low levels of endogenous CTLA-4 on 19_3z as observed in this study imply the possibility of the fusion receptor to outcompete the effect of endogenous CTLA-4. Another explanation can be seen in the strong CD28 signal delivered from the fusion receptor that simply overrides the negative signal of endogenous CTLA-4, rather than directly competing with it⁵². Since the binding affinity to CD80 and CD86 is 100-fold higher for CTLA-4 than for CD28^{62,71}, such a strong CD28 signaling might not be provided for CAR T cells without fusion receptor.

7.5 Potential enhancement of conventional CAR T cells by CTLA-4/CD28 fusion receptor in specific settings

To address the question whether CAR T cell functionality is influenced by the presence of the CTLA-4/CD28 fusion receptor, activation potential, cytokine release and cytotoxic capacity of first generation CAR T cells with and without fusion receptor were compared. Similar activation potential and high killing capacities were observed for both tested CAR T cell constructs upon antigen contact. Unexpectedly, the presence of the CTLA-4 ligands CD80 and CD86, did not improve killing potential of the fusion receptor CAR. The reason for this observation may be due to the interaction of CD80/CD86 with CD28, a stimulatory surface molecule, which is present on all T cells, physiologically resulting in T cell activation. Since CTLA-4 has the highest affinity for CD80 amongst its ligands⁷², target cells were transduced with either CD80 or CD86 to detect possible differences in cytotoxic capacity. CAR T cells with CTLA-4/CD28 fusion receptor still demonstrated equally high killing capacities as conventional first and second generation CAR T cells. Interestingly, CAR T cells with CTLA-4/CD28 fusion receptor outcompeted conventional first generation CAR T cells in terms of cytokine secretion in presence of CD80 and CD86 on target cells. However, biological relevance of this effect needs to be further addressed in *in vitro* models. The fusion receptor CAR showed no drawbacks in cytokine secretion and killing capacity, when being compared to a conventional second generation CAR with 4-1BB-based co-stimulation. In co-culture with CD19⁻ target cells, CAR T cells secreted significantly lower amounts of cytokines, demonstrating the CAR mediated specificity, although a donor dependent background was detectable.

To mimic a more physiologic setting, where CAR T cells have to face multiple contact with leukemic cells and show serial killing, CAR T cell functionality was examined upon repetitive stimulation with the CD80⁺ and CD86⁺ leukemic Daudi cell line over a period of 19 days. Both tested CAR T cell constructs with and without fusion receptor showed strong IFN- γ and TNF- α secretion upon first stimulation with target cells. In accordance with previous data, the presence of the CTLA-4/CD28 fusion receptor led to significantly higher cytokine secretion at the first measuring time point. After four stimulations no

differences between the tested CAR constructs in terms of cytokine release could be detected. Surface expression of endogenous CTLA-4 on conventional first generation CAR T cells increased continuously over time. For CAR T cells with CTLA-4/CD28 fusion the amount of endogenous CTLA-4 was not appraisable. With lower expression levels of exhaustion marker PD-1 and higher expression of activation marker CD25 on CAR T cell surface, it is tempting to speculate a less exhausted but more activated condition of the fusion receptor CAR. However, these results must be interpreted with caution since experiments were performed with one donor in technical triplicates and thus can overestimate biologic significance especially in presence of low quantitative differences.

Few attempts at evaluating the long-term killing capacity of CAR T cells *in vitro* have been published with differing methods of re-stimulation^{73,74}. In this approach 2×10^3 CAR T cells were re-stimulated every three to four days with 1×10^4 Daudi cells at each time point. Long-term cytotoxicity was observed for both CAR T cell conditions with and without fusion receptor. Consistent with previous publications⁷⁴, long-term cytotoxicity could be shown for both, conventional first generation CAR T cells and CAR T cells with CTLA-4/CD28 fusion receptor during the examination time of 19 days. With this model, we were able to reveal elusive differences in cytotoxicity of CAR T cells due to long-term co-cultivation. The superiority of the fusion receptor CAR in killing potential was demonstrated with significantly higher killing percentages at any time. Higher killing rates after the first stimulation compared to results shown in 6.6 might be due to the usage of a leukemic cell line, rather than the previously used K562 control cell line.

7.6 Clinical potential of the CTLA-4/CD28 fusion receptor

The opportunity of selectively circumventing the inhibitory CTLA-4 signal and turning it into CD28-mediated stimulation in tumor-specific T cells might be appealing for clinical use. Previous work of our group made use of a similar mechanism by integrating a PD-1/CD28 fusion receptor into conventional CAR T cells to bypass inhibition through PD-1⁷⁵. The incorporation of a PD-1/CD28 fusion receptor can increase anti-leukemic functionality of conventional CAR T cells *in vivo* and *in vitro*^{75,76}. In comparison, the CTLA-4/CD28 fusion receptor evaluated in this work displayed a low functional effect *in vitro*. Therefore, this approach needs to be further investigated and many steps are to be climbed before CAR T cells with CTLA-4/CD28 fusion receptor could be considered for clinical administration.

To confirm biological relevance of the observed effects of the CTLA-4/CD28 fusion receptor on CAR T cells, experiments must be repeated with more donors. Since second generation CAR T cells showed enhanced functionality *in vivo*⁷⁷, the superiority of the CTLA-4/CD28 fusion receptor in presence of CD80 and CD86 on target cells should also be confirmed in second generation CAR T cells. Further investigations, regarding anti-leukemic efficacy of the fusion receptor on first and second

generation CAR T cells *in vivo* should be addressed in murine models. Although no unspecific activation of the CAR and the fusion receptor could be observed in this study, these experiments do not allow to draw conclusions on potential off-target side effects. Therefore, inclusion of a safety switch into the CAR should be considered prior to clinical use.

Another approach to improve anti-tumor efficacy before clinical administration could be the evaluation of the most functional molecular design of the CTLA-4/CD28 fusion receptor in an *in vivo* model. Kobold et al. have shown superior functionality of a PD-1/CD28 fusion receptor with a PD-1 transmembrane domain compared to a CD28 transmembrane domain⁷⁸. Blaeschke et al. tested different designs of a TIM-3/CD28 fusion receptor and revealed that fusion receptors with a CD28 transmembrane and intracellular domain were particularly effective and functional⁷⁹. Thus, investigation on different constellations of extracellular, transmembrane and intracellular domains within the CTLA-4/CD28 fusion receptor might lead to stronger anti-tumor response of CAR T cells.

Analysis of patient's immune checkpoint profile prior to CAR T cell administration might play a role, since a high CD80/CD86 expression on blasts would be a favorable constellation for this fusion receptor CAR. As shown in this study, the checkpoint profile of neither tumor nor T cell is stable, rather than adaptable to varying situations. Thus, the detection of changes in checkpoint expression might be even more important than the initial checkpoint expression on the patients' blasts. Nevertheless, patients with low initial PDL-1/PD-1 expression were reported to benefit from anti-PDL-1 blockade against renal cell carcinoma and melanoma^{80,81}. Therefore, even patients with low CD80/CD86 expression might profit from the CTLA-4/CD28 fusion receptor approach even though possibly in smaller extent.

The incorporation of a CTLA-4/CD28 fusion receptor into CAR T cells could contribute to overcome T cell exhaustion, maintain long-term cytotoxic capacity and increase CAR T cell functionality. Taken together, these results demonstrate the possibility of being one step ahead of the leukemic malignancy by preventing escape mechanisms to achieve durable and long-term remission due to CAR T cell therapy.

8 Summary

Adoptive transfer of CD19 specific T cells with a chimeric antigen receptor (CAR) has revolutionized anti-cancer therapy for patients with advanced B-precursor acute lymphoblastic leukemia (ALL). Unprecedented response rates up to 90% have been observed in clinical trials and resulted in FDA approvals. Nevertheless, 50% of the patients treated with anti-CD19 CAR T cells suffer from relapse within 24 months. This emphasizes the need to elucidate mechanisms that lead to success or failure of CAR T cell therapy and provide a potential strategy to overcome possible escape mechanisms.

In this study, the immune checkpoint profiles of leukemic cell lines and CAR T cells were analyzed before and after activation. A significant increase in mean surface expression of inhibitory surface markers like PD-L1, TIM-3 and CTLA-4 was observed in CD19 specific CAR T cells after target cell recognition. Next, we detected that overexpression of CTLA-4 on CAR T cells leads to diminished activation and proliferation potential upon antigen stimulation.

To circumvent the suppressing effect of CTLA-4, CAR T cells with a CTLA-4/CD28 fusion receptor were designed. The fusion receptor contains the extracellular and transmembrane domain of CTLA-4 fused to the intracellular domain of CD28, which is meant to turn the inhibitory CTLA-4 signal into CD28-mediated T cell stimulation. First generation CAR T cells with (19_3z_CTLA_28) and without (19_3z) fusion receptor and second generation CAR T cells (19_3z_BB) were successfully generated via retroviral transduction and characterized by flow cytometry. High viability and expansion as well as a favorable stem-cell/central memory like phenotype were observed. *In vitro* functionality assays of 19_3z_CTLA_28 revealed strong CD19-dependent activation, proliferation and killing capacities as well as high IFN- γ and TNF- α secretion upon target cell contact. Inclusion of the fusion receptor did not impair activation capability of conventional first generation CAR T cells. Comparably high killing capacities were detected for all tested CAR T cell constructs. CAR T cells with fusion receptor showed slightly increased cytokine secretion in presence of CD80/CD86 on target cells.

To assess long-term anti-tumor efficacy, CAR T cells with and without fusion receptor were stimulated repetitively with CD19⁺ CD80⁺ CD86⁺ target cells over a time period of 19 days. Upon serial stimulation, 19_3z_CTLA_28 showed stable killing potency as well as significantly higher killing percentages compared to conventional first generation CAR T cells. *In vivo* functionality of CAR T cells with a CTLA-4/CD28 fusion receptor will have to be addressed in future studies.

The incorporation of fusion receptors into CAR T cells could be a promising strategy to optimize CAR T cell therapy for treatment of advanced pediatric leukemia and relapse-prone patients.

9 Zusammenfassung

Der adoptive Transfer von CD19-spezifischen T-Zellen mit chimärem Antigenrezeptor (CAR) hat die Therapie der fortgeschrittenen B-Vorläufer ALL revolutioniert. Hohe initiale Ansprechraten bis zu 90% resultierten in der Zulassung in den USA und in Europa. Nichtsdestotrotz erleiden 50% der mit anti-CD19 CAR-T-Zellen behandelten Patienten innerhalb von 24 Monaten einen Rückfall. Dies unterstreicht die Notwendigkeit, Mechanismen aufzuklären, die zum Erfolg oder Misserfolg der CAR-T-Zelltherapie führen, sowie eine mögliche Strategie zur Überwindung dieser Mechanismen bereitzustellen.

In diesem Projekt wurden die Immuncheckpoint-Profile von Leukämiezelllinien und CAR-T-Zellen vor und nach Aktivierung analysiert. Eine signifikante Zunahme der Expression inhibitorischer Oberflächenmarker wie PD-L1, TIM-3 und CTLA-4 wurde auf CD19-spezifischen CAR-T-Zellen nach Erkennung der Zielzellen beobachtet. Es konnte gezeigt werden, dass eine Überexpression von CTLA-4 auf CAR-T-Zellen, nach Antigenstimulation, zu einem verminderten Aktivierungs- und Proliferationspotential führt.

Um den hemmenden Effekt von CTLA-4 zu umgehen, wurden CAR-T-Zellen mit einem CTLA-4/CD28 Fusionsrezeptor entwickelt. Dieser Rezeptor enthält eine extrazelluläre CTLA-4- und eine intrazelluläre CD28-Domäne, wodurch das inhibitorische CTLA-4-Signal in eine CD28-vermittelte T-Zell-Stimulation umgewandelt werden soll. Erst-Generations CAR-T-Zellen mit (19_3z_CTLA_28) und ohne (19_3z) Fusionsrezeptor sowie Zweit-Generations CAR-T-Zellen (19_3z_BB) wurden mittels retroviraler Transduktion erfolgreich generiert und durchflusszytometrisch charakterisiert. Hohe Viabilität, gute Expansionsfähigkeit und ein mehrheitlich Stammzell-/Gedächtniszell-Phänotyp wurden beobachtet. *In vitro* Funktionalitätstests des 19_3z_CTLA_28 zeigten eine starke CD19-abhängige Aktivierung, Proliferation und Zytotoxizität sowie eine hohe IFN- γ und TNF- α Sekretion bei Zielzellenkontakt. Der Einbau des Fusionsrezeptors beeinträchtigte nicht die Aktivierungsfähigkeit konventioneller CAR-T-Zellen der ersten Generation. Vergleichbar hohe Zytotoxizität wurde für alle getesteten CAR-T-Zellkonstrukte nachgewiesen. In Gegenwart von CD80/CD86 auf Zielzellen zeigten CAR T-Zellen mit Fusionsrezeptor eine leicht erhöhte Zytokinausschüttung.

Zur Beurteilung der langfristigen anti-Tumor Effektivität wurden CAR-T-Zellen mit und ohne Fusionsrezeptor über einen Zeitraum von 16 Tagen wiederholt mit CD19⁺ CD80⁺ CD86⁺ Zielzellen stimuliert. Bei wiederholter Stimulation zeigte 19_3z_CTLA_28 eine stabile sowie signifikant höhere Zytotoxizität im Vergleich zu konventionellen CAR-T-Zellen der ersten Generation. Die *in vivo* Funktionalität von CAR-T-Zellen mit CTLA 4/CD28 Fusionsrezeptor wird in zukünftigen Studien untersucht werden müssen. Der Einbau von Fusionsrezeptoren in CAR-T-Zellen könnte eine vielversprechende Strategie zur Optimierung der CAR-T-Zelltherapie bei der Behandlung von fortgeschrittener pädiatrischer Leukämie und Hochrisiko-Patienten darstellen.

10 Literature

1. Hunger SP, Mullighan CG. Acute Lymphoblastic Leukemia in Children. *The New England journal of medicine* 2015;373(16):1541-52. (In eng). DOI: 10.1056/NEJMra1400972.
2. Escherich G, Schrappe M, Creutzig U. S1-Leitlinie 025/014: Akute lymphoblastische- (ALL) Leukämie im Kindesalter. (https://www.awmf.org/uploads/tx_szleitlinien/025-014l_S1_Akute-lymphoblastische-Leukaemie-ALL-im-Kindesalter_2021-07.pdf).
3. Farber S, Diamond LK. Temporary remissions in acute leukemia in children produced by folic acid antagonist, 4-aminopteroyl-glutamic acid. *The New England journal of medicine* 1948;238(23):787-93. (In eng). DOI: 10.1056/nejm194806032382301.
4. Hunger SP, Lu X, Devidas M, et al. Improved survival for children and adolescents with acute lymphoblastic leukemia between 1990 and 2005: a report from the children's oncology group. *Journal of clinical oncology : official journal of the American Society of Clinical Oncology* 2012;30(14):1663-9. (In eng). DOI: 10.1200/jco.2011.37.8018.
5. Cooper SL, Brown PA. Treatment of pediatric acute lymphoblastic leukemia. *Pediatric clinics of North America* 2015;62(1):61-73. (In eng). DOI: 10.1016/j.pcl.2014.09.006.
6. Borowitz MJ, Devidas M, Hunger SP, et al. Clinical significance of minimal residual disease in childhood acute lymphoblastic leukemia and its relationship to other prognostic factors: a Children's Oncology Group study. *Blood* 2008;111(12):5477-85. (In eng). DOI: 10.1182/blood-2008-01-132837.
7. Locatelli F, Schrappe M, Bernardo ME, Rutella S. How I treat relapsed childhood acute lymphoblastic leukemia. *Blood* 2012;120(14):2807-16. (In eng). DOI: 10.1182/blood-2012-02-265884.
8. Swann JB, Smyth MJ. Immune surveillance of tumors. *The Journal of clinical investigation* 2007;117(5):1137-46. (In eng). DOI: 10.1172/jci31405.
9. Wedekind MF, Denton NL, Chen CY, Cripe TP. Pediatric Cancer Immunotherapy: Opportunities and Challenges. *Paediatric drugs* 2018;20(5):395-408. (In eng). DOI: 10.1007/s40272-018-0297-x.
10. Pardoll DM. The blockade of immune checkpoints in cancer immunotherapy. *Nature reviews Cancer* 2012;12(4):252-64. (In eng). DOI: 10.1038/nrc3239.
11. Sharon E, Streicher H, Goncalves P, Chen HX. Immune checkpoint inhibitors in clinical trials. *Chinese journal of cancer* 2014;33(9):434-44. (In eng). DOI: 10.5732/cjc.014.10122.
12. Hamid O, Robert C, Daud A, et al. Safety and tumor responses with lambrolizumab (anti-PD-1) in melanoma. *The New England journal of medicine* 2013;369(2):134-44. (In eng). DOI: 10.1056/NEJMoa1305133.
13. Hodi FS, O'Day SJ, McDermott DF, et al. Improved survival with ipilimumab in patients with metastatic melanoma. *The New England journal of medicine* 2010;363(8):711-23. (In eng). DOI: 10.1056/NEJMoa1003466.
14. Feucht J, Kayser S, Gorodezki D, et al. T-cell responses against CD19+ pediatric acute lymphoblastic leukemia mediated by bispecific T-cell engager (BiTE) are regulated contrarily by PD-L1 and CD80/CD86 on leukemic blasts. *Oncotarget* 2016;7(47):76902-76919. DOI: 10.18632/oncotarget.12357.
15. Boekstegers AM, Blaeschke F, Schmid I, et al. MRD response in a refractory paediatric T-ALL patient through anti-programmed cell death 1 (PD-1) Ab treatment associated with induction of fatal GvHD. *Bone Marrow Transplant* 2017;52(8):1221-1224. (In eng). DOI: 10.1038/bmt.2017.107.
16. U.S. Food and Drug Administration DoHaHS. BLA 125557, BLA accelerated approval BLINCYTO. (https://www.accessdata.fda.gov/drugsatfda_docs/applletter/2014/125557Orig1s000ltr.pdf).
17. von Stackelberg A, Locatelli F, Zugmaier G, et al. Phase I/Phase II Study of Blinatumomab in Pediatric Patients With Relapsed/Refractory Acute Lymphoblastic Leukemia. *Journal of clinical*

- oncology : official journal of the American Society of Clinical Oncology 2016;34(36):4381-4389. (In eng). DOI: 10.1200/jco.2016.67.3301.
18. June CH, Sadelain M. Chimeric Antigen Receptor Therapy. *The New England journal of medicine* 2018;379(1):64-73. (In eng). DOI: 10.1056/NEJMra1706169.
 19. Sadelain M, Brentjens R, Riviere I. The basic principles of chimeric antigen receptor design. *Cancer discovery* 2013;3(4):388-98. (In eng). DOI: 10.1158/2159-8290.cd-12-0548.
 20. Maus MV, Grupp SA, Porter DL, June CH. Antibody-modified T cells: CARs take the front seat for hematologic malignancies. *Blood* 2014;123(17):2625-35. (In eng). DOI: 10.1182/blood-2013-11-492231.
 21. U.S. Food and Drug Administration DoHaHS. Approval Letter - KYMRIAHA, STN:BL 125646/0. (<https://www.fda.gov/media/106989/download>).
 22. O'Leary MC, Lu X, Huang Y, et al. FDA Approval Summary: Tisagenlecleucel for Treatment of Patients with Relapsed or Refractory B-cell Precursor Acute Lymphoblastic Leukemia. *Clin Cancer Res* 2019;25(4):1142-1146. DOI: 10.1158/1078-0432.CCR-18-2035.
 23. Agency EM. Assessment report for Kymriah (tisagenlecleucel), Procedure No. EMEA/H/C/004090/0000. Committee for Medicinal Products for Human Use (CHMP). (https://www.ema.europa.eu/en/documents/assessment-report/kymriah-epar-public-assessment-report_en.pdf).
 24. Klebanoff CA, Yamamoto TN, Restifo NP. Immunotherapy: Treatment of aggressive lymphomas with anti-CD19 CAR T cells. *Nature reviews Clinical oncology* 2014;11(12):685-6. (In eng). DOI: 10.1038/nrclinonc.2014.190.
 25. Klebanoff CA, Khong HT, Antony PA, Palmer DC, Restifo NP. Sinks, suppressors and antigen presenters: how lymphodepletion enhances T cell-mediated tumor immunotherapy. *Trends Immunol* 2005;26(2):111-7. (In eng). DOI: 10.1016/j.it.2004.12.003.
 26. Lee DW, Kochenderfer JN, Stetler-Stevenson M, et al. T cells expressing CD19 chimeric antigen receptors for acute lymphoblastic leukaemia in children and young adults: a phase 1 dose-escalation trial. *Lancet (London, England)* 2015;385(9967):517-528. (In eng). DOI: 10.1016/S0140-6736(14)61403-3.
 27. Klebanoff CA, Yamamoto TN, Restifo NP. Treatment of aggressive lymphomas with anti-CD19 CAR T cells. *Nature Reviews Clinical Oncology* 2014;11:685. DOI: 10.1038/nrclinonc.2014.190.
 28. Gardner RA, Finney O, Annesley C, et al. Intent-to-treat leukemia remission by CD19 CAR T cells of defined formulation and dose in children and young adults. *Blood* 2017;129(25):3322-3331. (In eng). DOI: 10.1182/blood-2017-02-769208.
 29. Ghorashian S, Jacoby E, De Moerloose B, et al. Tisagenlecleucel therapy for relapsed or refractory B-cell acute lymphoblastic leukaemia in infants and children younger than 3 years of age at screening: an international, multicentre, retrospective cohort study. *Lancet Haematol* 2022;9(10):e766-e775. DOI: 10.1016/S2352-3026(22)00225-3.
 30. Brudno JN, Kochenderfer JN. Recent advances in CAR T-cell toxicity: Mechanisms, manifestations and management. *Blood reviews* 2019;34:45-55. (In eng). DOI: 10.1016/j.blre.2018.11.002.
 31. Maude SL, Laetsch TW, Buechner J, et al. Tisagenlecleucel in Children and Young Adults with B-Cell Lymphoblastic Leukemia. *The New England journal of medicine* 2018;378(5):439-448. (In eng). DOI: 10.1056/NEJMoa1709866.
 32. Kansagra AJ, Frey NV, Bar M, et al. Clinical Utilization of Chimeric Antigen Receptor T Cells in B Cell Acute Lymphoblastic Leukemia: An Expert Opinion from the European Society for Blood and Marrow Transplantation and the American Society for Blood and Marrow Transplantation. *Biology of blood and marrow transplantation : journal of the American Society for Blood and Marrow Transplantation* 2019;25(3):e76-e85. (In eng). DOI: 10.1016/j.bbmt.2018.12.068.
 33. U.S. Food and Drug Administration CfDEaR. Approval Package for: Application number: 125276Orig1s114, ACTEMRA tocilizumab. (https://www.accessdata.fda.gov/drugsatfda_docs/nda/2017/125276Orig1s114Approv.pdf).
 34. Turtle CJ, Hay KA, Hanafi LA, et al. Durable Molecular Remissions in Chronic Lymphocytic Leukemia Treated With CD19-Specific Chimeric Antigen Receptor-Modified T Cells After

- Failure of Ibrutinib. *Journal of clinical oncology : official journal of the American Society of Clinical Oncology* 2017;35(26):3010-3020. (In eng). DOI: 10.1200/jco.2017.72.8519.
35. Norelli M, Camisa B, Barbiera G, et al. Monocyte-derived IL-1 and IL-6 are differentially required for cytokine-release syndrome and neurotoxicity due to CAR T cells. *Nat Med* 2018;24(6):739-748. DOI: 10.1038/s41591-018-0036-4.
 36. Giavridis T, van der Stegen SJC, Eyquem J, Hamieh M, Piersigilli A, Sadelain M. CAR T cell–induced cytokine release syndrome is mediated by macrophages and abated by IL-1 blockade. *Nature Medicine* 2018;24(6):731-738. DOI: 10.1038/s41591-018-0041-7.
 37. Shah NN, Fry TJ. Mechanisms of resistance to CAR T cell therapy. *Nature reviews Clinical oncology* 2019 (In eng). DOI: 10.1038/s41571-019-0184-6.
 38. Maude SL, Barrett DM, Rheingold SR, et al. Efficacy of humanized CD19-targeted chimeric antigen receptor (CAR)-modified T cells in children and young adults with relapsed/refractory acute lymphoblastic leukemia. *Am Soc Hematology*; 2016.
 39. Park JH, Riviere I, Gonen M, et al. Long-Term Follow-up of CD19 CAR Therapy in Acute Lymphoblastic Leukemia. *The New England journal of medicine* 2018;378(5):449-459. (In eng). DOI: 10.1056/NEJMoa1709919.
 40. Sotillo E, Barrett DM, Black KL, et al. Convergence of Acquired Mutations and Alternative Splicing of CD19 Enables Resistance to CART-19 Immunotherapy. *Cancer discovery* 2015;5(12):1282-95. (In eng). DOI: 10.1158/2159-8290.Cd-15-1020.
 41. Fischer J, Paret C, El Malki K, et al. CD19 Isoforms Enabling Resistance to CART-19 Immunotherapy Are Expressed in B-ALL Patients at Initial Diagnosis. *Journal of immunotherapy (Hagerstown, Md : 1997)* 2017;40(5):187-195. (In eng). DOI: 10.1097/cji.0000000000000169.
 42. Jacoby E, Nguyen SM, Fountaine TJ, et al. CD19 CAR immune pressure induces B-precursor acute lymphoblastic leukaemia lineage switch exposing inherent leukaemic plasticity. *Nat Commun* 2016;7:12320. (In eng). DOI: 10.1038/ncomms12320.
 43. Gardner R, Wu D, Cherian S, et al. Acquisition of a CD19-negative myeloid phenotype allows immune escape of MLL-rearranged B-ALL from CD19 CAR-T-cell therapy. *Blood* 2016;127(20):2406-10. (In eng). DOI: 10.1182/blood-2015-08-665547.
 44. Ruella M, Xu J, Barrett DM, et al. Induction of resistance to chimeric antigen receptor T cell therapy by transduction of a single leukemic B cell. *Nat Med* 2018;24(10):1499-1503. (In eng). DOI: 10.1038/s41591-018-0201-9.
 45. Hamieh M, Dobrin A, Cabriolu A, et al. CAR T cell trogocytosis and cooperative killing regulate tumour antigen escape. *Nature* 2019;568(7750):112-116. (In eng). DOI: 10.1038/s41586-019-1054-1.
 46. Ghani K, Cottin S, Kamen A, Caruso M. Generation of a high-titer packaging cell line for the production of retroviral vectors in suspension and serum-free media. *Gene therapy* 2007;14(24):1705-11. (In eng). DOI: 10.1038/sj.gt.3303039.
 47. Ghani K, Wang X, de Campos-Lima PO, et al. Efficient human hematopoietic cell transduction using RD114- and GALV-pseudotyped retroviral vectors produced in suspension and serum-free media. *Human gene therapy* 2009;20(9):966-74. (In eng). DOI: 10.1089/hum.2009.001.
 48. Stitz J, Buchholz CJ, Engelstadter M, et al. Lentiviral vectors pseudotyped with envelope glycoproteins derived from gibbon ape leukemia virus and murine leukemia virus 10A1. *Virology* 2000;273(1):16-20. (In eng). DOI: 10.1006/viro.2000.0394.
 49. Schlegel P, Lang P, Zugmaier G, et al. Pediatric posttransplant relapsed/refractory B-precursor acute lymphoblastic leukemia shows durable remission by therapy with the T-cell engaging bispecific antibody blinatumomab. *Haematologica* 2014;99(7):1212-9. (In eng). DOI: 10.3324/haematol.2013.100073.
 50. Norde WJ, Hobo W, van der Voort R, Dolstra H. Coinhibitory molecules in hematologic malignancies: targets for therapeutic intervention. *Blood* 2012;120(4):728-36. (In eng). DOI: 10.1182/blood-2012-02-412510.
 51. Wherry EJ, Kurachi M. Molecular and cellular insights into T cell exhaustion. *Nature reviews Immunology* 2015;15(8):486-99. (In eng). DOI: 10.1038/nri3862.

52. Blackburn SD, Shin H, Haining WN, et al. Coregulation of CD8+ T cell exhaustion by multiple inhibitory receptors during chronic viral infection. *Nature immunology* 2009;10(1):29-37. (In eng). DOI: 10.1038/ni.1679.
53. Subklewe M. BiTEs better than CAR T cells. *Blood advances* 2021;5(2):607-612. DOI: 10.1182/bloodadvances.2020001792.
54. Kochenderfer JN, Dudley ME, Feldman SA, et al. B-cell depletion and remissions of malignancy along with cytokine-associated toxicity in a clinical trial of anti-CD19 chimeric-antigen-receptor-transduced T cells. *Blood* 2012;119(12):2709-20. (In eng). DOI: 10.1182/blood-2011-10-384388.
55. Alabanza L, Pegues M, Geldres C, et al. Function of Novel Anti-CD19 Chimeric Antigen Receptors with Human Variable Regions Is Affected by Hinge and Transmembrane Domains. *Molecular therapy : the journal of the American Society of Gene Therapy* 2017;25(11):2452-2465. (In eng). DOI: 10.1016/j.ymthe.2017.07.013.
56. Davis KL, Mackall CL. Immunotherapy for acute lymphoblastic leukemia: from famine to feast. *Blood advances* 2016;1(3):265-269. (In eng). DOI: 10.1182/bloodadvances.2016000034.
57. Blaesche F, Stenger D, Kaeuferle T, et al. Induction of a central memory and stem cell memory phenotype in functionally active CD4(+) and CD8(+) CAR T cells produced in an automated good manufacturing practice system for the treatment of CD19(+) acute lymphoblastic leukemia. *Cancer immunology, immunotherapy : CII* 2018;67(7):1053-1066. (In eng). DOI: 10.1007/s00262-018-2155-7.
58. Walunas TL, Lenschow DJ, Bakker CY, et al. CTLA-4 can function as a negative regulator of T cell activation. *Immunity* 1994;1(5):405-13. (In eng) ([https://www.cell.com/immunity/pdf/1074-7613\(94\)90071-X.pdf?_returnURL=https%3A%2F%2Flinkinghub.elsevier.com%2Fretrieve%2Fpii%2F107476139490071X%3Fshowall%3Dtrue](https://www.cell.com/immunity/pdf/1074-7613(94)90071-X.pdf?_returnURL=https%3A%2F%2Flinkinghub.elsevier.com%2Fretrieve%2Fpii%2F107476139490071X%3Fshowall%3Dtrue)).
59. Walunas TL, Bakker CY, Bluestone JA. CTLA-4 ligation blocks CD28-dependent T cell activation. *The Journal of experimental medicine* 1996;183(6):2541-50. (In eng) (<https://escholarship.org/content/qt6133s41s/qt6133s41s.pdf?t=qafp7h>).
60. Kim GR, Choi JM. Current Understanding of Cytotoxic T Lymphocyte Antigen-4 (CTLA-4) Signaling in T-Cell Biology and Disease Therapy. *Mol Cells* 2022;45(8):513-521. DOI: 10.14348/molcells.2022.2056.
61. Linsley PS, Bradshaw J, Greene J, Peach R, Bennett KL, Mittler RS. Intracellular trafficking of CTLA-4 and focal localization towards sites of TCR engagement. *Immunity* 1996;4(6):535-43. (In eng). DOI: 10.1016/S1074-7613(00)80480-x.
62. Linsley PS, Greene JL, Brady W, Bajorath J, Ledbetter JA, Peach R. Human B7-1 (CD80) and B7-2 (CD86) bind with similar avidities but distinct kinetics to CD28 and CTLA-4 receptors. *Immunity* 1994;1(9):793-801. (In eng) ([https://www.cell.com/immunity/pdf/S1074-7613\(94\)80021-9.pdf?_returnURL=https%3A%2F%2Flinkinghub.elsevier.com%2Fretrieve%2Fpii%2FS1074761394800219%3Fshowall%3Dtrue](https://www.cell.com/immunity/pdf/S1074-7613(94)80021-9.pdf?_returnURL=https%3A%2F%2Flinkinghub.elsevier.com%2Fretrieve%2Fpii%2FS1074761394800219%3Fshowall%3Dtrue)).
63. Krummel MF, Allison JP. CD28 and CTLA-4 have opposing effects on the response of T cells to stimulation. *The Journal of experimental medicine* 1995;182(2):459-65. (In eng). DOI: 10.1084/jem.182.2.459.
64. Buchbinder EI, Desai A. CTLA-4 and PD-1 Pathways: Similarities, Differences, and Implications of Their Inhibition. *Am J Clin Oncol* 2016;39(1):98-106. (In eng). DOI: 10.1097/coc.0000000000000239.
65. Brown RD, Pope B, Yuen E, Gibson J, Joshua DE. The expression of T cell related costimulatory molecules in multiple myeloma. *Leukemia & lymphoma* 1998;31(3-4):379-84. (In eng). DOI: 10.3109/10428199809059231.
66. Agency EM. Assessment Report for Yervoy (ipilimumab), Procedure No.: EMEA/H/C/002213. (https://www.ema.europa.eu/en/documents/assessment-report/yervoy-epar-public-assessment-report_en.pdf).

67. Bajwa R, Cheema A, Khan T, et al. Adverse Effects of Immune Checkpoint Inhibitors (Programmed Death-1 Inhibitors and Cytotoxic T-Lymphocyte-Associated Protein-4 Inhibitors): Results of a Retrospective Study. *Journal of clinical medicine research* 2019;11(4):225-236. (In eng). DOI: 10.14740/jocmr3750.
68. Attia P, Phan GQ, Maker AV, et al. Autoimmunity correlates with tumor regression in patients with metastatic melanoma treated with anti-cytotoxic T-lymphocyte antigen-4. *Journal of clinical oncology : official journal of the American Society of Clinical Oncology* 2005;23(25):6043-53. (In eng). DOI: 10.1200/jco.2005.06.205.
69. Shin JH, Park HB, Oh YM, et al. Positive conversion of negative signaling of CTLA4 potentiates antitumor efficacy of adoptive T-cell therapy in murine tumor models. *Blood* 2012;119(24):5678-87. (In eng). DOI: 10.1182/blood-2011-09-380519.
70. Park HB, Lee JE, Oh YM, Lee SJ, Eom HS, Choi K. CTLA4-CD28 chimera gene modification of T cells enhances the therapeutic efficacy of donor lymphocyte infusion for hematological malignancy. *Experimental & molecular medicine* 2017;49(7):e360. (In eng). DOI: 10.1038/emm.2017.104.
71. Linsley PS, Brady W, Urnes M, Grosmaire LS, Damle NK, Ledbetter JA. CTLA-4 is a second receptor for the B cell activation antigen B7. *The Journal of experimental medicine* 1991;174(3):561-9. (In eng) (<https://rupress.org/jem/article-pdf/174/3/561/1267974/561.pdf>).
72. Rowshanravan B, Halliday N, Sansom DM. CTLA-4: a moving target in immunotherapy. *Blood* 2018;131(1):58-67. (In eng). DOI: 10.1182/blood-2017-06-741033.
73. Kunkele A, Johnson AJ, Rolczynski LS, et al. Functional Tuning of CARs Reveals Signaling Threshold above Which CD8+ CTL Antitumor Potency Is Attenuated due to Cell Fas-FasL-Dependent AICD. *Cancer Immunol Res* 2015;3(4):368-79. (In eng). DOI: 10.1158/2326-6066.Cir-14-0200.
74. Lai Y, Weng J, Wei X, et al. Toll-like receptor 2 costimulation potentiates the antitumor efficacy of CAR T Cells. *Leukemia* 2018;32(3):801-808. (In eng). DOI: 10.1038/leu.2017.249.
75. Blaeschke F, Stenger D, Apfelbeck A, et al. Augmenting anti-CD19 and anti-CD22 CAR T-cell function using PD-1-CD28 checkpoint fusion proteins. *Blood Cancer J* 2021;11(6):108. DOI: 10.1038/s41408-021-00499-z.
76. Liu H, Lei W, Zhang C, et al. CD19-specific CAR T Cells that Express a PD-1/CD28 Chimeric Switch-Receptor are Effective in Patients with PD-L1-positive B-Cell Lymphoma. *Clin Cancer Res* 2021;27(2):473-484. DOI: 10.1158/1078-0432.CCR-20-1457.
77. Barrett DM, Singh N, Porter DL, Grupp SA, June CH. Chimeric antigen receptor therapy for cancer. *Annual review of medicine* 2014;65:333-47. (In eng). DOI: 10.1146/annurev-med-060512-150254.
78. Kobold S, Grassmann S, Chaloupka M, et al. Impact of a New Fusion Receptor on PD-1-Mediated Immunosuppression in Adoptive T Cell Therapy. *Journal of the National Cancer Institute* 2015;107(8) (In eng). DOI: 10.1093/jnci/djv146.
79. Blaeschke F, Ortner E, Stenger D, et al. Design and Evaluation of TIM-3-CD28 Checkpoint Fusion Proteins to Improve Anti-CD19 CAR T-Cell Function. *Front Immunol* 2022;13:845499. DOI: 10.3389/fimmu.2022.845499.
80. Motzer RJ, Rini BI, McDermott DF, et al. Nivolumab for Metastatic Renal Cell Carcinoma: Results of a Randomized Phase II Trial. *Journal of clinical oncology : official journal of the American Society of Clinical Oncology* 2015;33(13):1430-7. (In eng). DOI: 10.1200/jco.2014.59.0703.
81. Robert C, Long GV, Brady B, et al. Nivolumab in previously untreated melanoma without BRAF mutation. *The New England journal of medicine* 2015;372(4):320-30. (In eng). DOI: 10.1056/NEJMoa1412082.

11 Supplements

11.1 Primer sequences

CAR_ident_forw	GCCAAACATTATTACTACGGTGGTA
CAR_ident_rev	TATGGGAATAAATGGCGGTAAGATG

11.2 T cell sequences

Coding sequences are shown. Kozak sequence GCCGCCACC was attached to the 5' end to increase expression. Restriction sites Not1 and EcoR1 were added for cloning into pMP71.

11.2.1 Sequence of 19_3z CAR

ATGCTTCTCCTGGTGACAAGCCTTCTGCTCTGTGAGTTACCACACCCAGCATTCTCCTGATCCCAGACATCCAGATGACAC
 AGACTACATCCTCCCTGTCTGCCTCTCTGGGAGACAGAGTCACCATCAGTTGCAGGGCAAGTCAGGACATTAGTAAATATT
 TAAATTGGTATCAGCAGAAACCAGATGGAAGTGTAACTCCTGATCTACCATACATCAAGATTAACTCAGGAGTCCCAT
 CAAGTTTCAAGTGGCAGTGGGTCTGGAACAGATTATTCTCTCACCATTAGCAACCTGGAGCAAGAAGATATTGCCACTTACT
 TTTGCCAACAGGGTAATACGCTTCCGTACACGTTCCGAGGGGGGACTAAGTTGGAAATAACAGGCTCCACCTCTGGATCC
 GGCAAGCCCGGATCTGGCGAGGGATCCACCAAGGGCGAGGTGAACTGCAGGAGTCAGGACCTGGCCTGGTGGCGCCC
 TCACAGAGCCTGTCCGTACATGCACTGTCTCAGGGGTCTCATTACCCGACTATGGTGTAAAGCTGGATTGCGCCAGCCTCCA
 CGAAAGGGTCTGGAGTGGCTGGGAGTAATATGGGGTAGTGAAACACATACTATAATTGAGCTCTCAAATCCAGACTGAC
 CATCATCAAGGACAACCTCAAGAGCCAAGTTTTCTTAAAAATGAACAGTCTGCAAACCTGATGACACAGCCATTTACTACTGT
 GCCAAACATTATTACTACGGTGGTAGCTATGCTATGGACTACTGGGGTCAAGGAACCTCAGTCACCGTCTCCTCAGAGCAA
 AAGCTCATTCTGAAGAGGACTTGTTCGTGCCGGTCTTCTGCCAGCGAAGCCACCACGACGCCAGCGCCGCGACCACCA
 ACACCGGCGCCACCATCGCGTCGACGCCCTGTCCCTGCGCCAGAGGCGTGCCGGCCAGCGGGGGGGCGCAGTGC
 ACACGAGGGGGCTGGACTTCGCTGTGATATCTACATCTGGGCGCCCTTGGCCGGGACTTGTGGGGTCTTCTCCTGTAC
 TGGTTATCACCTTTACTGCAACCACAGGAACAGAGTGAAGTTCAGCAGGAGCGCAGACGCCCCCGGTACCAGCAGGGC
 CAGAACCAGCTCTATAACGAGCTCAATCTAGGACGAAGAGAGGAGTACGATGTTTTGGACAAGAGACGTGGCCGGGACC
 CTGAGATGGGGGGAAAGCCGAGAAGGAAGAACCCTCAGGAAGGCCTGTACAATGAACTGCAGAAAGATAAGATGGCGG
 AGGCCTACAGTGAAGTGGGATGAAAGGCGAGCGCCGGAGGGGCAAGGGGCACGATGGCCTTACCAGGGTCTCAGTA
 CAGCCACCAAGGACACCTACGACGCCCTTACATGCAGGCCCTGCCCCCTCGCTAA

11.2.2 Sequence of 19_3z_CTLA CAR

ATGCTTCTCCTGGTGACAAGCCTTCTGCTCTGTGAGTTACCACACCCAGCATTCTCCTGATCCCAGACATCCAGATGACAC
 AGACTACATCCTCCCTGTCTGCCTCTCTGGGAGACAGAGTCACCATCAGTTGCAGGGCAAGTCAGGACATTAGTAAATATT
 TAAATTGGTATCAGCAGAAACCAGATGGAAGTGTAACTCCTGATCTACCATACATCAAGATTAACTCAGGAGTCCCAT
 CAAGTTTCAAGTGGCAGTGGGTCTGGAACAGATTATTCTCTCACCATTAGCAACCTGGAGCAAGAAGATATTGCCACTTACT
 TTTGCCAACAGGGTAATACGCTTCCGTACACGTTCCGAGGGGGGACTAAGTTGGAAATAACAGGCTCCACCTCTGGATCC
 GGCAAGCCCGGATCTGGCGAGGGATCCACCAAGGGCGAGGTGAACTGCAGGAGTCAGGACCTGGCCTGGTGGCGCCC
 TCACAGAGCCTGTCCGTACATGCACTGTCTCAGGGGTCTCATTACCCGACTATGGTGTAAAGCTGGATTGCGCCAGCCTCCA
 CGAAAGGGTCTGGAGTGGCTGGGAGTAATATGGGGTAGTGAAACACATACTATAATTGAGCTCTCAAATCCAGACTGAC
 CATCATCAAGGACAACCTCAAGAGCCAAGTTTTCTTAAAAATGAACAGTCTGCAAACCTGATGACACAGCCATTTACTACTGT
 GCCAAACATTATTACTACGGTGGTAGCTATGCTATGGACTACTGGGGTCAAGGAACCTCAGTCACCGTCTCCTCAGAGCAA

AAGCTCATTCTGAAGAGGACTTGTTCTGCGCGTCTTCTGCCAGCGAAGCCACCACGACGCCAGCGCCGCGACCACCA
ACACCGGCGCCACCATCGCGTCGCAGCCCCTGTCCCTGCGCCAGAGGCGTGCCGGCCAGCGGCGGGGGGCGCAGTGC
ACACGAGGGGGCTGGACTTCGCTGTGATATCTACATCTGGGCGCCCTTGCCGGGACTTGTGGGGTCTTCTCTGTAC
TGTTATCACCTTTACTGCAACCACAGGAACAGAGTGAAGTTCAGCAGGAGCGCAGACGCCCCGCGTACCAGCAGGGC
CAGAACCAGCTCTATAACGAGCTCAATCTAGGACGAAGAGAGGAGTACGATGTTTTGGACAAGAGACGTGGCCGGACC
CTGAGATGGGGGAAAGCCGAGAAGGAAGAACCCTCAGGAAGGCCTGTACAATGAACTGCAGAAAGATAAGATGGCGG
AGGCCTACAGTGAGATTGGGATGAAAGGCGAGCGCCGGAGGGGCAAGGGGCACGATGGCCTTACCAGGGTCTCAGTA
CAGCCACCAAGGACACCTACGACGCCCTTACATGCAGGCCCTGCCCCCTCGCGTGAAACAGACTTTGAATTTGACCTTCT
CAAGTTGGCGGGAGACGTGGAGTCCAACCCAGGCCCGCTTGCCCTGGATTTAGCGGCACAAGGCTCAGCTGAACCTG
GCTACCAGGACCTGGCCCTGCACTCTCTGTTTTTCTTCTTTCATCCCTGTCTTCTGCAAAGCAATGCACGTGGCCAGCC
TGCTGTGGTACTGGCCAGCAGCCGAGGCATCGCCAGCTTTGTGTGTGAGTATGCATCTCCAGGCAAAGCCACTGAGGTCC
GGGTGACAGTGCTTCGGCAGGCTGACAGCCAGGTGACTGAAGTCTGTGCGGCAACCTACATGATGGGGAATGAGTTGAC
CTTCTAGATGATTCCATCTGCACGGGCACCTCCAGTGGAAATCAAGTGAACCTCACTATCCAAGGACTGAGGGCCATGGA
CACGGGACTCTACATCTGCAAGGTGGAGCTCATGTACCCACCGCCATACTACCTGGGCATAGGCAACGGAACCCAGATTT
ATGTAATTGATCCAGAACCCTGCCAGATTCTGACTTCTCTCTGGATCCTTGCAGCAGTTAGTTGGGGTTGTTTTTTAT
AGCTTCTCTCACAGCTGTTTCTTTGAGCAAAATGCTAAAGAAAAGAAGCCCTTACAACAGGGGTCTATGTGAAAATG
CCCCAACAGAGCCAGAATGTGAAAAGCAATTTAGCCTTATTTTATCCCATCAATTGA

11.2.3 Sequence of 19_3z_CTLA_CD28 CAR

ATGCTTCTCTGGTGACAAGCCTTCTGCTCTGTGAGTTACCACACCAGCATTCTCTGATCCAGACATCCAGATGACAC
AGACTACATCTCCCTGTCTGCCTCTCTGGGAGACAGAGTACCATCAGTTGCAGGGCAAGTCAGGACATTAGTAAATATT
TAAATTGGTATCAGCAGAAACCAGATGGAAGTGTAAACTCTGATCTACCATACATCAAGATTACACTCAGGAGTCCCAT
CAAGTTTCAAGTGGCAGTGGGTCTGGAACAGATTATTCTCTACCATAGCAACCTGGAGCAAGAAGATATTGCCACTTACT
TTTGCCAACAGGGTAATACGCTTCCGTACACGTTCCGGAGGGGGGACTAAGTTGGAAATAACAGGCTCCACCTCTGGATCC
GGCAAGCCCGATCTGGCGAGGATCCACCAAGGGCGAGGTGAAACTGCAGGAGTCAAGGACCTGGCCTGGTGGCGCCC
TCACAGAGCTGTCCGTACATGCACTGTCTCAGGGGTCTCATTACCCGACTATGGTGTAAAGTGGATTCGCCAGCCTCCA
CGAAAGGGTCTGGAGTGGCTGGGAGTAATATGGGGTAGTGAACCACATACTATAATTAGCTCTCAAATCCAGACTGAC
CATCATCAAGGACAACCTCCAAGAGCCAAGTTTTCTTAAAAATGAACAGTCTGCAAACCTGATGACACAGCCATTTACTACTGT
GCCAAACATTACTACGGTGGTAGCTATGCTATGGACTACTGGGGTCAAGGAACCTCAGTCACCGTCTCCTCAGAGCAA
AAGCTCATTCTGAAGAGGACTTGTTCTGCGCGTCTTCTGCCAGCGAAGCCACCACGACGCCAGCGCCGCGACCACCA
ACACCGGCGCCACCATCGCGTCGCAGCCCCTGTCCCTGCGCCAGAGGCGTGCCGGCCAGCGGCGGGGGGCGCAGTGC
ACACGAGGGGGCTGGACTTCGCTGTGATATCTACATCTGGGCGCCCTTGCCGGGACTTGTGGGGTCTTCTCTGTAC
TGTTATCACCTTTACTGCAACCACAGGAACAGAGTGAAGTTCAGCAGGAGCGCAGACGCCCCGCGTACCAGCAGGGC
CAGAACCAGCTCTATAACGAGCTCAATCTAGGACGAAGAGAGGAGTACGATGTTTTGGACAAGAGACGTGGCCGGACC
CTGAGATGGGGGAAAGCCGAGAAGGAAGAACCCTCAGGAAGGCCTGTACAATGAACTGCAGAAAGATAAGATGGCGG
AGGCCTACAGTGAGATTGGGATGAAAGGCGAGCGCCGGAGGGGCAAGGGGCACGATGGCCTTACCAGGGTCTCAGTA
CAGCCACCAAGGACACCTACGACGCCCTTACATGCAGGCCCTGCCCCCTCGCGTGAAACAGACTTTGAATTTGACCTTCT
CAAGTTGGCGGGAGACGTGGAGTCCAACCCAGGCCCGCTTGCCCTGGATTTAGCGGCACAAGGCTCAGCTGAACCTG
GCTACCAGGACCTGGCCCTGCACTCTCTGTTTTTCTTCTTTCATCCCTGTCTTCTGCAAAGCAATGCACGTGGCCAGCC
TGCTGTGGTACTGGCCAGCAGCCGAGGCATCGCCAGCTTTGTGTGTGAGTATGCATCTCCAGGCAAAGCCACTGAGGTCC
GGGTGACAGTGCTTCGGCAGGCTGACAGCCAGGTGACTGAAGTCTGTGCGGCAACCTACATGATGGGGAATGAGTTGAC
CTTCTAGATGATTCCATCTGCACGGGCACCTCCAGTGGAAATCAAGTGAACCTCACTATCCAAGGACTGAGGGCCATGGA
CACGGGACTCTACATCTGCAAGGTGGAGCTCATGTACCCACCGCCATACTACCTGGGCATAGGCAACGGAACCCAGATTT
ATGTAATTGATCCAGAACCCTGCCAGATTCTGACTTCTCTCTGGATCCTTGCAGCAGTTAGTTGGGGTTGTTTTTTAT
AGCTTCTCTCACAGGAGTAAGAGGAGCAGGCTCCTGCACAGTACTACATGAACATGACTCCCCGCCGCCCGGGCC
CACCCGCAAGCATTACCAGCCCTATGCCCCACCACGCGACTTCGCAGCCTATCGCTCCTGA

11.2.5 Sequence of 19_BB_3z CAR

ATGCTTCTCCTGGTGACAAGCCTTCTGCTCTGTGAGTTACCACACCCAGCATTCTCCTGATCCCAGACATCCAGATGACAC
AGACTACATCCTCCCTGTCTGCCTCTCTGGGAGACAGAGTCACCATCAGTTGCAGGGCAAGTCAGGACATTAGTAAATATT
TAAATTGGTATCAGCAGAAACCAGATGGAAGCTGTTAACTCCTGATCTACCATACATCAAGATTACACTCAGGAGTCCCAT
CAAGGTTCAAGTGGCAGTGGGTCTGGAACAGATTATTCTCTCACCATTAGCAACCTGGAGCAAGAAGATATTGCCACTTACT
TTTGCCAACAGGGTAATACGCTTCCGTACACGTTCCGAGGGGGGACTAAGTTGGAAATAACAGGCTCCACCTCTGGATCC
GGCAAGCCCGGATCTGGCGAGGGATCCACCAAGGGCGAGGTGAACTGCAGGAGTCAGGACCTGGCCTGGTGGCGCCC
TCACAGAGCCTGTCCGTACATGCACTGTCTCAGGGGTCTCATTACCCGACTATGGTGTAAAGCTGGATTGCGCAGCCTCCA
CGAAAGGGTCTGGAGTGGCTGGGAGTAATATGGGGTAGTGAAACCACATACTATAATTAGCTCTCAAATCCAGACTGAC
CATCATCAAGGACAACCTCAAGAGCCAAGTTTTCTTAAAAATGAACAGTCTGCAAACCTGATGACACAGCCATTTACTACTGT
GCCAAACATTATTACTACGGTGGTAGCTATGCTATGGACTACTGGGGTCAAGGAACCTCAGTCACCGTCTCCTCAGAGCAA
AAGCTCATTCTGAAGAGGACTTGTTTCGTGCCGGTCTTCTGCCAGCGAAGCCACCACGACGCCAGCGCCGCGACCACCA
ACACCGGCGCCACCATCGCGTCGACGCCCTGTCCCTGCGCCAGAGGCGTGCCGGCCAGCGGCGGGGGGCGCAGTGC
ACACGAGGGGGCTGGACTTCGCTGTGATATCTACATCTGGGCGCCCTTGGCCGGGACTTGTGGGGTCTTCTCCTGTAC
TGTTTATCACCTTTACTGCAACCACAGGAACAAACGGGGCAGAAAGAACTCCTGTATATATTCAAACAACCATTTATGA
GACCAGTACAACTACTCAAGAGGAAGATGGCTGTAGCTGCCGATTTCCAGAAGAAGAAGAAGGAGGATGTGAAGTGA
AGTGAAGTTCAGCAGGAGCGCAGACGCCCCCGCTACCAGCAGGGCCAGAACCAGCTCTATAACGAGCTCAATCTAGGA
CGAAGAGAGGAGTACGATGTTTTGGACAAGAGACGTGGCCGGGACCCTGAGATGGGGGGAAAGCCGAGAAGGAAGAA
CCCTCAGGAAGGCCTGTACAATGAACTGCAGAAAGATAAGATGGCGGAGGCCTACAGTGAGATTGGGATGAAAGGCGA
GCGCCGGAGGGGCAAGGGGCACGATGGCCTTACCAGGGTCTCAGTACAGCCACCAAGGACACCTACGACGCCCTTAC
ATGCAGGCCCTGCCCCCTCGCTAA

11.2.6 Sequence of 19_BB_3z CTLA CAR

ATGCTTCTCCTGGTGACAAGCCTTCTGCTCTGTGAGTTACCACACCCAGCATTCTCCTGATCCCAGACATCCAGATGACAC
AGACTACATCCTCCCTGTCTGCCTCTCTGGGAGACAGAGTCACCATCAGTTGCAGGGCAAGTCAGGACATTAGTAAATATT
TAAATTGGTATCAGCAGAAACCAGATGGAAGCTGTTAACTCCTGATCTACCATACATCAAGATTACACTCAGGAGTCCCAT
CAAGGTTCAAGTGGCAGTGGGTCTGGAACAGATTATTCTCTCACCATTAGCAACCTGGAGCAAGAAGATATTGCCACTTACT
TTTGCCAACAGGGTAATACGCTTCCGTACACGTTCCGAGGGGGGACTAAGTTGGAAATAACAGGCTCCACCTCTGGATCC
GGCAAGCCCGGATCTGGCGAGGGATCCACCAAGGGCGAGGTGAACTGCAGGAGTCAGGACCTGGCCTGGTGGCGCCC
TCACAGAGCCTGTCCGTACATGCACTGTCTCAGGGGTCTCATTACCCGACTATGGTGTAAAGCTGGATTGCGCAGCCTCCA
CGAAAGGGTCTGGAGTGGCTGGGAGTAATATGGGGTAGTGAAACCACATACTATAATTAGCTCTCAAATCCAGACTGAC
CATCATCAAGGACAACCTCAAGAGCCAAGTTTTCTTAAAAATGAACAGTCTGCAAACCTGATGACACAGCCATTTACTACTGT
GCCAAACATTATTACTACGGTGGTAGCTATGCTATGGACTACTGGGGTCAAGGAACCTCAGTCACCGTCTCCTCAGAGCAA
AAGCTCATTCTGAAGAGGACTTGTTTCGTGCCGGTCTTCTGCCAGCGAAGCCACCACGACGCCAGCGCCGCGACCACCA
ACACCGGCGCCACCATCGCGTCGACGCCCTGTCCCTGCGCCAGAGGCGTGCCGGCCAGCGGCGGGGGGCGCAGTGC
ACACGAGGGGGCTGGACTTCGCTGTGATATCTACATCTGGGCGCCCTTGGCCGGGACTTGTGGGGTCTTCTCCTGTAC
TGTTTATCACCTTTACTGCAACCACAGGAACAAACGGGGCAGAAAGAACTCCTGTATATATTCAAACAACCATTTATGA
GACCAGTACAACTACTCAAGAGGAAGATGGCTGTAGCTGCCGATTTCCAGAAGAAGAAGAAGGAGGATGTGAAGTGA
AGTGAAGTTCAGCAGGAGCGCAGACGCCCCCGCTACCAGCAGGGCCAGAACCAGCTCTATAACGAGCTCAATCTAGGA
CGAAGAGAGGAGTACGATGTTTTGGACAAGAGACGTGGCCGGGACCCTGAGATGGGGGGAAAGCCGAGAAGGAAGAA
CCCTCAGGAAGGCCTGTACAATGAACTGCAGAAAGATAAGATGGCGGAGGCCTACAGTGAGATTGGGATGAAAGGCGA
GCGCCGGAGGGGCAAGGGGCACGATGGCCTTACCAGGGTCTCAGTACAGCCACCAAGGACACCTACGACGCCCTTAC
ATGCAGGCCCTGCCCCCTCGCTGAAACAGACTTTGAATTTGACCTTCTCAAGTTGGCGGGAGACGTGGAGTCCAACCCA
GGCCCGGCTTGCCTTGGATTTAGCGGCACAAGGCTCAGCTGAACCTGGCTACCAGGACCTGGCCCTGCACTCTCCTGTTT
TTTCTTCTTTCATCCCTGTCTTCTGCAAAGCAATGCACGTGGCCAGCCTGCTGTGGTACTGGCCAGCAGCCGAGGCATCG
CCAGCTTTGTGTGTGAGTATGCATCTCCAGGCAAAGCCACTGAGGTCCGGGTGACAGTGTCTCGGCAGGCTGACAGCCAG

GTGACTGAAGTCTGTGCGGCAACCTACATGATGGGGAATGAGTTGACCTTCTAGATGATTCCATCTGCACGGGCACCTCC
AGTGAAATCAAGTGAACCTCACTATCCAAGGACTGAGGGCCATGGACACGGGACTCTACATCTGCAAGGTGGAGCTCAT
GTACCCACCGCCATACTACCTGGGCATAGGCAACGGAACCCAGATTTATGTAATTGATCCAGAACCGTGCCAGATTCTGA
CTTCCTCTCTGGATCCTTGACAGTTAGTTCGGGGTTGTTTTTATAGCTTCTCCTCACAGCTGTTTCTTTGAGCAAAAT
GCTAAAGAAAAGAAGCCCTCTTACAACAGGGGTCTATGTGAAAATGCCCCAACAGAGCCAGAATGTGAAAAGCAATTTCC
AGCCTTATTTTATCCCATCAATTGA

11.2.7 Sequence of 19t CAR

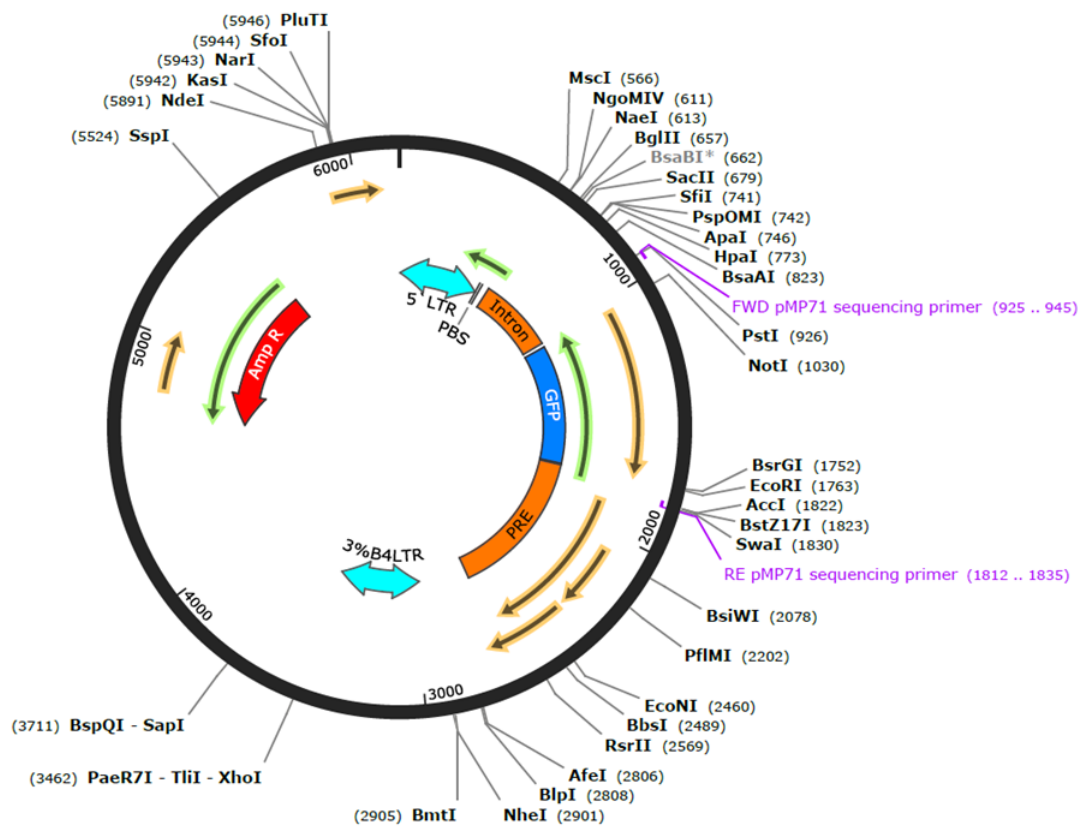
ATGCTTCTCCTGGTGACAAGCCTTCTGCTCTGTGAGTTACCACACCCAGCATTCTCCTGATCCCAGACATCCAGATGACAC
AGACTACATCCTCCCTGTCTGCCTCTCTGGGAGACAGAGTCACCATCAGTTGCAGGGCAAGTCAGGACATTAGTAAATATT
TAAATTGGTATCAGCAGAAACCAGATGGAACCTGTTAACTCCTGATCTACCATACATCAAGATTACACTCAGGAGTCCCAT
CAAGGTTCAAGTGGCAGTGGGTCTGGAACAGATTATTCTCTACCATAGCAACCTGGAGCAAGAAGATATTGCCACTTACT
TTTGCCAACAGGGTAATACGCTTCCGTACACGTTCCGGAGGGGGGACTAAGTTGGAATAACAGGCTCCACCTCTGGATCC
GGCAAGCCCGGATCTGGCGAGGGATCCACCAAGGGCGAGGTGAACTGCAGGAGTCAGGACCTGGCCTGGTGGCGCCC
TCACAGAGCCTGTCCGTACATGCACTGTCTCAGGGGTCTCATTACCCGACTATGGTGTAAAGCTGGATTCGCCAGCCTCCA
CGAAAGGGTCTGGAGTGGCTGGGAGTAATATGGGGTAGTGAAACCACATACTATAATTCAGCTCTCAAATCCAGACTGAC
CATCATCAAGGACAACCTCAAGAGCCAAGTTTTCTTAAAAATGAACAGTCTGCAAACCTGATGACACAGCCATTTACTACTGT
GCCAAACATTATTACTACGGTGGTAGCTATGCTATGGACTACTGGGGTCAAGGAACCTCAGTCACCGTCTCCTCAGAGCAA
AAGCTCATTCTGAAGAGGACTTGTTCGTGCCGGTCTTCTGCCAGCGAAGCCACCACGACGCCAGCGCCGCGACCACCA
ACACCGGCGCCACCATCGCGTCGACGCCCTGTCCCTGCGCCAGAGGCGTGCCGGCCAGCGCGGGGGGCGCAGTGC
ACACGAGGGGGCTGGACTTCGCTGTGATATCTACATCTGGGCGCCCTTGGCCGGGACTTGTGGGGTCTTCTCCTGTAC
TGTTATCACCTTTACTGCAACCACAGGAACTGA

11.2.8 Sequence for CTLA-4 overexpression

ATGGCTTGCCTTGGATTTCAAGCGGCACAAGGCTCAGCTGAACCTGGCTACCAGGACCTGGCCCTGCACTCTCCTGTTTTTTC
TTCTTTCATCCCTGTCTTCTGCAAAGCAATGCACGTGGCCAGCCTGCTGTGGTACTGGCCAGCAGCCGAGGCATCGCCA
GCTTTGTGTGTGAGTATGCATCTCCAGGCAAAGCCACTGAGGTCCGGGTGACAGTGCTTCGGCAGGCTGACAGCCAGGTG
ACTGAAGTCTGTGCGGCAACCTACATGATGGGGAATGAGTTGACCTTCTAGATGATTCCATCTGCACGGGCACCTCCAGT
GGAAATCAAGTGAACCTCACTATCCAAGGACTGAGGGCCATGGACACGGGACTCTACATCTGCAAGGTGGAGCTCATGTA
CCCACCGCCATACTACCTGGGCATAGGCAACGGAACCCAGATTTATGTAATTGATCCAGAACCGTGCCAGATTCTGACTT
CCTCCTCTGGATCCTTGACAGTTAGTTCGGGGTTGTTTTTATAGCTTCTCCTCACAGCTGTTTCTTTGAGCAAAATGC
TAAAGAAAAGAAGCCCTCTTACAACAGGGGTCTATGTGAAAATGCCCCAACAGAGCCAGAATGTGAAAAGCAATTTCCAG
CCTTATTTTATCCCATCAATTGA

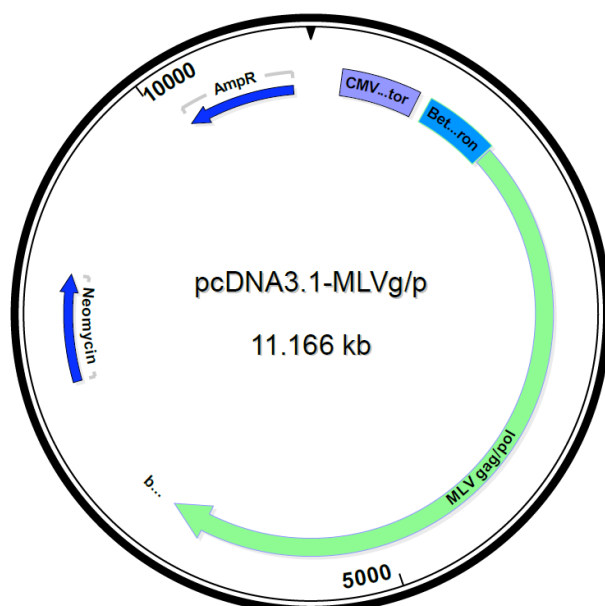
11.3 Vector Maps

11.3.1 Vector map of pMP71



CAR constructs were inserted instead of GFP

11.3.2 Vector map of gag/pol (pcDNA3.1-MLV-g/p)



12 Publication list

Blaeschke, F., E. Ortner, D. Stenger, J. Mahdawi, A. Apfelbeck, N. Habjan, T. Weisser, T. Kaeuferle, S. Willier, S. Kobold, and T. Feuchtinger. 2022. Design and Evaluation of TIM-3-CD28 Checkpoint Fusion Proteins to Improve Anti-CD19 CAR T-Cell Function. *Front Immunol* 13:845499. doi: 10.3389/fimmu.2022.845499.

Blaeschke, F., D. Stenger, A. Apfelbeck, B. L. Cadilha, M. R. Benmebarek, J. Mahdawi, E. Ortner, M. Lepenies, N. Habjan, F. Rataj, S. Willier, T. Kaeuferle, R. G. Majzner, D. H. Busch, S. Kobold, and T. Feuchtinger. 2021. Augmenting anti-CD19 and anti-CD22 CAR T-cell function using PD-1-CD28 checkpoint fusion proteins. *Blood Cancer J* 11 (6):108. doi: 10.1038/s41408-021-00499-z.